Hormonal modulation of auditory processing in a seasonally breeding songbird

Melissa L. Caras

A dissertation

submitted in partial fulfillment of the

requirements for the degree of

Doctor of Philosophy

University of Washington

2013

Reading Committee:

Eliot Brenowtiz, Chair

Edwin W Rubel

Joseph Sisneros

Program Authorized to Offer Degree:

Neurobiology and Behavior

University of Washington

Abstract

Hormonal modulation of auditory processing in a seasonally breeding songbird

Melissa L. Caras

Chair of the Supervisory Committee:
Professor Eliot Brenowitz
Department of Psychology

Sex steroid hormones modulate vocal communication in a number of species. While much is known about the impact of these hormones on the motor systems responsible for generating vocal output, less is known about the influence of these hormones on auditory processing. I addressed this issue in a neuroethological context by studying Gambel's white-crowned sparrow (*Zonotrichia leucophrys gambelii*). White-crowned sparrows are wild songbirds that undergo dramatic fluctuations in sex steroid levels as a function of season. I manipulated photoperiod and hormone levels in the laboratory and found that sex steroids have disparate effects along the ascending auditory pathway. Specifically, I report the following: First, breeding condition elevates auditory brainstem response thresholds and prolongs peak latencies compared to non-breeding condition, but does not affect distortion product otoacoustic emissions. These results are described in detail in chapter 2. Next, in chapter 3, I demonstrate that single cells in the avian primary auditory forebrain, field L, are selectively responsive to hormonal state. When

plasma hormone levels are elevated, cells with monotonic responses to pure tone stimuli demonstrate enhanced auditory function, and their physiological response properties strongly correlate with the concentration of circulating hormone. Finally, the findings described in chapter 4 show that a neural code based on spike timing reliability more accurately discriminates the intensity of incoming vocalization signals compared with a spike count-based strategy, and is sensitive to hormonal condition. My results are summarized and placed into a broader context in chapter 5, and future studies are proposed.

TABLE OF CONTENTS

LIST OF FIGURES

LIST OF TABLES

GLOSSARY

ABR	auditory brainstem response
AR	androgen receptor
CLM	caudolateral mesopallium
CM	caudal mesopallium
CMM	caudomedial mesopallium
dB SPL	decibel sound pressure level
DPOAE	distortion product otoacoustic emission
E_2	17β-estradiol
ELISA	enzyme-linked immunosorbent assay
ER	estrogen receptor
F1	first primary tone
F2	second primary tone
GWCS	Gambel's white-crowned sparrow
L1	level of the first primary tone*
L2	level of the second primary tone*
LD	long-day
LH	hyperpallial lamina
LMD	dorsal medullary lamina
MLd	mesencephalicus lateralis pars dorsalis
NA	nucleus angularis
NL	nucleus laminaris
NM	nucleus magnocellularis
NCM	caudomedial nidopallium
OAE	otoacoustic emission
Ov	ovoidalis
Q	quality factor
RMS	root mean squared
SD	short-day
T	testosterone

*L1 and L2 only refer to tone levels in Chapter 2. In the remainder of this dissertation, L1 and L2 refer to specific subdivisions of field L, an auditory forebrain region that is the focus of Chapters 3 and 4.

PREFACE

Chapters 2 has been published previously as:

Caras ML, Brenowitz E, Rubel EW (2010) Peripheral auditory processing changes seasonally in Gambel's white-crowned sparrow. J Comp Physiol A Neuroethol Sens Neural Behav Physiol 196:581-599.

Chapter 3 has been published previously as:

Caras ML, O'Brien M, Brenowitz E, Rubel EW (2012) Estradiol selectively enhances auditory function in avian forebrain neurons. J Neurosci 32(49): 17597-17611

Chapter 4 has been prepared in publication format. Therefore, I ask the reader to forgive some apparent redundancies in the figures and text.

ACKNOWLEDGEMENTS

A heartfelt thank you to my parents, brother, and grandparents. Your complete confidence in my abilities has shaped me into the person that I am today. I love you all and hope that I continue to make you proud.

I am grateful for the advice and support I have received from members of the Brenowitz and Rubel labs over the years: Rachel Cohen, Dale Cunningham, Karin Lent, John Meitzen, Tracy Larson Parichy, Kristen Richards Preble, Jason Sanchez, Armin Seidl, Melissa Strong, Kate Tabor, Nivi Thatra, Christopher Thompson, Christopher Vaaga, Yuan Wang and Tsu-Wei Wang. Each of you made going to work a joy; I look forward to future collaborations and continued friendships. Additional thanks goes to David Schneider and Sarah M.N. Woolley for technical assistance, members of the Perkel lab for hours of thoughtful discussion, and Jenny Stone and Christine Portfors for critical insights and advice.

A very special thank you to Brandon Warren for the creation and maintenance of all of my data acquisition software and to Matt O'Brien for help with the histology in Chapters 3 and 4.

Thank you to all of the friends I have made while on this journey: Stephanie Furrer, Adrienne Mueller, Ilana Cohen, Geoff Bucks, James Lawton, Craig Bierle, Charlie Hass, Grant Storey, Helen Gerns, Mike Famulare and Stephanie Seeman. I consider each and every one of you to be

like family. You are all amazing people, and I will miss you terribly. Thank you from the bottom of my heart for bringing so much joy into my life.

I thank my committee, David Perkel, Joseph Sisneros, and Kelly Tremblay, for thoughtful advice throughout my graduate school career. I am a better scientist because of your unwavering support and constructive criticism. Truly, thank you.

A thousand thanks to the administrators that make daily life in the lab possible: Lucia Wisdom, Ann Wilkinson, Ann Simons, Liz MacCready, and Susan Carpenter-Brandt. Each of you are absolute gems.

Last, I thank my advisors, Eliot Brenowitz and Ed Rubel. Eliot, I thank you for all of your advice about becoming a successful, independent scientist; your lessons will not be forgotten as I now begin my career. Ed, I feel so incredibly lucky that our initial collaboration evolved into such a strong mentor-student relationship. I cannot express how truly grateful I am to have had you as a role-model these past 5 years; your influence has been profound. I am honored to say that I am your last graduate student. (If you ever retire, that is.) Many thanks to both of you.

This work was supported by the NIH/NIDCD grants R01DC000033, R01DC003829, P30DC004661, F31DC010938, the Seattle Chapter of Achievement Rewards for College Scientists Foundation, and the Washington Research Foundation.

DEDICATION

This work is dedicated to the life and memory of a friend and scientist, Robin Harris.

Chapter 1. Background and Significance

A fundamental area of neurobiological study is the hormonal modulation of behavior. Hormones regulate both internal states, such as mood and appetite, and external interactions, including aggressive and reproductive encounters, in a wide range of taxa. In humans, hormones and their receptors are the targets of many therapeutic drugs aimed at alleviating disease or dysfunction. It is therefore no surprise that research on this topic has far reaching implications for both basic science and human health.

1.1 Sex steroid hormones and sensory processing

Sex steroids are one class of hormones that have received particular scientific attention. Derived from cholesterol, sex steroid hormones are synthesized primarily in the gonads and brain (Schlinger and Remage-Healey, 2012), and are especially involved in various aspects of mating, parental caregiving, and aggression. Like other hormones, they exert their influence by binding to specific receptors located in the cytoplasm or within the plasma membrane of cellular targets. The classical view is that receptor binding initiates an intracellular cascade of events that eventually leads to gene transcription; however, rapid modulations, including changes in cellular excitability, can also occur (Zakon, 1998; Kelly and Rønnekleiv, 2009; Chow et al., 2010). This dissertation focuses on the effects on the avian auditory system of two of these steroid hormones: testosterone (T) and 17β-estradiol (E_2). T exerts its effects by binding selectively to androgen receptors (ARs). E_2, on the other hand, is estrogenic, and therefore selectively binds to estrogen receptors (ERs). It should be noted that *in vivo*, T can be transformed into E_2 via the enzymatic

action of aromatase, but this conversion is one-way: E_2 is at the end of the synthesis pathway, and cannot be changed back into T or any of its androgenic metabolites (Luu-The and Labrie, 2010).

Growing evidence points to a substantial modulatory role of sex steroid hormones in sensory processing. In stingrays (*Dasyatis sabina*), androgen treatment alters frequency tuning and sensitivity of electrosensory primary afferent neurons (Sisneros and Tricas, 2000). Similarly, Cardwell et. al (1995) showed that androgens modulate electro-olfactogram response amplitude and sensitivity in juvenile South-East Asian Cyprinids (*Puntius schwanenfeldi*). Furthermore, approximately 50% of patients with Kennedy's disease, an abnormality caused by an X-linked recessive mutation in the androgen receptor, demonstrate sensory abnormalities, often involving visual and somatosensory systems (Finsterer, 2010). Estrogens also modulate sensory function, particularly nociception, though the exact nature of this modulation depends on a host of interacting factors, including, but not limited to, the type and duration of pain, the species under study, and the level of circulating estrogen (Evrard, 2006; Craft, 2007).

1.2 Sex steroid hormones and auditory function

Perhaps the strongest argument for hormonally regulated sensory processing comes from the impact of sex steroids on the auditory system. Steroid receptors are expressed in the auditory system of many organisms, including humans (Stenberg et al., 2001), rodents (Stenberg et al., 1999; Charitidi and Canlon, 2010; Tremere et al., 2011), fish (Forlano et al., 2005), and birds (Metzdorf et al., 1999; Noirot et al., 2009; Jeong et al., 2011).

1.2.1 Sex steroid hormones and auditory health

Traditionally, estrogen and its metabolites are thought to protect the auditory system. In the periphery, evidence for this idea comes from studies using otoacoustic emissions (OAEs) to assess adult outer hair cell function (Kemp, 2002). OAEs are more numerous and are stronger in women than in men (McFadden, 1998), and are weaker and less numerous in women taking oral contraceptives than in women cycling naturally (Snihur and Hampson, 2012). Male mice exhibit age-related decreases in OAE amplitudes earlier than females, and females show the greatest OAE amplitude decline following menopause (Guimaraes et al., 2004).

Cellular and molecular findings at the peripheral level further the case for estrogenic protection. Activation of one particular class of ER, ERβ, protects the inner ear against acoustic trauma (Meltser et al., 2008). More recently, Nakamagoe et. al (2010, 2011) demonstrated that estrogens protect hair cells against gentamicin-induced ototoxicity in cochlear explants, and that this protection is mediated by ER binding.

Estrogenic protection of auditory function also extends into the central nervous system. Auditory brainstem response (ABR) peak latencies are prolonged in rats after ovariectomy and are shortened after estrogen replacement (Coleman et al., 1994). Similarly, post-menopausal women demonstrate greater age-related increases in ABR peak latencies than age-matched males (Wharton and Church, 1990). Additionally, women with Turner's syndrome, who have only a single X chromosome and are estrogen deficient, demonstrate general hearing impairments, including difficulty with sound source localization (Hederstierna et al., 2009).

Less known is about the role of T in auditory protection or dysfunction. Work in both rhesus monkeys (McFadden et al., 2006), and more recently, adult men (Snihur and Hampson, 2012), have demonstrated a negative correlation between circulating T levels and OAE amplitudes. In green treefrogs (*Hyla cinerea*), T treatment increases multiunit auditory midbrain thresholds in a sex and stimulus-specific manner (Miranda and Wilczynski, 2009b). Together, these findings suggest a possible negative influence of circulating T on auditory function, but more studies are needed.

1.2.2 Sex steroid hormones and context-dependent regulation of auditory function

While the findings above suggest that T and E_2 have important effects on general auditory health, sex steroid hormones also interact with an organism's surroundings and past experience to fine-tune auditory processing. An excellent example of experience-dependent regulation comes from studies of pup retrieval by female mice. When a mouse pup is isolated from the nest, it emits an ultrasonic vocalization, which prompts search and retrieval behavior by the mother; virgin mice do not respond to these calls. This behavioral difference is attributed at least in part to adaptive changes in the cortical auditory representation of pup vocalizations (for review see Miranda and Liu, 2009).

Studies of a second-order auditory forebrain region, the caudomedial nidopallium (NCM), further illustrate how sex steroid hormones interact with an organism's social context and stimulus experience to regulate auditory function in one particular species: the zebra finch (*Taeniopygia guttata*). First, T and E_2 levels are rapidly modulated in NCM after exposure to

male song playback (Remage-Healey et al., 2008; Remage-Healey et al., 2012). Second, infusions of E_2 increase stimulus-evoked activity, while blockade of local ERs or interruption of endogenous E_2 synthesis reduces auditory-evoked firing rates in NCM (Tremere et al., 2009; Remage-Healey et al., 2010; Tremere and Pinaud, 2011; Remage-Healey et al., 2012). Third, ER activation in NCM is necessary for neural and perhaps behavioral discrimination of song stimuli (Remage-Healey et al., 2010; Tremere and Pinaud, 2011). For a more thorough review of these and other related studies, the reader is referred to Yoder and Vicario (2012), and Maney and Pinaud (2011).

1.3 Seasonal plasticity

While there are many approaches one could use to study hormonal modulation of auditory processing, I have chosen to take advantage of a naturally occurring type of adult plasticity: seasonally-induced changes in reproductive state. Seasonal plasticity consists of adaptive changes in the brain and behavior of an organism in response to environmental variations in day length, ambient temperature, or rainfall (Brenowitz, 2004). These environmental cues stimulate the production of sex steroid hormones, which can dramatically reshape the neural substrates underlying reproductive and communication behaviors (Bass, 2008; Meitzen and Thompson, 2008; Sisneros, 2009b).

Previous research has demonstrated the utility of studying hormonal influences of auditory function in a seasonal context. A growing body of work using electrophysiological, behavioral, and immunohistochemical techniques has demonstrated seasonal auditory plasticity in many

anuran species (Arch and Narins, 2009). Similarly, a number of studies have shown sex-steroid mediated shifts in sensitivity and frequency encoding in the auditory end organ of the vocal midshipman fish (*Porichthys notatus*; Sisneros, 2009b; Rohmann and Bass, 2011). A recent publication by Coffin et al. (2012) identified seasonally-mediated saccular hair cell addition as the potential anatomical substrate underlying these functional changes.

1.3.1 Seasonal plasticity and songbirds

Of all seasonally breeding animals, songbirds are particularly advantageous for studies of hormonally regulated plasticity. Songbirds demonstrate predictable, seasonal changes in vocal output (Meitzen et al., 2009b), and in the morphology and physiology of the neural circuit underlying song production (Nottebohm, 1981; Smith, 1996; Smith et al., 1997; Brenowitz et al., 1998; Moore et al., 2004; Meitzen et al., 2007b). Additionally, photoperiod and hormone manipulations can be used to mimic breeding and non-breeding conditions in laboratory-housed songbirds, allowing for more carefully controlled experiments (Tramontin et al., 2000, 2003; Park et al., 2005; Meitzen et al., 2009a). De Groof et al. (2009) made use of these advantages in a Diffusion Tensor Imaging study of the European starling (*Sturnus vulgaris*). They showed that high levels of circulating T, typical of the spring breeding season, were correlated with a volumetric increase in NCM volume.

Despite the advantages that songbirds provide, previous studies of seasonally-induced hormonal regulation of the songbird auditory system have some limitations. For example, seasonal differences in peripheral and brainstem auditory-evoked responses have been reported in several

songbird species, but hormonal measurements were never made to verify breeding condition (Lucas et al., 2002, 2007; Henry and Lucas, 2009). Similarly, immediate early gene immunoreactivity varies across seasons in NCM of black-capped chickadees (*Poecile atricapillus*; Phillmore et al., 2011), but again, hormonal state was not assessed.

1.4 Gambel's white-crowned sparrow

One particular songbird sub-species, Gambel's white-crowned sparrow (*Zonotorichia leucophrys gambelii*), stands out as an excellent model to further our understanding of how sex steroid hormones modulate auditory function in a seasonal, reproductive context. Gambel's white-crowned sparrow (GWCS) is one of five subspecies of White-crowned sparrow, all of which live and breed in North America. The Gambel's subspecies spends the non-breeding season (fall and winter) in the southwest portion of the United States and northern Mexico; its long-distance migration takes it as far as the Arctic circle for the breeding season (spring and summer; Cortopassi and Mewaldt, 1965). Though GWCS are closed-ended learners, producing only a single song type during the breeding season (Marler and Tamura, 1964), specific song parameters change on a seasonal basis. During the breeding season, song rate increases, and songs become longer and more stereotyped in structure (Meitzen et al., 2009b). It should be noted that while only male GWCS produce the learned vocalizations known as songs, both sexes produce presumably unlearned vocalizations, such as calls and chirps. Though GWCS have been studied for more than 50 years, and much is known about steroid-mediated plasticity of the vocal motor pathway in this species, we know nothing about how (or whether) sex hormones modulate GWCS auditory processing.

To address this issue, I brought male and female GWCS into "breeding" and "non-breeding" conditions in the laboratory using the photoperiod and hormone manipulations alluded to above. Specifically, to induce a "non-breeding" condition, I exposed birds to short day lengths (8 hours of light; 16 hours of darkness). Birds housed under these conditions maintain regressed gonads and basal levels of circulating sex steroids (Middleton, 1965; Smith et al., 1995). To induce a "breeding" condition, I exposed birds to substantially longer day lengths, typical of their Alaskan summer breeding grounds (20 hours of light; 4 hours of darkness). In addition, because photoperiod alone is not sufficient to raise plasma hormone levels in captive GWCS up to the concentrations measured in wild breeding birds, I implanted subjects with subcutaneous implants that released supplementary hormone systemically (Smith et al., 1995). All of the experiments outlined in this dissertation were performed on GWCS exposed to these laboratory manipulations designed to mimic natural seasonal conditions.

1.5 Organization of the songbird auditory system

1.5.1 The auditory periphery and sub-telencephalon

I began my investigation of the GWCS auditory system in the basilar papilla (the avian auditory end organ), and the auditory brainstem. Mechanical stimulation of the hair cells of the inner ear results in the generation of action potentials in the innervating spiral ganglion afferents. This activity is transmitted via the VIIIth cranial nerve to the avian cochlear nuclei: nucleus magnocellularis (NM) and nucleus angularis (NA). From there, the signal diverges into parallel brainstem pathways, each involving multiple synapses, before converging again in the dorsal lateral nucleus of the mesencephalon (MLd), from which it is transmitted up to the auditory

thalamic nucleus, Ovoidalis (Ov; Karten, 1967; Conlee and Parks, 1986; Krützfeldt et al., 2010a; Krützfeldt et al., 2010b; Wild et al., 2010; Fig. 1.1).

ERs are expressed in auditory hair cells and supporting cells in zebra finch (Noirot et al., 2009) and GWCS (Fig. 1.2). ER expression has also been observed in both male and female GWCS spiral ganglion neurons (Fig. 1.2) and in auditory brainstem nuclei of the non-oscine chicken (*Gallus gallus*; Wang, Brenowitz and Rubel, unpublished observations). AR expression, on the other hand, seems to be restricted to the spiral ganglion cells, at least in GWCS (Fig. 1.2). No known sex steroid receptors are expressed in MLd or Ov (Maney and Pinaud, 2011). Thus, the GWCS auditory periphery and brainstem, but not the midbrain or thalamus, are potential targets of androgen or estrogen-mediated plasticity.

1.5.2 The auditory forebrain

After completing a series of experiments at the brainstem and peripheral level, I focused my investigation on the avian analogue of the mammalian auditory cortex, Field L. A heterogenous nucleus, field L is actually a complex of 4 subregions (L1, L2a, L/L2b, and L3), distinct based on cellular morphology and connectivity, but all interconnected. L2a receives the vast majority of auditory input from Ov, though L2b also receives some direct input from Ov. Subregions make specific, reciprocal connections with secondary auditory regions, including NCM (Fortune and Margoliash, 1992; Vates et al., 1996; Fig. 1.1).

Like many other auditory nuclei, field L is tonotopically organized, with low frequencies represented dorsally and caudally, and higher frequencies represented ventrally and rostrally (Zaretsky and Konishi, 1976; Müller and Leppelsack, 1985; Wild et al., 1993). The intrinsic electrical and response properties of each Field L cell type are unknown, though differences in tuning, and perhaps stimulus selectivity, have been demonstrated among the different subregions (Bonke et al., 1979; Sen et al., 2001; Nagel and Doupe, 2008; Woolley et al., 2009; Kim and Doupe, 2011).

Unlike mammalian auditory cortex (Charitidi and Canlon, 2010; Tremere et al., 2011), field L neurons do not express ARs or ERs (Maney and Pinaud, 2011; Fig. 1.1). Therefore, the effects of sex steroids on field L that are described in chapters 3 and 4 are likely due to indirect hormonal action, though other possibilities (such as efferent modulation) cannot be ruled out at this time.

I chose to focus my investigation on field L for a few reasons. First, while many recent studies have begun to elucidate the modulatory role of sex steroid hormones in second-order auditory forebrain regions, almost nothing is known about steroid effects on the primary auditory forebrain, field L. Second, given the importance of ethological context in interpreting hormonal effects, I wished to use a representative sample of song stimuli in my experiments. Field L neurons are particularly sensitive to conspecific songs, but do not display a high degree of selectivity for specific song exemplars, as is typical of many other auditory forebrain regions (Leppelsack and Vogt, 1976; Grace et al., 2003; Theunissen et al., 2004). In addition, field L

neurons also respond to simple, pure tone stimuli (Zaretsky and Konishi, 1976; Capsius and Leppelsack, 1999; Grace et al., 2003). The use of similar stimuli in both brainstem and forebrain experiments is advantageous in that it allows for more general conclusions to be drawn about the role of sex steroid hormones in the auditory pathway. Thus, field L was particularly well-suited for the investigations described in Chapters 3 and 4.

1.6 Questions addressed in this work

As alluded to above, the overarching goal of this dissertation is to answer the following question: Do sex steroid hormones affect auditory function in GWCS? Using a combination of physiological, computational, and endocrinological techniques, under an ethological framework, I have investigated this issue at different levels within the auditory pathway. More specifically, I asked the following questions:

1.6.1 Do sex steroid hormones modulate peripheral and/or brainstem auditory function?

I address this question in Chapter 2 by recording ABRs and distortion-product OAEs from male and female GWCS under breeding and non-breeding conditions. The results from these studies provide the rationale for further investigation in the ascending auditory pathway.

1.6.2 Do sex steroid hormones affect fundamental aspects of auditory function in Field L?

I address this question in Chapter 3 by making *in vivo* extracellular recordings of single-unit auditory responses in GWCS under breeding and non-breeding conditions. Using both pure tone and conspecific song stimuli, I determine whether hormonal state impacts basic aspects of

auditory processing, including sensitivity, tuning, and response strength. I also examine whether the physiological response properties of single neurons correlate with specific hormone concentrations measured within individual birds.

1.6.3 Do sex steroid hormones affect neural discrimination of sound intensity in the auditory forebrain?

While the results from Chapter 3 demonstrate that hormones affect firing rate-based properties of auditory function, the influence of spike timing remained unexplored. I address this issue in Chapter 4 by applying computational methods to a larger dataset of single-unit responses collected from male and female GWCS under breeding and non-breeding conditions. Specifically, I create a pattern classifier to test the hypothesis that sex steroids differentially modulate spike timing-based and spike-count based intensity discrimination.

The next three chapters of this dissertation will provide the reader with a deeper understanding of the role of sex steroid modulation in auditory function. While these experiments highlight the complexity of studying hormonally-driven sensory plasticity, this work points to new directions for future research. One potential avenue is an investigation of other steroid hormones (such as progesterone and cortisol) and their role in sensory processing. Further work could elucidate the downstream (and perhaps secondary neuromodulatory) signaling pathways involved in the hormone-mediated plasticity demonstrated here. Additional future directions include expanding these experiments to other seasonally breeding bird species, particularly to those that learn new songs seasonally, such as the canary (Brenowitz and Beecher, 2005).

1.7 Figures

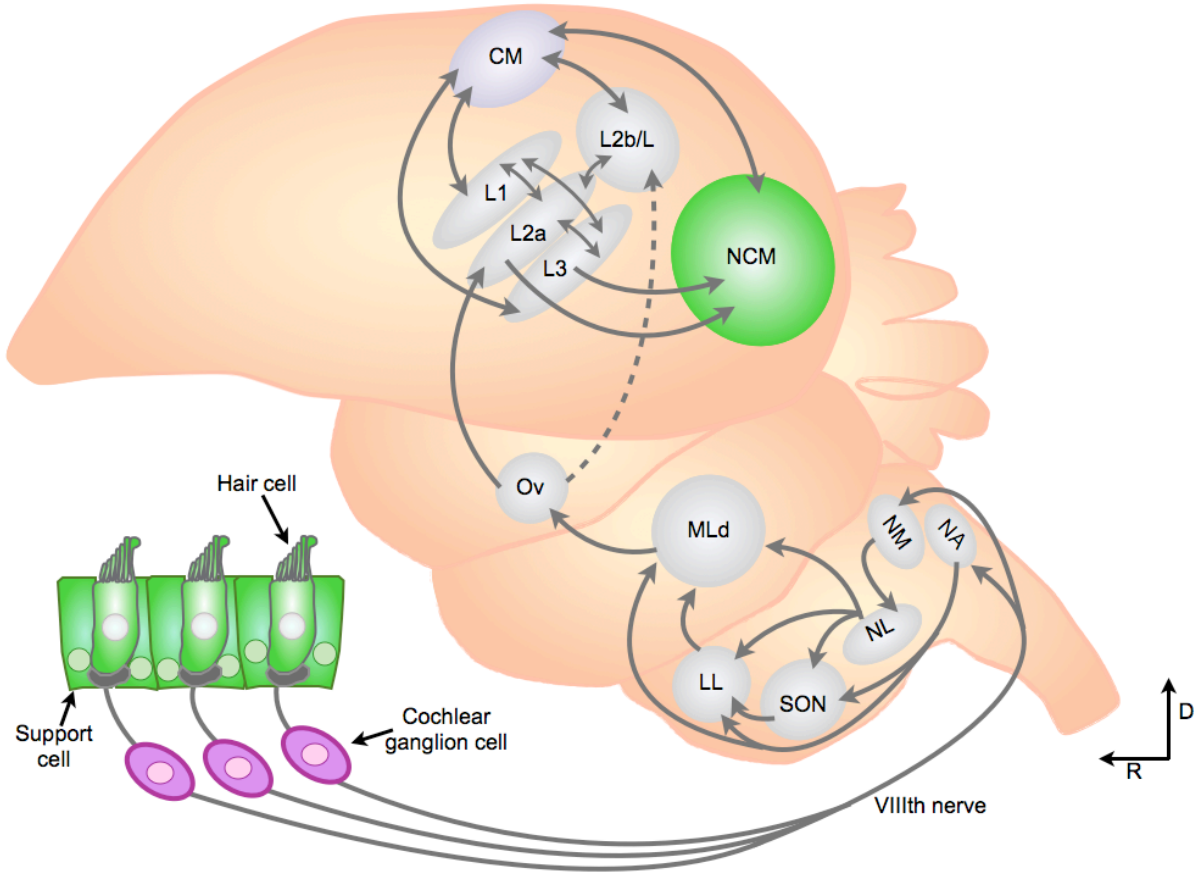

Figure 1.1. Schematic of ascending songbird auditory system. The dashed line connecting Ov to L2b indicates that this projection is a smaller input than the one to L2a, and its origin is restricted to the medial portion of Ov. Areas in green indicate sites of known ER expression in songbirds. Areas in purple indicate sites of both AR and ER expression. No areas of the ascending auditory system exclusively express ARs. Note that portions of this schematic have been simplified for clarity. L1, L2a, L2b/L and L3 refer to individual subregions in the field L complex. (NA, nucleus angularis; NM, nucleus magnocellularis; SON, superior olivary nucleus; NL, nucleus laminaris; LL, lateral lemniscus; MLd, mesencephalicus lateralis pars dorsalis; Ov, ovidalis; CM, caudal mesopallium; NCM, caudomedial nidopallium; D, dorsal; R, rostral.)

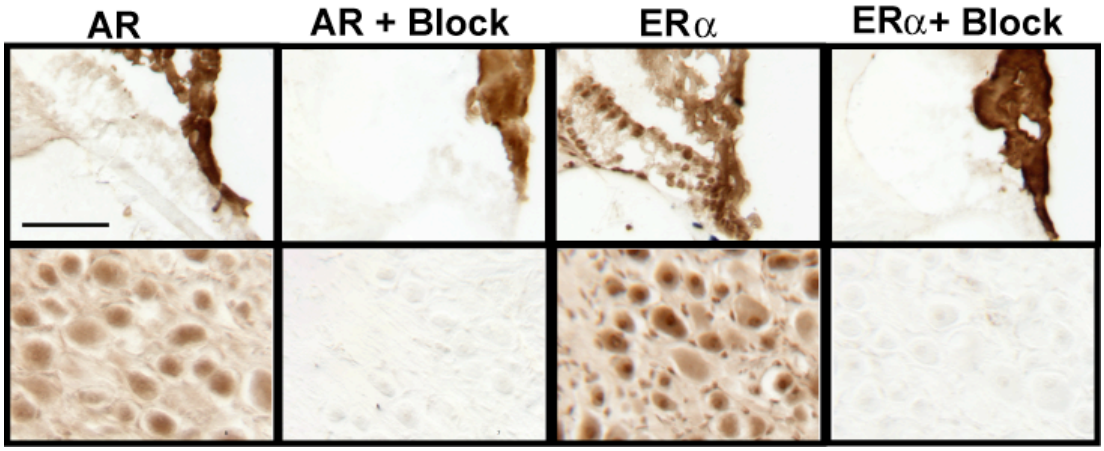

Figure 1.2. ER and AR expression in the inner ear of GWCS. Hair cells and support cells (top row) and spiral ganglion cells (bottom row) of non-breeding male GWCS express at least one subtype of ER, ERα. AR is not expressed in hair cells or support cells, but is expressed in spiral ganglion cells. Staining was appropriately blocked when antibody serum was pre-incubated with the antigenic peptide. A similar pattern of expression is observed in female GWCS. Expression patterns were detected using antibody labeling and visualized using DAB staining. Scale bar = 50 μm. Image provided by Yuan Wang.

Chapter 2. Peripheral auditory processing changes seasonally in Gambel's white-crowned sparrow

2.1 Summary

Song in oscine birds is a learned behavior that plays important roles in breeding. Pronounced seasonal differences in song behavior, and in the morphology and physiology of the neural circuit underlying song production are well documented in many songbird species. Androgenic and estrogenic hormones largely mediate these seasonal changes. While much work has focused on the hormonal mechanisms underlying seasonal plasticity in songbird vocal production, relatively little work has investigated seasonal and hormonal effects on songbird auditory processing, particularly at a peripheral level. We addressed this issue in Gambel's white-crowned sparrow (*Zonotrichia leucophrys gambelii*), a highly seasonal breeder. Photoperiod and hormone levels were manipulated in the laboratory to simulate natural breeding and non-breeding conditions. Peripheral auditory function was assessed by measuring the auditory brainstem response (ABR) and distortion product otoacoustic emissions (DPOAEs) of males and females in both conditions. Birds exposed to breeding-like conditions demonstrated elevated thresholds and prolonged peak latencies compared with birds housed under non-breeding-like conditions. There were no changes in DPOAEs, however, which indicates that the seasonal differences in ABRs do not arise from changes in hair cell function. These results suggest that seasons and hormones impact auditory processing as well as vocal production in wild songbirds.

2.2 Introduction

Seasons and hormones play an important role in coordinating the breeding activity of many animals. In songbirds, song is important in mate attraction and territorial defense. During the breeding season, songs are typically produced more often, are longer, and are more stereotyped in structure than during the rest of the year (Brenowitz, 2008). Morphological and physiological changes occur in the underlying song control circuitry (Brenowitz, 2008). During the breeding season, some song nuclei are larger (Nottebohm, 1981; Brenowitz, 1991; Brenowitz et al., 1998) and fire spontaneously at a higher rate (Park et al., 2005; Meitzen et al., 2007b). These seasonal differences in song behavior and neural circuitry are primarily regulated by the sex steroid hormones testosterone and estrogen (Marler et al., 1988; Tramontin et al., 2003; Soma et al., 2004; Meitzen et al., 2007a).

Many studies have used songbirds as model system for examining the effects of seasons and hormones on vocal production (Brenowitz, 2008), but relatively few studies have investigated seasonal and hormonal influences on songbird auditory processing. Seasonal changes in auditory processing have been reported for other animals. Seasonal changes in frequency tuning and temporal response properties have been found in the midbrain inferior colliculus of Northern leopard frogs (Goense and Feng, 2005). In female green tree frogs (*Hyla cinerea*), testosterone increases midbrain multiunit thresholds to pure tones that lie within the range of the male advertisement calls (Miranda and Wilczynski, 2009b), and females that have mated show frequency-specific, decreased multiunit response strength to noise bursts (Miranda and Wilczynski, 2009a). Recordings from auditory nerve afferents in female midshipman fish

(*Porichthys notatus*) demonstrate more precise phase locking during the breeding season, and this auditory phenotype can be induced in non-reproductive fish by administering testosterone or 17β-estradiol (Sisneros and Bass, 2003; Sisneros et al., 2004). Both sex-specific and seasonal differences have been found in click-evoked otoacoustic emissions of Rhesus monkeys (McFadden et al., 2006; McFadden, 2009).

Behavioral, physiological and morphological observations raise the possibility that seasons and hormones also affect auditory processing in songbirds. Male and female zebra finches housed on a long-day photoperiod learned an operant song discrimination paradigm faster than those housed on a short-day photoperiod (Cynx and Nottebohm, 1992a), suggesting that day length may influence song perception (though the effect simply may instead reflect seasonal differences in activity or motivation). Similarly, some evidence suggests that estrogen treatment modulates the song-elicited behavioral responses of female birds (Vyas et al., 2009). There are several reports of seasonal and/or hormonal effects on physiological processing in forebrain areas known to respond to auditory stimuli. For instance, the spontaneous electrophysiological profile of neurons in the song nucleus HVC varies as a function of season in male and female canaries (Del Negro and Edeline, 2002) and Del Negro and colleagues reported that photoperiod and breeding condition affected song selective neural responses in HVC (Del Negro et al., 2000, 2005). Similar effects were found on both passive and active electrophysiological properties of neurons in the white-crowned sparrow robust nucleus of the arcopallium, but the electrical properties of HVC neurons were stable across seasons (Meitzen et al., 2009a). Seasonal effects may also exist in the caudomedial nidopallium (NCM), a forebrain auditory region (Terleph et al., 2008).

Estradiol increases evoked activity in NCM (Tremere et al., 2009), and modulates song-induced expression of the immediate early gene egr-1 in several auditory nuclei (Maney et al., 2006; Sanford et al., 2009). Additionally, a recent study using diffusor tensor imaging suggests that the volume of NCM is larger in breeding-condition European starlings (*Sturnus vulgaris*) (De Groof et al., 2009).

Most of this literature has focused on seasonal changes in auditory function in the forebrain. Seasonal cues, however, may also influence auditory processing at the peripheral level. Seasonal changes at the periphery may be conserved throughout the auditory pathway, giving rise to the seasonal effects observed in higher processing centers. In this respect, it is interesting to note that expression of the alpha subtype of the estrogen receptor (ERα), and aromatase (which catalyzes the synthesis of estrogen from testosterone), were recently reported in the inner ear of zebra finches (Noirot et al., 2009). We have also observed ERα in hair cells and support cells and both ERα and the androgen receptor (AR) in ganglion cells of the inner ear of young chickens and adult white-crowned sparrows (Wang, Brenowitz, Rubel, McCullar, and Oesterle unpublished observations). Lucas and colleagues examined seasonal changes in the amplitude and latencies of evoked responses in six different species of birds (Lucas et al., 2002, 2007). Their data suggest that the effect of seasonal cues differs between species, but these authors only measured threshold sensitivity in one species (House sparrow, *Passer domesticus*). Those results were inconclusive, however, due to inadequate sample sizes (Henry and Lucas, 2009).

Our study addresses the issue of whether hormonal and photoperiod manipulations that mimic the breeding and non-breeding season affect peripheral auditory processing in Gambel's white-crowned sparrow (*Zonotrichia leucophrys gambelii*), a migratory species with highly seasonal breeding. Auditory brainstem response (ABR) and distortion product otoacoustic emission (DPOAE) recordings were used as a measure of peripheral auditory processing.

The ABR is a short-latency neural response typically emitted 10-15 msec after the presentation of an auditory stimulus (Hall, 1992). ABR recording has a long history of use as a diagnostic measure of peripheral and brainstem auditory function in humans and animals (Jewett et al., 1970; Achor and Starr, 1980; Despland and Galambos, 1980; Liberman et al., 2006), and this method has been used to assess avian auditory function (Corwin et al., 1982; Brown-Borg et al., 1987; Burkard et al., 1994; Woolley et al., 2001; Brittan-Powell et al., 2002; Lucas et al., 2002).

Otoacoustic emissions are low-intensity sounds generated by the compressively nonlinear cochlear amplification process of the inner ear (Kemp, 1978; Probst et al., 1991; Kemp, 2002). In mammals, it is thought that the outer hair cells of the cochlea produce the amplification responsible for emission generation (Dallos, 2008; Dallos et al., 2008). Although the exact cellular origin of otoacoustic emission production in non-mammalian vertebrates is currently unknown (Bergevin et al., 2008), DPOAEs can still be effectively used as an indicator of avian inner ear function (Kettembeil et al., 1995; Bergevin et al., 2008).

We report that ABR thresholds were elevated and ABR peak latencies were prolonged in breeding birds, whereas DPOAE amplitudes and thresholds were not affected. Our results show a seasonal effect on auditory thresholds, and suggest that the effect originates post-synaptic to the hair cells.

2.3 Methods and Materials

2.3.1 Subjects

Adult male (n=24) and female (n=24) Gambel's white-crowned sparrows (*Zonotrichia leucophrys gambelii*) were collected during autumn and spring migrations between 2006 and 2008. Most birds were captured in mist nets in eastern Washington State; a small subset were captured in Davis, California. Birds were housed in outdoor aviaries at the University of Washington for up to 30 weeks before being moved to indoor aviaries. Once inside, all birds were housed in groups on a short-day photoperiod (SD, 8-hr light: 16hr dark) for a minimum of 10 weeks to ensure sensitivity to the stimulating effects of hormones and photoperiod (i.e., photosensitive; Wingfield et al., 1979). Food and water were available *ad libitum*. All procedures were approved by the Institutional Animal Care and Use Committee at the University of Washington, Seattle.

2.3.2 Seasonal manipulations

Birds were randomly divided into two groups mimicking breeding and non-breeding conditions. To induce a non-breeding-like condition, birds were housed on a SD photoperiod as above. Birds housed on a SD photoperiod maintain regressed gonads and song nuclei and have basal

plasma sex hormone levels typical of the non-breeding season (Wingfield and Farner, 1978; Tramontin et al., 2000; Park et al., 2005; Meitzen et al., 2007b). To induce a breeding-like condition, birds were housed on a long day (LD; 20 hr light – 4 hr dark) photoperiod typical of their Alaskan breeding grounds. Additionally, these birds were implanted subcutaneously with capsules made from SILASTIC tubing (i.d. 1.0mm; o.d. 2.0mm, length 12mm; VWR, West Chester, PA) filled with crystalline testosterone (males) or estradiol (females) (Tramontin et al., 2003). Implants were rinsed in ethanol and soaked overnight in 0.1M phosphate buffered saline prior to implantation. Supplemental hormone is necessary to raise plasma hormone levels of laboratory-housed birds to physiological levels observed in breeding birds in the wild (Smith et al., 1995). Birds were housed under these conditions for three weeks; this time period is sufficient to induce full breeding-like growth of the song circuits in male white-crowned sparrows (Tramontin et al., 2000; Meitzen et al., 2009b).

2.3.3 Drugs

Birds were anesthetized with 25% urethane (6 μl/g body weight) for all recordings. Body weight (mean +/- S.E.M) was 27.6 +/- 0.64 g (males) and 27.7 +/- 0.75 g (females). The total drug volume was divided evenly into three intramuscular injections separated by 30 minutes. Additional doses (0.67 μl/g) were delivered as necessary to maintain anesthetic state as assessed by toe-pinch.

2.3.4 Experimental set-up

All experiments took place in an acoustically isolated chamber (Acoustic Systems, Austin, TX) between 10:30 and 15:30. We prepared each bird for ABR or DPOAE recording by removing feathers from the top of the head and surrounding the left ear. We swabbed the skin with alcohol and made a small incision at the anterior portion of the dorsal midline of the skull. The skin was retracted and fascia was removed. We cleaned and dried the skull with alcohol and glued a custom-made metal post to the head. The post was securely mounted on a magnetic stand to prevent head movement. We placed the bird on an electric heating pad and maintained the body temperature at 40-42 ^{o}C using a cloacal thermal probe and digital controller (TC-1000 Temperature Controller, CWE Inc., Ardmore, PA). For a subset of birds, we placed subcutaneous needle electrodes in the left wing and right leg to monitor electrocardiogram activity throughout the experiment. An electrode in the left leg served as a single-point ground for both the electrocardiogram (when recorded) and the ABR recordings described below. We amplified electrocardiogram signals 1000x (Grass Technologies P15, West Warwick, RI), band-pass filtered them at 100-1000 Hz and displayed them on a digital oscilloscope. The output of a small speaker (Etymotics ER-2B, Elk Grove Village, IL) and microphone (Etymotics ER-10B, Elk Grove Village, IL) were enclosed within a custom-made sound delivery tube affixed to a micromanipulator. We positioned the tube flush against the skull surrounding the left external auditory meatus, and sealed it with petroleum jelly, creating a closed sound delivery system.

At the beginning of each recording session, we calibrated dB SPL values (re: 20 μPa) on-line using a custom written software program. Click stimuli were presented in dB peak equivalent

(pe) SPL. Unless otherwise noted, all pure tones were 10 msec in duration with 2 msec rise-fall times. Clicks were 0.1 msec in duration. We presented all stimuli with alternating polarity. We generated sound stimuli using custom software and delivered them one of two ways. We routed some stimuli through a Delta-44 digital/analog converter (M-Audio, Irwindale, CA), fed them through a PA5 programmable attenuator (Tucker Davis Technologies, Alachua, FL) and delivered them directly to the speaker. We routed the remaining stimuli through an RX6 (Tucker Davis Technologies, Alachua, FL) multifunction processor that performed both digital/analogue conversion and attenuation of the signal before delivery to the speaker.

2.3.5 ABR recording

We recorded ABRs using standard subcutaneous needle electrodes. We placed the positive electrode at the vertex of the skull and positioned the reference electrode just dorsal to the (sound stimulated) external auditory meatus. We pre-amplified responses 100x (Grass Technologies P15 amplifier, West Warwick, RI), ran them through a MA3 amplifier with an additional 50 dB post-preamp gain (Tucker Davis, Technologies, Alachua, FL), band pass filtered them from 300-3000 Hz with a 24dB/octave roll-off (Krohn-Hite filter model 3550, Brockton, MA), fed them through a digital oscilloscope and audio monitor, digitized them at a rate of 24.400 kHz, and recorded them using a custom written software program. We sampled responses for a 20 msec window (with a 2 msec stimulus onset delay) or a 30 msec window (with a 10 msec stimulus delay). We used ABR recording in four different paradigms, each of which explored a different aspect of auditory processing. The rationale and methodological details for each paradigm are described below.

2.3.5.1 Minimum audibility paradigm

We used a total of 17 females (8 non-breeding, 9 breeding) and 24 males (13 non-breeding, 11 breeding) in this paradigm. A subset of these birds also participated in other ABR paradigms and/or DPOAE recording. One non-breeding female was housed in a rooftop aviary up until the day of recording in mid November, and was therefore exposed to day length changes natural to Washington State. Data from this female fell within the range of data from non-breeding females that were housed indoors, so we included them in the subsequent analysis.

The purpose of this experiment was to determine if breeding condition affects basic ABR parameters (i.e. thresholds and response latencies). We tested seven different frequencies (0.5, 1, 2, 3, 4, 6, 8 kHz) within the hearing range of most songbirds, and completely encompassing the spectrum of white-crowned sparrow song (Dooling et al. 2000; Meitzen et al. 2009b). We presented each stimulus at a rate of 19.6/sec starting at 70 dB SPL and decreased the amplitude in 10 dB steps; at or near threshold, we switched to 5 dB intervals. We averaged responses to suprathreshold stimuli across 500 stimulus presentations; for responses at or near threshold, we averaged across 1000 stimulus presentations and recorded the ABR at least twice to determine repeatability. We randomized stimulus presentation order for each subject.

We analyzed all ABR responses offline using custom written software. We defined threshold as the lowest intensity stimulus to elicit a repeatable, visually discernible response of any ABR wave within 10 msec of stimulus onset. To verify threshold estimates, we took two approaches. First, we gave a blind observer trained in audiology a subset (10%) of responses that represented

all stimuli and conditions tested. We instructed the observer to estimate the threshold visually, using any ABR wave readily observable. Threshold estimates by one of us (MLC) and the blind observer were highly correlated (Pearson's Correlation coefficient r = 0.989, $p < 0.01$, Supplementary Figure 2.1a in Appendix 2.1). Second, we used a quantitative approach to estimate threshold for the same subset of data. For this approach, a custom written software program automatically detected the largest peak-to-peak voltage difference in a 10 msec window after stimulus onset. Offline, we calculated the maximum peak-to-peak voltage + 2 standard deviations in the pre-stimulus window. Threshold was defined as the lowest stimulus intensity tested that elicited a post-stimulus measurement greater than the pre-stimulus measurement. Quantitative and visually estimated thresholds were significantly correlated (Pearson's r = 0.941 p <0.0001, Supplementary Figure 2.1b in Appendix 2.1). We conclude that visually-determined thresholds are valid, representative estimates of auditory sensitivity and therefore present only these data for the remainder of this report.

We determined latency values from the time of stimulus onset for the first two positive peaks numbered sequentially with Arabic numerals as in Brittan-Powell et al. (2005). We generated latency input/output (I/O) functions for each subject and compared latencies across subjects at an iso-intensity level (70 dB SPL). Because many factors can independently affect ABR amplitude measurements (such as head size and electrode placement), we did not compare them in this study.

2.3.5.2 Forward masking frequency resolution paradigm

Because findings from the minimum audibility paradigm suggested that seasonal and hormonal effects on auditory processing are similar in male and female white-crowned sparrows (see Results section below), we only used males for the additional ABR paradigms described below. We used a total of 11 males (5 non-breeding, 6 breeding) in this experiment. All of these males also participated in the other ABR paradigms.

Breeding condition may affect aspects of auditory processing that are independent of ABR thresholds and wave peak latencies. To determine which other auditory processing parameters were worth closely investigating, we examined the structure of the white-crowned sparrow song. Males produce a single song type, consisting of five syllables: a whistle, a warble, and three buzzes (DeWolfe et al., 1974; Meitzen et al. 2009b, Fig. 2.1). The introductory whistle is a pure tone, the frequency of which does not change seasonally (Meitzen et al., 2009b); many studies suggest that it plays a particularly important role in song identification and learning (Baptista and Morton, 1981; Margoliash, 1983; Soha and Marle,r 2000). These findings led us to hypothesize that breeding condition may influence the ability of white-crowned sparrows to resolve the frequency of the introductory whistle.

To address this possibility, we used a forward masking paradigm to examine the effect of breeding condition on ABR-derived frequency tuning curves. We set a 10 msec probe tone **[**3.3 kHz, roughly equivalent to the fundamental frequency of the white-crowned sparrow whistle (Meitzen et al., 2009b)] to a fixed amplitude of 70 dB SPL. Masker stimuli (2.50, 2.70, 2.90,

3.10, 3.20, 3.25, 3.35, 3.40, 3.50, 3.70 and 3.90 kHz) were 100 msec long with 16 msec rise-fall times. We presented the masker after a 10 msec onset delay (to allow for baseline noise capture). The onset of the probe tone occurred 10 msec after the offset of the masker (Fig. 2.2a). We presented each masker-probe combination at a rate of 6.2/sec. We captured the elicited ABR during a 140 msec recording window and averaged it across 500 masker-probe presentations.

At the beginning of each recording, we presented the probe tone alone at 70 dB SPL, which was approximately 20-40 dB above threshold for every subject. We calculated the maximum peak-to-peak voltage difference of the ABR response online for a 10 msec measurement window (starting at the time of probe onset). After obtaining this baseline response amplitude, we began masker-probe trials. In each trial, we presented the masker at an initial amplitude of 40 dB SPL and gradually raised the amplitude by 10 dB steps. We defined threshold as the masker level necessary to reduce the maximum peak-to-peak voltage in the 10 msec measurement window by 50% or more. We verified threshold by repeating the masker-probe presentation. If two out of three repetitions failed to verify the threshold estimation, we raised the masker amplitude by 5 dB until a new threshold was verified. We randomized the order of masker frequency presentations for each subject.

We generated tuning curves offline for each subject and used the quality factor (Q_{10}) as indicator of sharpness of tuning. Q_{10} is calculated as the signal (probe) frequency divided by the bandwidth of the tuning curve at 10 dB above the tip. Larger Q values indicate sharper tuning.

2.3.5.3 Forward masking temporal adaptation paradigm

We used a total of 11 males (5 non-breeding, 6 breeding) in this paradigm. All of these males also participated in the other ABR paradigms.

White-crowned sparrows exhibit seasonal changes in the duration of some song syllables and in the length of the overall song (Meitzen et al., 2009b). These findings raise the possibility that temporal processing also changes seasonally. To address this possibility, we used a forward masking paradigm to examine the effect of breeding condition on temporal adaptation capabilities. We set a 10 msec probe tone (3.3 kHz) to a fixed amplitude of 70 dB SPL as above. The masker stimulus was band-pass filtered white-noise (0.2 – 6 kHz) with a 100 msec duration and 16 msec rise-fall times. We presented the masker after a 10 msec onset delay. The onset of the probe tone occurred 5, 10, 25 or 50 msec after the offset of the masker (Fig. 2.2b). Masker-probe presentations occurred at a rate of 4.9/sec. We captured the elicited ABR during a 161 msec recording window and averaged them across 500 masker-probe presentations.

At the beginning of each recording, we presented the probe tone alone and calculated the maximum peak-to-peak voltage difference online for a 10 msec measurement window as above (starting at the time of probe onset). We then presented the masker at amplitudes of 40, 50, 60 and 70 dB SPL for each masker-probe interval. We randomized the order of masker-probe interval presentations for each subject.

We calculated the decrease of the probe-elicited ABR response amplitude for each masker amplitude and masker-probe interval as follows:

Response decrease = [(baseline amplitude - response amplitude)/baseline amplitude] x 100%

The more the response amplitude decreases, the greater the effect of the masker.

2.3.5.4 Temporal variability paradigm

We used a total of 10 males (4 non-breeding, 6 breeding) in this paradigm. All of these males also participated in the other ABR paradigms.

In addition to seasonal changes in syllable and song length, white-crowned sparrows also exhibit seasonal fluctuations in song structure variability. During the breeding season, song and syllable duration are less variable than in the non-breeding season (Meitzen et al., 2009b), suggesting that breeding condition may affect other aspects of temporal processing more directly related to temporal variability. To address this issue, we presented clicks (0.1 msec duration) at three presentation rates (19.6/sec, 30.3/sec and 23.2/sec). Rates were either fixed (such that the inter-click interval was constant) or variable (such that the inter-click interval was randomized, but the average rate over the course of all click presentations equaled 19.6/sec, 30.3/sec or 23.2/sec; see Fig. 2.2c).

We initially presented clicks at 70 dB SPL and gradually decreased the amplitude by 10 dB; at or near threshold, we switched to 5 dB intervals. We averaged responses to suprathreshold stimuli across 500 stimulus presentations; at or near threshold we averaged across 1000 stimulus

presentations and recorded the ABR at least twice to determine repeatability. We randomized the order of presentation rates for each subject. We determined thresholds visually and measured wave peak latencies offline (as described for the minimum audibility paradigm.)

2.3.6 Distortion Product Otoacoustic Emission (DPOAE) recording

Differences in auditory processing as measured by ABR recording could reflect changes in the VIIIth nerve and/or brainstem, or could reflect changes in sensory processing prior to neuronal activation at the hair cell - ganglion cell synapse (i.e. changes in the external ear canal, middle ear, or inner ear mechanics). To dissociate these possibilities, we recorded DPOAEs from 10 males (5 non-breeding, 5 breeding) and 12 females (6 non-breeding, 6 breeding). Five of the females (2 non-breeding, 3 breeding) and all of the males also participated in the ABR minimum audibility paradigm.

Sounds were delivered as described for ABR recording. Two primary tones (F1 and F2) were presented simultaneously. The frequency of F2 varied (0.5, 1.0, 1.5, 2.0, 2.5, 3.0, 3.5, 4.0, 4.5, 5.0, 5.5, 6.0, 6.5, 7.0, 7.5, 8.0, 8.5, 9.0, 9.5 kHz) but we fixed the F2/F1 ratio at 1.15. We determined this ratio value to be optimal for white-crowned sparrows during pilot studies (data not shown). We initially presented the first primary tone (F1) at an amplitude (L1) of 20 dB SPL and systematically increased the amplitude by 5 dB steps to a maximum of 90 dB SPL. The amplitude of the second primary tone (L2) was consistently 10 dB lower than L1. The cubic distortion tone, which corresponds to a frequency of 2F1-F2, is the largest distortion product

generated, and was therefore the focus of this study. The presentation order of stimulus frequencies was randomized for each subject.

We measured the amplitude (dB SPL) of the DPOAE for each tone presentation (Fig. 2.3). In addition to absolute amplitude, we estimated DPOAE thresholds for six different F2 frequencies that were also used in the ABR minimum audibility paradigm (1, 2, 3, 4, 6, and 8 kHz). We defined threshold as the lowest L1 amplitude (dB SPL) that met the following three criteria: *1*) The amplitude of the DPOAE was at least 3 dB above the immediately surrounding noise floor. *2*) The difference between L1 and DPOAE amplitudes did not exceed 85 dB. (This criterion was formed from offline determinations of instrumental and cavity distortions.) *3*) The next two DPOAE measurements (elicited by 5 and 10dB increases in L1, respectively) also fit the first two criteria.

2.3.7 Hormone Measurement

At the end of each recording session, we rapidly decapitated subjects and removed basilar papillae for histological processing for a separate study. We collected trunk blood in heparinized tubes and immediately centrifuged it. We separated the plasma and stored it at -80°C until Enzyme-Linked ImmunoSorbent Assay (ELISA). Testosterone and estradiol concentrations were measured using standard kits (Assay Designs, Ann Arbor, MI) and compared to those measured in the wild (Wingfield and Farner, 1978).

2.3.7.1 Assay Validation

We used a testosterone immunoassay kit (Assay Designs catalogue # 900-065) previously validated for the congeneric white-throated sparrow *(Zonotrichia albicollis*) (Swett and Breuner, 2008). No publications reporting the use of the estrogen kit (Assay Designs catalogue # 900-174) in any avian species were found. We therefore validated the use of this kit for white-crowned sparrows. We pooled plasma samples from multiple sparrows and stripped the plasma of steroids with dextran-coated charcoal in assay buffer (Sigma-Aldrich, St. Louis, MO). We spiked stripped plasma with estradiol to ~19.6 ng/ml and assayed a serial dilution of the spiked plasma. The serial dilution paralleled the kit's standard curve, indicating that endogenous protein elements in white-crowned plasma do not substantially interfere with hormone measurement.

2.3.7.2 Immunoassay Procedures

We followed the kit instructions to determine testosterone or estradiol levels of experimental subjects. Briefly, we added steroid displacement buffer (1% of raw plasma volume) to each plasma sample, brought the total volume to 200 μl with assay buffer and vortexed. Because LD+ testosterone conditions can generate plasma testosterone levels beyond the highest range of the kit's detectability (2 ng/ml), a 1:20 dilution of each LD+ testosterone sample was made with assay buffer. We ran 100 μl aliquots of each sample (or LD dilution) in duplicate along with either five testosterone standards (0.008 – 2.000 ng/ml) or 6 estrogen standards (.0293-30.00 ng/ml). We incubated each sample with 50 μl of steroid antibody and alkaline phosphotase-conjugated steroid, emptied and washed all sample wells and added 200 μl of substrate. After

adding the stop solution (50µl/well), we read the plate immediately on a Dynex MRX II microplate reader (Chantilly, VA) at 405 nm.

We analyzed samples from subjects tested in the DPOAE paradigm in separate assays from those tested only in the ABR paradigms. The minimum detectable plasma testosterone concentrations were 5.72×10^{-4} ng/ml (ABR tested) and 3.17×10^{-3} ng/ml (DPOAE tested); minimum estradiol concentrations were 1.91×10^{-2} ng/ml (ABR tested) and 5.15×10^{-2} ng/ml (DPOAE tested). Intra-assay variabilities for testosterone measurement were 5.99% (ABR tested) and 5.90% (DPOAE tested); intra-assay variabilities for estradiol measurement were 9.23% (ABR tested) and 7.84% (DPOAE tested). Inter-assay variabilities were 22.4% (testosterone) and 21.7% (estradiol).

One male (ABR) sample fell below the detection limit of the assay. For statistical analysis, we multiplied the detection limit (5.72×10^{-4} ng/ml) by the dilution factor of the sample in question (2.5). We used the resulting value (1.43×10^{-3} ng/ml) for subsequent analysis. One male sample was too concentrated to be detected by the assay, even after a 1:20 dilution. In this case, the concentration of the highest standard (2.0 ng/ml) was multiplied by the dilution factor (20) to give a result of 4.0 ng/ml. All female samples fell within the range of the estradiol assay; however, blood samples were lacking for two females that we used to optimize the DPOAE recording parameters.

2.3.8 Statistics

We made all comparisons with three-way or two-way mixed-model ANOVA (Sex x Breeding Condition x Stimulus Frequency/Stimulus Level) or independent samples t-test. All statistical analyses were made using PASW Statistics 18.0 for Mac (Chicago, IL). Data in all figures are presented as means +/- S.E.M.

2.4 Results

2.4.1 Plasma Hormone Levels

Male and female birds housed under breeding (LD + testosterone or LD + estradiol) conditions had significantly higher plasma testosterone or estradiol levels than those housed under non-breeding (SD) conditions. Table 2.1 shows that testosterone levels from males housed under LD + testosterone were comparable to those observed in breeding condition males in the wild (Wingfield and Farner, 1978). Estradiol levels from LD + estradiol females, however, were higher than the physiological range of wild females in breeding condition (4.919 +/- 0.726 vs 0.300-0.400 ng/ml, Wingfield and Farner, 1978).

2.4.2 ABR

2.4.2.1 Minimum audibility paradigm

ABR thresholds were significantly affected by breeding condition and stimulus frequency. Males and females had similar overall ABR thresholds (means +/- S.E.M., 51.6 +/- 0.92 vs. 53.5 +/- 1.07 dB SPL, respectively; [$F(1,35) = 0.279$, $p = 0.601$]); we therefore pooled their data for analysis. Figure 2.4 shows representative averaged responses to a 4.0 kHz tone from a non-

breeding female (2.4a) and a breeding female (2.4b). In these examples, we judged threshold to be 35 dB SPL (2.4a) and 45 dB SPL (2.4b). Figure 2.4c shows group data for thresholds to clicks and tone bursts at 0.5, 1, 2, 3, 4, 6 and 8 kHz. Stimulus frequency significantly affected threshold estimates, with birds showing maximal sensitivity to clicks and 4 kHz pure tones [$F(7,245)= 70.54$, $p < 0.001$]. Thresholds in white-crowned sparrows housed under breeding-like conditions were higher by 3.90 – 12.3 dB (average 8.23 dB) than in birds housed under non-breeding–like conditions. The effect of breeding condition was significant [$F(1,35) = 12.99$, $p = 0.001$]. No significant interactions were found between any of the independent variables (sex, stimulus frequency, or breeding condition; all $p > 0.05$).

Many ABR peak latency values were not measurable at 70 dB SPL, either because of high thresholds at the extremes of the stimulus frequencies tested (500 and 8000 Hz) or because of elevated thresholds in breeding condition birds. As a result, the missing values (11.5% of the total number of data points) were not randomly distributed among the data set (see Table 2.1 in Appendix 2.1 for more detailed information). A biased sample of missing data can confound statistical analyses and obscure interpretation of the results. Therefore, we calculated average peak latency values for each stimulus and experimental group (breeding males, non-breeding males, breeding females, and non-breeding females). Missing data points were filled in with the appropriate mean values and the completed dataset was analyzed by ANOVA, as above. ABR peak latencies were significantly affected by breeding condition and stimulus frequency. Males and females had similar latency values for peak 1 (mean +/- S.E.M., 2.28 +/- 0.02 vs. 2.34 +/- 0.03 msec, respectively) and peak 2 (3.55 +/- 0.031 vs. 3.65 +/- 0.04 msec). The effect of sex

was not significant (peak 1 [F (1,35) = 0.694, p = 0.411]; peak 2 [F(1,37) = 0.887, p = 0.353] we therefore pooled their data for analysis. Figure 2.5a shows representative ABR traces from a breeding and non-breeding female overlaid. Peak latencies from the breeding bird were delayed relative to the non-breeding bird. Group data for peak latencies generated by 70 dB SPL clicks and pure tone bursts are shown in figure 2.5b-c. Latency values depended on stimulus frequency, with clicks evoking the lowest values. The effect of frequency was highly significant for both peak 1 [F(7,259) = 63.40, p < 0.001] and peak 2 [F(7,259) = 31.52, p < 0.001]. The differences between breeding and non-breeding peak 1 latencies ranged from 0.135-0.349 msec (average 0.233 msec); peak 2 latencies differed by more (range 0.286-0.513 msec, average 0.378 msec). The effect of breeding condition was statistically significant across all stimuli tested (peak 1; [F (1,37) = 18.94, p < 0.001]; peak 2 [F(1,37) = 26.06, p < 0.001]). A significant interaction between stimulus frequency and sex was observed for peak 1 latency values [F(7,259) = 2.846, p = 0.007]; no other interactions were found (all p > 0.05).

Breeding condition also affected inter-peak intervals (Fig. 2.5d). Males and females had similar inter-peak intervals (mean +/- S.E.M.; 1.28 +/- 0.02 msec vs. 1.31 +/- 0.02 msec, respectively). The effect of sex was not significant [F(1,37) = 0.557, p = 0.460]; we again pooled their data for analysis. Birds in breeding condition had longer inter-peak intervals than birds in non-breeding condition. These differences ranged from 0.067-0.256 msec (average 0.146 msec) and were statistically significant [F(1,37) = 17.09, p < 0.001]. While stimulus frequency did not affect inter-peak intervals independently [F(7,259) = 1.681, p = 0.114], a significant interaction was

found between all three independent variables (stimulus frequency, breeding condition and sex), [$F(7,259) = 2.747$, $p = 0.009$].

These data suggest that seasons and hormones affect peripheral auditory sensitivity. One possible concern was that these findings reflected group differences in baseline noise levels, rather than differences in sensory processing, *per se*. High baseline noise levels could cause difficulty in the extraction of responses at low stimulus amplitudes, leading to higher threshold estimates. To examine this possibility, we calculated the root mean square deviation (RMSD) of the voltage values during the first two msec of the pre-stimulus window for each response. A large RMSD value indicates greater variability in the pre-stimulus window, reflecting a higher baseline noise level. We averaged RMSD values across all responses to obtain a single value for each bird. We then compared these values as a function of breeding condition.

We only used responses averaged over 1000 stimulus presentations for this analysis. We chose this selection criterion because the effect of baseline noise on threshold detection was of primary interest, and all traces at or near threshold were averaged over 1000 stimulus presentations. Birds in breeding and non-breeding condition had similar RMSD values (mean +/- S.E.M., 0.077 +/- 0.025 μV vs. 0.073 +/- 0.022 μV, respectively) that did not differ statistically [$F(1,37) = 0.093$, $p = 0.762$]). The results of this analysis suggest that seasonal and hormonal differences in ABR thresholds and latencies and reflect differences in auditory sensitivity at the level of the inner ear and/or central nervous system.

2.4.2.2 Forward masking frequency resolution paradigm

Breeding condition did not affect frequency tuning. Figure 2.6a shows averaged frequency tuning curves from breeding males and non-breeding males. The curves show substantial overlap at all masker frequencies tested and did not differ statistically [F (1,9) = 0.057, p = 0.817]. We calculated and compared Q_{10} values for each subject to determine whether tuning sharpness varied as a function of breeding condition. Average Q_{10} values are shown in figure 2.6b. Breeding males and non-breeding males had similar Q_{10} values (means +/- S.E.M.; breeding 4.70 +/- 0.54; non-breeding 5.21 +/- 0.84). A two-sample t-test revealed no significant difference between the groups [t = 2.447, p = 0.651].

2.4.2.3 Forward masking temporal processing paradigm

Breeding condition did not affect temporal adaptation. Figures 2.7a-d show the percent decrease of the probe response as a function of masker level (40, 50, 60 and 70 dB SPL) for four different masker-probe intervals (5, 10, 25 and 50 msec). Response amplitudes of breeding males and non-breeding males decrease by similar amounts across all masker levels for 5, 10, and 25 msec masker-probe intervals (Fig. 2.7a-c). Separate two-way ANOVAs revealed no effect of breeding condition for these three intervals (all $p > 0.4$). At the longest masker-probe interval, however, breeding condition did affect the amount by which response amplitudes decreased (Fig. 2.7d). Response amplitudes of males in breeding condition decreased an average of 5.84% more than males in non-breeding condition when the masker and probe were separated by 50 msec. This difference was significant [F(1,8) = 6.867, p = 0.031].

2.4.2.4 Temporal variability paradigm

Breeding condition did not affect processing of temporally variable stimuli. Figure 2.8a-c shows the peak 1, peak 2, and inter-peak latencies, respectively, as a function of click rate. Fixed and variable rates elicited similar latencies from breeding and non-breeding males. Separate two-way ANOVAs revealed no effect of temporal variability on peak 1, peak 2 or inter-peak latencies (all $p > 0.2$).

As expected from the latency analyses presented above, breeding males showed a trend of longer peak latencies and inter-peak intervals than non-breeding males. These differences did not reach significance, however, probably due to small sample sizes (n = 4-6).

2.4.3 DPOAE

The results from the ABR study indicated that breeding condition affects auditory sensitivity. To determine whether the effect could be explained by processing changes at levels prior to synaptic responses, DPOAEs were elicited by a range of frequencies (1 – 9.5 kHz) from males and females in breeding and non-breeding conditions.

Breeding condition and sex did not affect iso-intensity DPOAE amplitudes. DPOAE amplitudes of males and females were similar overall, and did not differ significantly [$F(1,15) = 1.181$, $p > 0.20$]; we therefore pooled their data for analysis. Figure 2.9a shows DPOAE amplitudes as a function of the second primary (F2) frequency. These DPOAEs were elicited while L1 was held constant at 70 dB SPL. DPOAE amplitudes depended on primary tone frequency, with mid to

high frequencies eliciting the largest DPOAEs. The effect of frequency was significant [$F(17,255) = 17.95$, $p < 0.001$]. DPOAE amplitudes were similar for birds in breeding and non-breeding conditions across all frequencies (mean +/- S.E.M.-9.12 +/- 0.82 vs. 8.17 +/- 0.83 dB SPL) and did not differ statistically [$F(1,15) = 0.009$, $p = 0.927$]. No significant interactions were observed (all $p > 0.05$).

While breeding condition did not affect iso-intensity DPOAE amplitudes, it was possible that seasons/hormones affected amplitudes across the dynamic range of stimulus levels. Figure 2.9b shows DPOAE amplitudes as a function of the level of the first primary tone (L1). These DPOAEs were elicited while F2 was held constant at 7 kHz. This F2 value was chosen because it elicited relatively strong DPOAE amplitudes at 70 dB (see Fig. 2.9a). DPOAE amplitudes were similar for males and females across stimulus levels [$F(1,15) = 2.35$, $p = 0.146$); we again pooled their data for analysis. DPOAE amplitudes increased with higher stimulus levels; this effect was significant [$F(14,210) = 141.8$, $p < 0.001$]). DPOAE amplitudes were similar, however, for birds in breeding and non-breeding conditions across all stimulus levels [$F(1,15) = 2.62$, $p = 0.127$)]. No significant interactions were observed (all $p > 0.2$).

While DPOAE thresholds depend on DPOAE amplitudes, other factors can affect threshold independently, such as the level of the noise floor. This fact raised the possibility that breeding condition affected DPOAE thresholds without directly affecting DPOAE absolute amplitude measurements. To address this issue, DPOAE thresholds were measured for six F2 frequencies that were also used in the ABR minimum audibility paradigm (1, 2, 3, 4, 6 and 8kHz). Figure

2.9c shows DPOAE threshold as a function of F2 frequency. Again, males and females had similar threshold values (51.9 +/- 2.89 vs. 60.2+/- 3.07 dB SPL; mean +/- S.E.M.) that did not differ statistically [$p > 0.20$] and we pooled their data for analysis. In general, the frequencies that elicited that highest amplitude DPOAEs (6-8 kHz) also elicited the lowest thresholds. The effect of stimulus frequency was significant [$F(5, 85) = 15.29$, $p < 0.001$]. Threshold values of birds in breeding condition and non-breeding condition were similar (mean +/- S.E.M., 58.1 +/- 3.18 vs. 54.9 +/- 2.92 dB SPL) and did not differ statistically, [$F(1,17) = 0.092$, $p = 0.77$)].

2.4.4 Summary of results

To summarize, we found that birds housed under breeding-like laboratory conditions had higher ABR thresholds, longer peak latencies, and increased inter-peak intervals. As measured by ABR methods, temporal processing and frequency tuning were unaffected by breeding state. In addition, otoacoustic emissions appeared to be unaffected by breeding state.

2.5 Discussion

The main purpose of this study was to determine whether breeding condition affects auditory processing at the level of the inner ear and brainstem pathways in a highly seasonal songbird. A robust effect of breeding condition was found. Birds exposed to breeding-like conditions had higher ABR thresholds, longer peak latencies, and longer inter-peak intervals than birds housed under non-breeding-like conditions. No measurable effects were found for ABR analyses of frequency resolution or temporal adaptation or for more peripheral measures of auditory function (otoacoustic emissions).

One important note is that while males in this study demonstrated testosterone levels comparable to male white-crowned sparrows free living in the wild, females had much higher estradiol levels than free living birds, even when housed under non-breeding conditions. While the exogenous treatment can account for the high estradiol levels in the breeding condition females, the underlying cause of elevated estradiol in non-breeding females remains unclear. It is possible that the ELISA kit used to measure estradiol levels detected endogenous estrogen-like compounds in the white-crowned sparrow plasma, giving artificially high measurements, though this explanation seems unlikely given that stripped and spiked white-crowned sparrow plasma dilutions paralleled the kit's standard curves. Alternatively, the social environment of the non-breeding females may have been a contributing factor. It is known that experimentally elevating hormone levels in female white-crowned sparrows can increase the hormone levels of their mates (Moore, 1982). Many of the non-breeding females in this study were housed in single sex aviaries before experimentation, and unidentified social or endocrine cues may have elevated estradiol levels in these birds. (It should be noted, however, that birds in single-sex aviaries always had full visual and auditory contact with members of the opposite sex.) Though the effect of social interactions between females on their hormone levels has not been addressed in birds, effects of this type have been documented in other taxa (McClintock, 1971). These reports, however, are controversial (see Schank, 2001). It is important to recognize, however, that even though we cannot explain the high estradiol levels measured in this study, our experimental groups did show large relative differences in estradiol levels (~4X higher in breeding vs. non-breeding conditions).

2.5.1 Breeding condition affects ABR thresholds

Both male and female white-crowned sparrows showed significantly higher ABR thresholds when housed under breeding-like conditions than under non-breeding like conditions. On average, this difference amounted to about 8 - 10 dB, a substantial amount given that a 10 dB amplitude increase is perceived as twice as loud by humans (Stevens and Poulton, 1956). We were careful to verify ABR threshold estimates in several ways. First, visually estimated thresholds showed strong correlations with both blind observer and quantitative estimates. Second, though ABR threshold estimates are approximately 10- 30 dB less sensitive than behavioral estimates (Borg and Engstrom, 1983; Brittan-Powell et al., 2002), the audiograms presented here are similar in shape to behavioral audiograms from song sparrows (*Melospiza melodia*) and swamp sparrows (*Melospiza Georgiana*) (Okanoya and Dooling, 1988). Third, RMSD analysis demonstrated that group differences in threshold estimates could not be attributed solely to differences in baseline noise levels. Last, given the fact that there are numerous reports in the literature of absolute peak latency delays as a function of hearing loss (Coats and Martin, 1977; Coats, 1978; Jerger and Mauldin, 1978; Rosenhamer et al., 1981), the fact that breeding condition birds demonstrated both elevated thresholds and prolonged peak latencies for all stimuli tested supports the validity of the threshold differences observed.

The results reported here differ from those of a previous study that showed no effect of season on ABR thresholds or latencies (Henry and Lucas, 2009). The discrepancy between the studies may result from a number of different factors. First, Henry and Lucas used house sparrows (*Passer domesticus*), a species that shows much less pronounced seasonal breeding (Nehls, 1981) than

does the Gambel's subspecies of white-crowned sparrow used in our study. Second, the birds in the Lucas study were divided into three different groups for seasonal comparisons (those caught in March-May, June-July and Sep-Nov). It is well known, however, that the seasonal fluctuations in hormone levels are not synchronous within the individuals in a population. Therefore, such comparisons are more robust when subjects are selected on the basis of their hormonal and breeding state, rather than by calendar date (Wingfield and Farner, 1978). It is possible that if Henry and Lucas had measured plasma hormone levels and examined their data on the basis of that comparison, they might have observed effects similar to those reported here.

The results of our study also differ from the published literature in another important way. Previous work has demonstrated seasonal differences in auditory processing in other taxa, including both frogs and fish (Goense and Feng, 2005; Miranda and Wilczynski, 2009a; Sisneros, 2009a). In all of these cases, sensitivity or frequency tuning has shifted in a direction that enhances reception of mating calls or vocalizations during breeding conditions. These findings led to the *a priori* hypothesis that white-crowned sparrows in breeding condition would have greater auditory sensitivity than birds in non-breeding condition. Surprisingly, the results here demonstrate the opposite of what was expected; sparrows in non-breeding condition have greater auditory sensitivity than birds in breeding condition. The possible behavioral significance and adaptive value of these findings are discussed below.

2.5.2 Breeding condition affects ABR latencies

Both absolute and inter-peak latencies were prolonged in breeding condition white-crowned sparrows. Studies of humans and other mammals suggest that the first peak of the ABR reflects activity of the auditory nerve (Sohmer et al., 1974; Buchwald and Huang, 1975; Starr and Hamilton, 1976; Achor and Starr, 1980; Moller et al., 1981; Moller and Jannetta, 1983). Similar wave 1 latencies have been reported for both mammalian (Buchwald and Huang, 1975; Achor and Starr, 1980; Katayama, 1985) and avian species (present data; Burkard et al., 1996; Brittan-Powell et al., 2002; Brittan-Powell et al., 2005), suggesting that the wave 1 generator is the same for both animal classes. Additionally, Brittan-Powell and Dooling (2002) demonstrated that wave 1 of the ABR corresponds to the first deflection of the compound action potential in budgerigars (*Melopsittacus undulatus*); this finding supports the notion that wave 1 of the avian ABR reflects activity of the auditory nerve. The breeding condition increase in white-crowned sparrow wave 1 latencies therefore suggests a hormonal effect that originates early in the auditory pathway.

The generator of wave 2 is less clear. Intracranial recordings, clinical evidence and estimates of conduction times and synaptic delays suggest that wave 2 of the human ABR reflects processing in the proximal portion of the auditory nerve (Moller and Jannetta, 1981,1983; Hall, 2007). The lack of such studies in birds and the dramatic difference in length of the auditory nerve axons in humans (25 mm, Hall 2007) and songbirds (1-3 mm, personal communication- E.W. Rubel), however, suggests that this conclusion does not necessarily apply to avian species. Additionally confounding is the fact that previous studies have suggested that components of wave 2 of the

avian ABR actually correspond to wave 3 of the human ABR (Katayama, 1985; Brittan-Powell et al., 2002; Hall, 2007), which is thought to have multiple brainstem generators (Hall 2007).

Though no conclusive statement can be made about the location of the wave 2 generator(s) in this study, much can still be learned from the effect of breeding condition on the wave 2 latency. In particular, wave 2 latency values increased more than wave 1 latencies in breeding condition birds, leading to a significant difference in inter-peak intervals. Inter-wave latencies reflect signal conduction times along the auditory pathway (Ponton et al., 1996). Longer inter-wave latencies therefore suggest that axonal conduction velocity and/or synaptic transmission is slower in breeding condition white-crowned sparrows. Possible mechanisms to explain these findings are discussed below.

2.5.3 Effect of acoustic stimulation on breeding condition differences

Breeding condition male birds, including white-crowned sparrows, sing at higher rates than non-breeding males (Catchpole and Slater, 1995; Meitzen et al., 2009b). Birds in different breeding conditions in our study were held in separate rooms, leading to the possibility that breeding birds were more acoustically stimulated than non-breeding birds and that this extra stimulation contributed to their lower auditory sensitivity. While we did not formally measure the differences in singing and calling rates between breeding and non-breeding birds during housing, breeding females were often housed in a room with no males. Wild female white-crowned sparrows rarely sing without testosterone stimulation, and almost never do so in captivity (Baptista and Petrinovich, 1986). (Indeed, the two authors who work with white-crowned sparrows routinely

(EB and MLC) have never observed a captive female sing under either breeding or non-breeding conditions). Therefore, breeding condition females that were housed without males would be *less* acoustically stimulated than their non-breeding counterparts that were housed in rooms with many males. Conversely, we would expect breeding condition males to be *more* stimulated than their non-breeding counterparts. As similar ABR findings were observed for males and females, it is unlikely that differences in acoustic stimulation can explain the differences in auditory sensitivity reported in this study.

2.5.4 Cellular origins of breeding condition differences

Increased ABR thresholds and prolonged wave 1 latencies in breeding condition white-crowned sparrows initially raised the possibility that seasons and hormones act on the hair cells or other auditory processing components presynaptic to the auditory nerve afferents. Others have suggested similar models (Sisneros et al., 2004; Henry and Lucas, 2009), and hair cells presented themselves as interesting candidates because of their known expression of hormone receptors in numerous species (Stenberg et al., 1999; Stenberg et al., 2001; Sisneros et al., 2004; Hultcrantz et al., 2006; Noirot et al., 2009). The distortion product otoacoustic emission (DPOAE) analyses, however, do not support the idea of a functional change at the hair cell level. DPOAEs, like other types of otoacoustic emissions, are indices of cochlear function and are now widely used in clinical diagnostic settings (Harris, 1990; Pak et al., 2000; Akdogan and Ozkan, 2006). Changes in DPOAE thresholds and input-output functions are reliable and valid indicators of changes in auditory sensitivity (Lonsbury-Martin et al., 1991; Kemp, 2002). If preneural changes in auditory function were responsible for the elevated ABR thresholds and increased peak 1 latencies found

in breeding condition birds, one would expect to find to decreased DPOAE amplitudes and/or increased DPOAE thresholds. No measurable effect of breeding condition was found for DPOAEs recorded from male or female birds, suggesting that the functional change does not occur peripheral to the hair cell-auditory nerve synapse. It is important to note, however, that the site of hormone action and the site of the functional change are not necessarily the same. For example, steroid hormones have been implicated in the regulation of synaptic signaling (Mitsushima et al., 2009), leading to the possibility that hormones act on hair cells to modulate neurotransmitter release at the hair cell-auditory nerve synapse. Similarly, elevated aromatase expression or activity in the auditory hair cells of breeding condition birds may contribute to functional changes at the level of the auditory nerve, an idea discussed more fully below.

Steroid hormones are well known regulators of ionic currents and neurotransmitter receptor expression (McEwen, 1991; Zakon, 1998). Hormone binding in cochlear ganglion cells or auditory nerve fibers could therefore directly affect axon conduction time and intrinsic excitability, leading to the latency and threshold differences observed here. Anatomical evidence supports this possibility. Positive staining for both ERα and ERβ has been documented in type I and II spiral ganglion cells of mice, rats and humans (Stenberg et al., 1999; Stenberg et al., 2001). Similarly, Forlano and colleagues found ERα mRNA and aromatase expression in the auditory nerve fibers of the midshipman fish (*Porichthys notatus*); aromatase was also found in the ganglion cell somata (Forlano et al., 2005). Additionally, both ERα and AR are expressed in the cochlear ganglion cells of white-crowned sparrows (Wang, Brenowitz and Rubel,

unpublished observations). The contribution of seasonal and hormonal effects on descending efferent pathways cannot be ruled out conclusively at this time, however.

Male and female white-crowned sparrows showed similar changes in auditory processing even though they were treated with two different hormones (testosterone and estradiol). Testosterone can be aromatized to estradiol *in vivo*, however, suggesting that estradiol may mediate the changes observed in both sexes. Previous research has shown that aromatase expression is elevated in breeding condition birds (Fusani et al., 2000), and aromatase activity is highest during the breeding season (Riters et al., 2001; Soma et al., 2003). Additionally, other investigators have demonstrated that testosterone treatment increases aromatase activity in the central nervous system of quails (Schumacher and Balthazart, 1986), doves (Steimer and Hutchison, 1981), canaries (Fusani et al., 2001) and possibly white-crowned sparrows (Park et al., 2005). Aromatase is expressed in the auditory hair cells of zebra finches (Noirot et al., 2009). Notably, aromatase is also expressed in the auditory nerve of two species of fish (Gelinas and Callard, 1997; Forlano et al., 2005), though it is not yet known whether this is also true for birds. These findings support the idea that estradiol production is elevated in breeding condition male white-crowned sparrows and available to bind to ERs in the cochlear ganglion cells.

It should be noted that the data presented here may partly result from steroid independent effects of photoperiod, such as seasonal regulation of aromatase or steroid receptor expression (Smith et al., 1997; Soma et al., 1999; Riters et al., 2001; Park et al., 2005). To investigate this possibility further, we looked for correlations between hormone level and ABR thresholds and latencies

(Figures 2.2 and 2.3 in Appendix 2.1). Though some of the latency measures significantly correlated with hormone levels in males, we observed no significant correlations for females, nor for ABR thresholds in either sex. These findings suggest that steroid independent effects of photoperiod may play a role in the regulation of auditory processing. One cannot necessarily rule out hormones as a causal factor, however; an alternative possibility is that after a threshold hormone concentration is reached, a physiological response occurs which then levels off when the concentration reaches a ceiling level. This model seems to explain seasonal changes in the morphology and electrical activity of neurons in the telencephalic song control nuclei (Brenowitz, 2008).

2.5.5 Behavioral Significance

We predicted that auditory thresholds would be lower in breeding condition birds than in non-breeding birds, but observed the opposite pattern. The thresholds observed in white-crowned sparrows exposed to breeding-like conditions (ranging from 25 – 90 dB SPL) are not outside the range of 'normal' thresholds of other songbirds (Dooling et al., 2000), suggesting that these findings may best be interpreted as enhanced sensitivity during the non-breeding season rather than impaired hearing during the breeding season.

One possible explanation for this finding relates to seasonal changes in vocal production. White-crowned sparrow song is known to be shorter, more variable, and less frequently produced outside the breeding season (Meitzen et al., 2009b). In addition, non-breeding song is produced at lower amplitudes (Figure 2.4 in appendix 2.1). Previous work in other avian species has indicated that song may serve as a flocking and/or roosting signal in birds that form social groups

outside the breeding season (Brenowitz, 1981). If non-breeding song plays a similar role in white-crowned sparrows, then increased auditory sensitivity may facilitate group cohesion in the non-breeding period. Future work should address this issue and other perceptual implications of seasonal/hormonal effects on auditory processing.

Note.: This work has been previously published as

Caras ML, Brenowitz E, Rubel EW (2010) Peripheral auditory processing changes seasonally in Gambel's white-crowned sparrow. J Comp Physiol A Neuroethol Sens Neural Behav Physiol 196:581-599.

2.6 Tables and Figures

Table 2.1. Plasma Testosterone and Estradiol Levels (mean +/- S.E.M. ng/ml)

	Non-breeding	Breeding	t[a]	*P*
Plasma Testosterone	0.496 +/- 0.146 (n=13)	13.95 +/- 2.970 (n=11)	2.07	<0.0001
Plasma Estradiol	1.143 +/- 0.243 (n=11)	4.919 +/- 0.726 (n=11)	2.09	<0.0001

[a]Independent samples t-test (two-tailed)

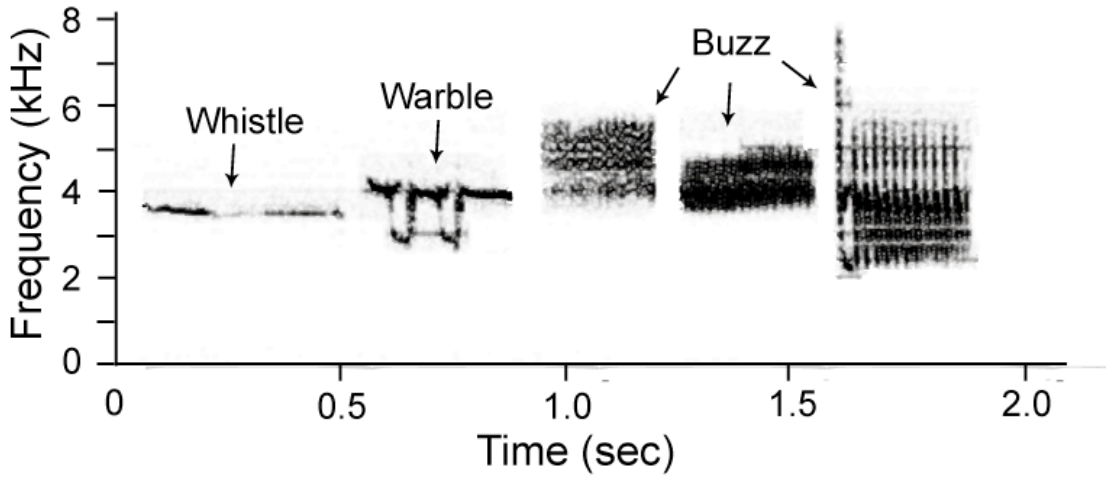

Figure 2.1. A representative white-crowned sparrow song from a breeding condition male. Songs typically consist of 5 syllables: a whistle, a warble, and 3 buzzes.

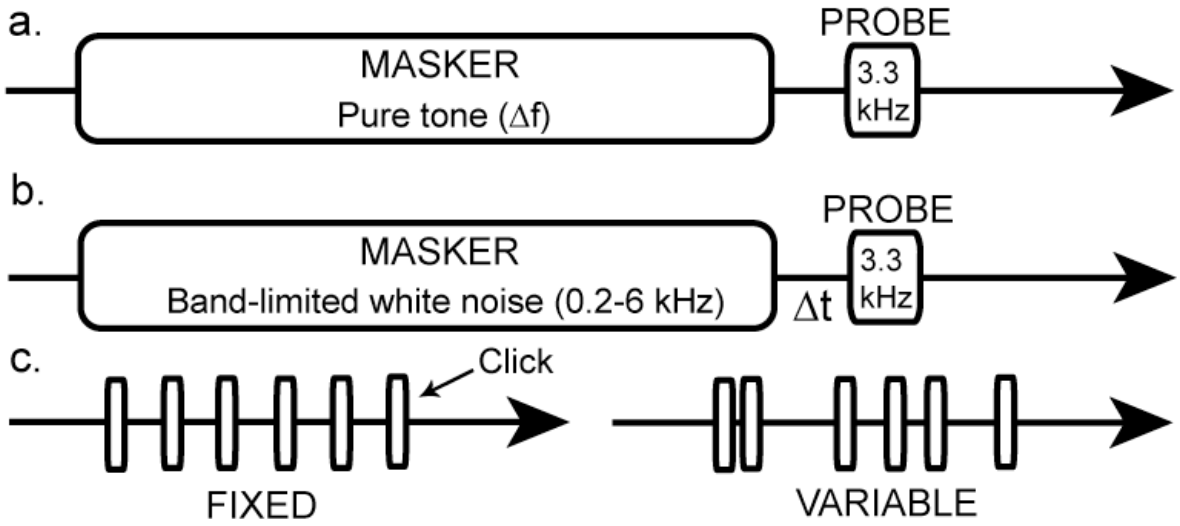

Figure 2.2. Stimulus delivery schematics for three of the ABR paradigms. Horizontal arrows indicate passage of time. *a*) Schematic for the forward masking frequency resolution paradigm. A 100 msec pure tone masker is varied in frequency (Δf). The offset of the masker always occurs 10 msec before the onset of 3.3 kHz probe tone. *b)* Schematic for the forward masking temporal adaptation paradigm. The offset of a 100 msec band-limited (0.2-6kHz) white noise masker occurs at varying time intervals (Δt) before the onset of the 3.3 kHz probe tone. *c*) Schematic for the temporal variability paradigm. Clicks were presented at three different rates, with both fixed (left) and variable (right) inter-peak intervals.

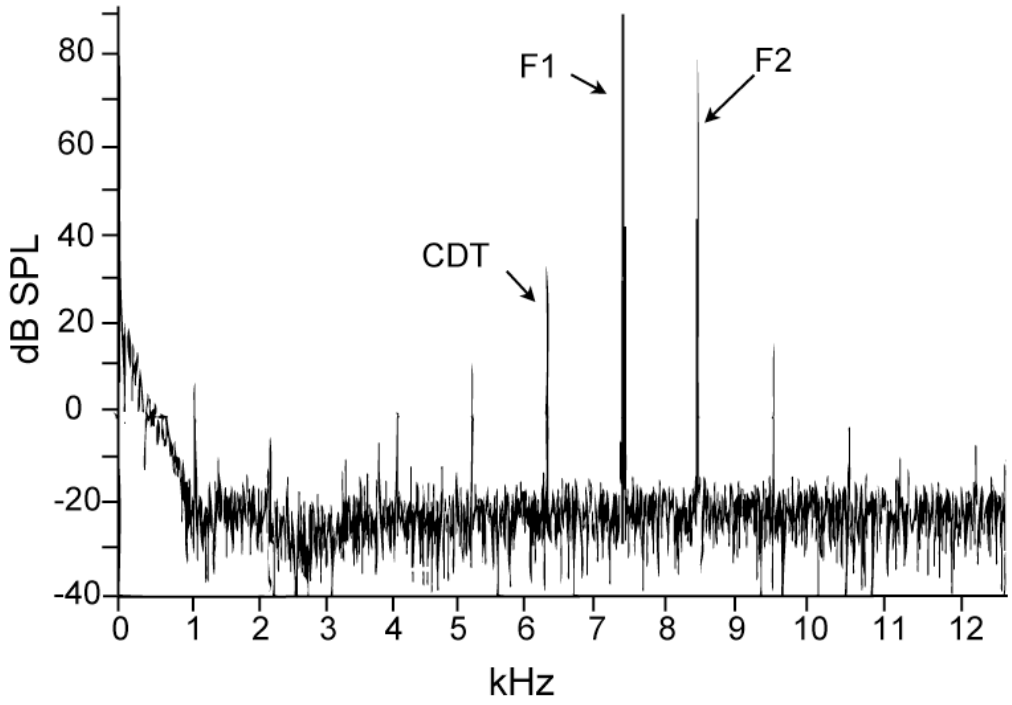

Figure 2.3. Representative frequency spectrum of a DPOAE recording from a breeding condition female. The primary tones (F1 and F2) were presented at the highest amplitudes (L1 = 90 dB SPL) to enable clear observation of the multiple distortion products. The distortion product with the largest amplitude is the cubic distortion tone (CDT), which corresponds to a frequency of 2F1-F2. F1 and F2 in this example are 7.4 and 8.5 kHz, respectively and the CDT is 6.3 kHz.

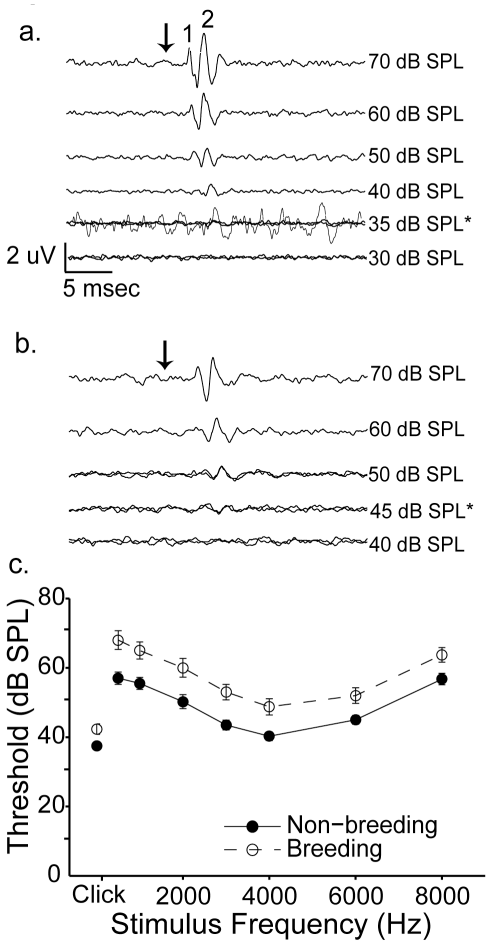

Figure 2.4 Birds housed under breeding-like conditions have higher auditory thresholds than those housed under non-breeding-like conditions. *a*) Representative ABRs decrease in amplitude and increase in latency as stimulus intensity is decreased. Traces were elicited by a 4000Hz tone from a non-breeding female. The top 4 traces represent averages of 500 stimulus presentations. 35 and 30 dB SPL traces represent averages of 1000 presentations. The black arrow indicates stimulus onset. Scale bars = 2 μV/ 5 msec. Threshold was estimated to be 35 dB SPL and is indicated by the asterisk. One trace elicited by a 35 dB SPL stimulus is enlarged and shown over the original traces to more clearly demonstrate a response. For this trace only, the scale bar = 0.3 uV/5 msec. *b*) Representative ABR traces from a breeding female demonstrate an elevated threshold. Experimental parameters and figure notations are as in *a*. The top two traces represent averages from 500 stimulus presentations; the remaining traces were averaged over 1000 presentations. Threshold was estimated at 45 dB SPL. Scale bar is the same for *a* and *b*. *c)* Mean +/- S.E.M. ABR thresholds of birds exposed to breeding-like conditions (open circles) are higher than those housed under non-breeding-like conditions (closed circles) across all stimulus frequencies. Data are presented linearly (rather than logarithmically) for clarity. Thresholds to clicks are shown at the left most portion of each graph and are measured in dB peak equivalent (p.e.) SPL. Each experimental group had an n = 20 (except for clicks, where breeding birds n = 21).

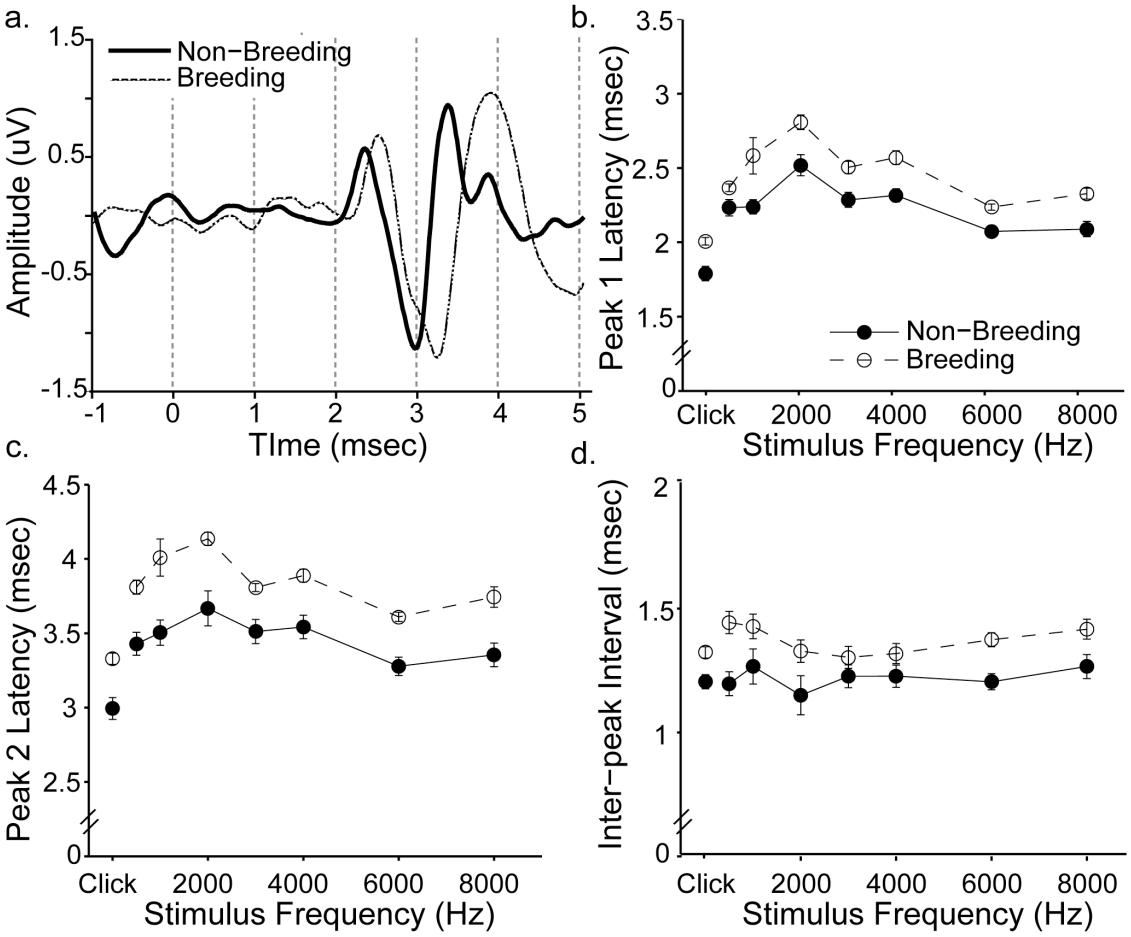

Figure 2.5 Birds housed under breeding-like conditions have longer ABR peak latencies and inter-peak intervals than those housed under non-breeding-like conditions. *a*) Representative ABR traces from a breeding (thin line) and non-breeding (thick line) female in response to a 4 kHz tone. Traces are aligned in time and stimulus onset occurs at time zero. The breeding bird has a delayed response compared to the non-breeding bird; note that this temporal disparity increases between peak 1 and peak 2. *b*) Peak 1 latencies of birds exposed to breeding-like conditions (open circles) are longer than those housed under non-breeding-like conditions (closed circles). The same pattern was observed for peak 2 latencies (*c*) and inter-peak intervals (*d*). Data are means +/- S.E.M. generated in response to iso-intensity tones (70 dB SPL) and clicks (70 dB p.e. SPL). Missing data points were filled in with appropriate group averages before data were plotted and analyzed (see main text). Breeding birds n = 19; non-breeding birds n = 20.

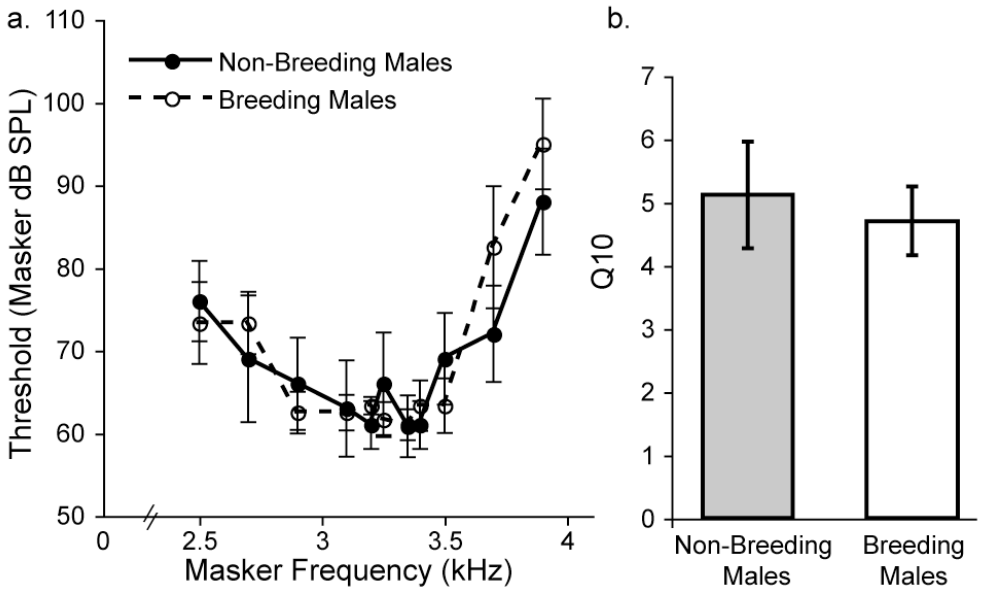

Figure 2.6 Breeding condition does not affect frequency tuning. *a)* Thresholds for a 3.3 kHz probe tone in a forward masking paradigm are similar for breeding males (open circles; n = 5) and non-breeding males (closed circles; n = 5) across all masker frequencies. *b)* Average Q_{10} values (indicative of tuning sharpness) did not differ between breeding males (open bar) and non-breeding males (shaded bar). One subject in each group had tuning curves too broad to accurately measure Q_{10}. Thus, n = 4 for each group in *b*.

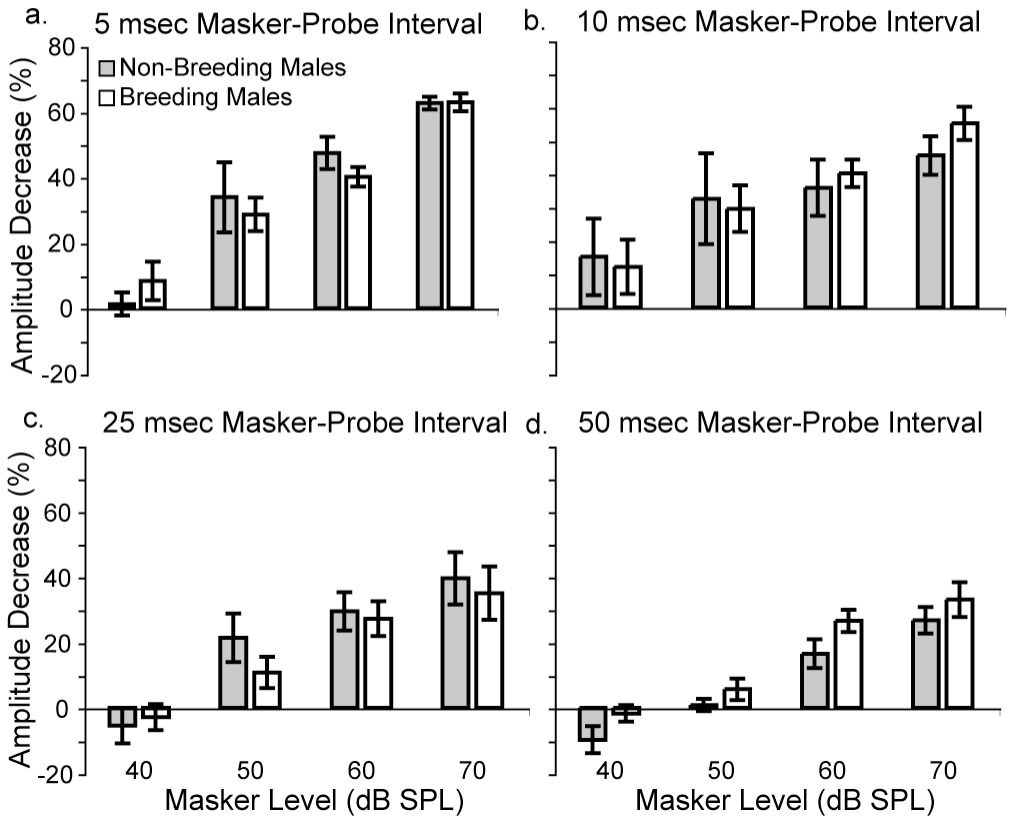

Figure 2.7 Breeding condition only affects temporal adaptation at the longest masker-probe interval tested. *a)* The probe-elicited ABR response amplitude decreases by a similar amount for males in breeding (open bars) and non-breeding (shaded bars) conditions when the masker and probe are separated by 5 msec. Similar results were found for (*b*) 10 msec and (*c*) 25 msec masker-probe intervals. *d*) When the masker and probe are separated by 50 msec, breeding males show a significantly greater decrease in response amplitude than non-breeding males. Data are means +/- S.E.M. Breeding males n = 6; non-breeding males n = 5 (except n = 4 at 40 and 50 dB SPL masker levels for 10, 25 and 50 msec intervals, and 40 dB SPL masker level for 5 msec interval).

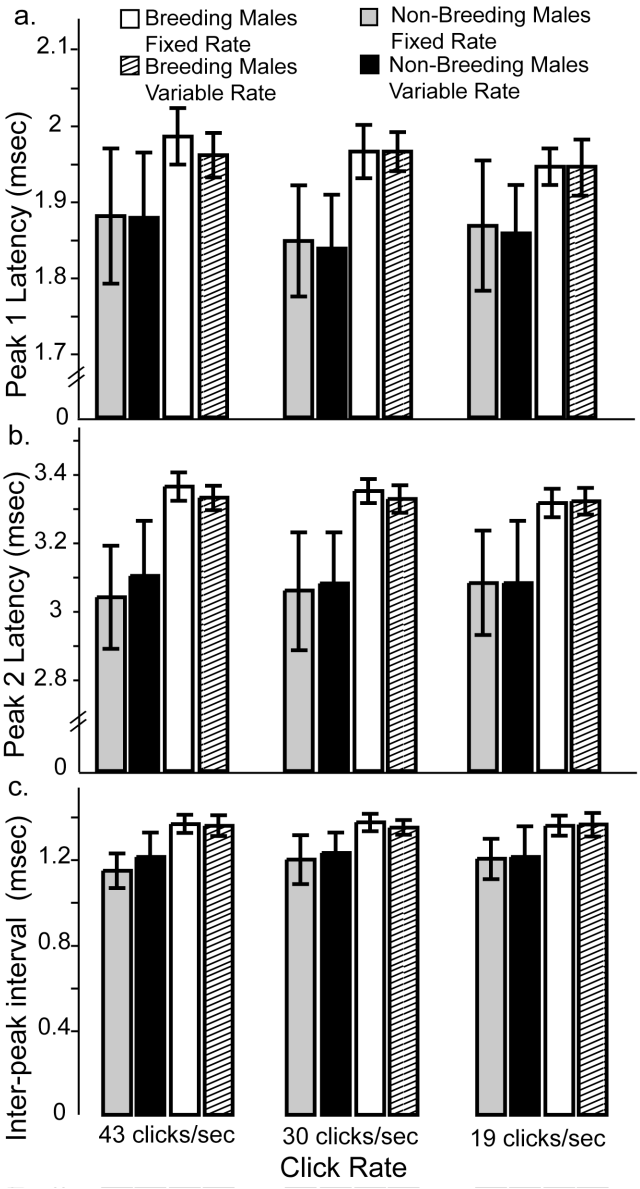

Figure 2.8 Breeding condition does not affect processing of temporally variable stimuli. Clicks were presented at three rates with both fixed and variable inter-click intervals. *a)* Non-breeding males show similar peak 1 latencies to fixed (grey bars) and variable (black bars) inter-click intervals for all presentation rates tested. Though breeding males showed a trend towards longer latencies in general, their responses to fixed (open bars) and variable (striped bars) stimuli were also similar. Similar results were found for peak 2 latencies (*b*) and inter-peak intervals (*c*). Data are mean +/- S.E.M. Breeding males n = 6, non-breeding males n = 4.

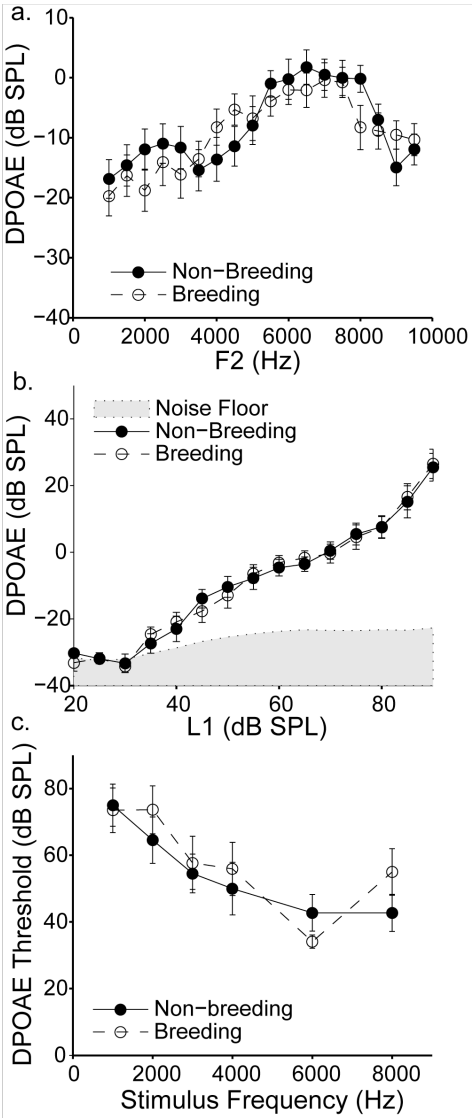

Figure 2.9 Breeding condition does not affect DPOAE amplitudes or thresholds. *a)* DPOAE amplitude changes systematically with F2 frequency, but no amplitude differences are observed between breeding (open circles) and non-breeding (closed circles) birds. DPOAEs were elicited by iso-intensity primary tones (L1 = 70 dB SPL) for all frequencies tested. *b*) DPOAE amplitude increases with increasing stimulus level, but no difference is observed between breeding (open circles) and non-breeding (closed circles) birds. The amplitude of the noise floor immediately surrounding the DPOAE frequency is indicated by the shaded grey area. DPOAEs were elicited by iso-frequency primary tones (F2 = 7 kHz) for all levels tested. *c*) DPOAE threshold decreases with increasing stimulus frequency, but no difference is observed between breeding (open circles) and non-breeding (closed circles) birds. Data are means +/- S.E.M. Breeding birds n = 11 (except n = 8 at 20 and 25 dB SPL in *b*); non-breeding birds n = 11 (except n = 7 at 1000Hz in *c*).

Chapter 3. Estradiol selectively enhances auditory function in avian forebrain neurons

3.1 Summary

Sex steroids modulate vertebrate sensory processing, but the impact of circulating hormone levels on forebrain function remains unclear. We tested the hypothesis that circulating sex steroids modulate single-unit responses in the avian telencephalic auditory nucleus, field L. We mimicked breeding or non-breeding conditions by manipulating plasma 17ß-estradiol levels in wild-caught female Gambel's white-crowned sparrows (*Zonotrichia leucophrys gambelii*). Extracellular responses of single neurons to tones and conspecific songs presented over a range of intensities revealed that estradiol selectively enhanced auditory function in cells that exhibited monotonic rate-level functions to pure tones. In these cells, estradiol treatment increased spontaneous and maximum evoked firing rates, increased pure tone response strengths and sensitivity, and expanded the range of intensities over which conspecific song stimuli elicited significant responses. Estradiol did not significantly alter the sensitivity or dynamic ranges of cells that exhibited non-monotonic rate-level functions. Notably, there was a robust correlation between plasma estradiol concentrations in individual birds and physiological response properties in monotonic, but not non-monotonic neurons. These findings demonstrate that functionally distinct classes of anatomically overlapping forebrain neurons are differentially regulated by sex steroid hormones in a dose-dependent manner.

3.2 Introduction

Sex steroid hormones modulate vocal signaling in adult vertebrates (Bass, 2008; Brenowitz, 2008), but how these modulations impact the auditory function of listeners remains unclear. Songbirds are well-suited for addressing this issue. Song is a complex, learned vocalization that serves several functions, including species and individual identification, mate attraction, and territory defense (Catchpole and Slater, 1995). In seasonal breeders, such as Gambel's white-crowned sparrow, song behavior is sensitive to hormonal state; high levels of circulating sex steroid hormones, typical of the breeding season (Wingfield and Farner, 1978), increase singing rate, song duration and song stereotypy (Smith et al., 1995; Meitzen et al., 2009b). Associated changes in the morphology and physiology of the neural circuit underlying song production are also observed (Nottebohm, 1981; Brenowitz et al., 1991; Smith et al., 1997; Tramontin et al., 2003; Soma et al., 2004; Park et al., 2005; Meitzen et al., 2007a, 2007b, 2009a; Phillmore et al., 2011).

Recent work has explored the effect of sex steroid hormones on songbird auditory sensitivity at the level of the periphery and brainstem (Henry and Lucas, 2009; Caras et al., 2010). Additional studies have examined the impact of sex steroid hormones on the processing of song stimuli in regions specialized for song perception or production such as the sensorimotor nucleus HVC (proper name), the caudomedial nidopallium (NCM) or the caudomedial mesopallium (CMM) (Maney et al., 2006; Tremere et al., 2009; Remage-Healey et al., 2010; Sanford et al., 2010; Tremere and Pinaud, 2011; Phillmore et al., 2011; Remage-Healey et al., 2012; Remage-Healey and Joshi, 2012).

Many issues remain unexplored. First, neurons in NCM, the main focus for the majority of studies on this topic, express hormone receptors (Bernard et al. 1999; Gahr, 2001; Jeong et al., 2011). Receptor expression is not a prerequisite for hormonal sensitivity, however, as steroid action can be mediated via other neuromodulatory systems (Maney and Pinaud, 2011). It is therefore of interest to determine whether auditory regions upstream of NCM, some of which lack sex steroid receptors, are also affected by hormonal state. Similarly, it is unclear whether circulating sex steroids modulate fundamental aspects of auditory processing in the forebrain, and if so, whether the magnitude of these modulations depends on the plasma level of hormone. To address these questions, we brought adult female sparrows into breeding (high 17ß-estradiol (E_2)) or non-breeding condition (low E_2) in the laboratory and made *in vivo* extracellular recordings from single-units in the forebrain field L complex. Field L is the primary thalamic recipient of auditory information and is analogous to mammalian primary auditory cortex (Fortune and Margoliash, 1992; Vates et al., 1996; Reiner et al., 2004, Fig. 3.1B). Unlike cells in downstream nuclei, field L neurons do not express steroid receptors (Jeong et al., 2011; Maney and Pinaud, 2011). We found that modulations of systemic E_2 affect many fundamental response properties in monotonic field L neurons.

3.3 Methods and Materials

3.3.1 Subjects

Adult female Gambel's white-crowned sparrows (n=21) were captured in eastern Washington state during autumn and spring migrations between 2007 and 2011. Birds were housed in outdoor aviaries at the University of Washington for up to 30 weeks before being moved to

indoor aviaries. Once inside, all birds were housed in groups on a short-day photoperiod (SD, 8 hr light : 16 hr dark) for a minimum of 10 weeks to ensure sensitivity to the stimulating effects of hormones and photoperiod (Wingfield et al., 1979). Food and water were available *ad libitum*. All procedures were approved by the Institutional Animal Care and Use Committee at the University of Washington, Seattle.

3.3.2 Hormone and photoperiod manipulations

Birds were brought into either non-breeding-like condition or breeding-like condition in the laboratory. To induce a non-breeding condition, we housed birds (n = 12) on a SD photoperiod as above. Birds housed on a SD photoperiod maintain regressed gonads, have basal plasma sex hormone levels, and display neural morphology and physiology typical of the non-breeding season (Middleton, 1965; Smith et al., 1995; Tramontin et al., 2000; Park et al., 2005; Meitzen et al., 2007a). To induce a breeding condition, we housed birds (n = 9) on a long day (LD; 20 hr light : 4 hr dark) photoperiod typical of their Alaskan breeding grounds and implanted them with subcutaneous hormone pellets made from SILASTIC tubing (i.d. 1.0mm; o.d. 2.0mm, length 12mm; VWR). Pellets were filled with crystalline E_2, rinsed in ethanol, and soaked overnight in 0.1M phosphate buffered saline prior to implantation (Tramontin et al., 2003). Supplemental hormone is necessary to raise plasma hormone levels of laboratory-housed birds to physiological levels observed in breeding birds in the wild (Smith et al., 1995). Birds were housed under these conditions for three weeks; this time period is sufficient to induce neural morphology and physiology typical of the breeding season (Tramontin et al., 2000; Park et al., 2005; Meitzen et al., 2007a).

3.3.3 Electrophysiology

3.3.3.1 Surgical procedures

All experiments took place in a double-walled acoustically isolated chamber (Acoustic Systems). At the beginning of each experiment, birds were anesthetized with 25% urethane (6 µl/g body weight, Thermo Fisher Scientific), divided evenly into three intramuscular injections separated by 30 minutes. Supplementary doses (0.67 µl/g) were delivered throughout the experiment to maintain anesthetic state as assessed by toe-pinch. After birds were fully anesthetized, we injected 0.1ml of 1% lidocaine (APP Pharmaceuticals) subcutaneously at the dorsal midline of the skull, made an incision and removed the skin and fascia. A metal post was fixed to the skull with dental cement (Lang Dental) and birds were secured to a head holder / stereotaxic device. Body temperature was maintained at 40-42 ^{o}C by a heating pad using a cloacal thermal probe and digital controller (TC-1000 Temperature Controller, CWE Inc.). A small craniotomy was made dorsal to field L in the right hemisphere using stereotaxic coordinates relative to the bifurcation of the midsagittal sinus (1.4 mm lateral, 1.8-2.3 mm anterior). The dura was removed and a glass micropipette electrode (5-19 MΩ impedance) filled with 10% fluororuby (10,000 MW tetramethylrhodamine dextran, Invitrogen) or 10% biontinylated detran amine (BDA 10,000 MW, Invitrogen) in 0.9% NaCl was positioned over the opening. The electrode was advanced by an electric microdrive (Newport), which was controlled by the experimenter from outside the sound attenuation booth. For some recording sessions, the craniotomy opening was covered in petroleum jelly to prevent tissue dehydration. We made one to three electrode penetrations in each bird. Though we recorded activity at a wide range of depths (~800 - 3300µm), we restricted our analysis to units that were confirmed histologically to be within field L (see *Electrode Track*

Reconstruction below).

Auditory processing is lateralized in songbirds, though the exact nature of hemisphere specificity depends on sex, species, brain area, anesthetic state, stimulus selection, and method of analysis (Cynx et al., 1992; George et al., 2004, 2005; Avey et al., 2005; Hauber et al., 2007; Poirier et al., 2009; Phan and Vicario, 2010). To avoid introducing a lateralization confound into our experimental design, we chose to focus only on the right hemisphere.

3.3.3.2 Stimulus delivery and calibration

The stimulus delivery system we employed has been used previously (Caras et al., 2010). Briefly, a small speaker (Etymotics ER-2B) and microphone (Etymotics ER-10B) were enclosed within a custom-made sound delivery tube and positioned flush against the skull surrounding the left external auditory meatus. Petroleum jelly was applied to the outside of the tube and skull, creating a closed sound delivery system. Sound delivery was controlled by custom scripts (Python) running on a computer located outside the sound attenuation chamber. Stimuli were routed through an RX6 multifunction processor (Tucker Davis Technologies) that performed both digital/analogue conversion and attenuation of the signal before delivery to the speaker.

Prior to each experiment, we used random-phase band-limited (6Hz -20 kHz) white noise to calibrate pure tone sound pressure levels (dB SPL re: 20 μPa). For our initial experiments, we used the white-noise generated calibration table to determine root-mean squared sound pressure

levels (RMS dB SPL) for song stimuli. In later experiments, we presented individual songs to the microphone and determined RMS dB SPL values separately for each song. The levels for earlier recordings were corrected for each song type presented. RMS amplitudes for song stimuli were reliable within ≤ 4.9 dB SPL.

3.3.3.3 Auditory stimuli

We presented two different types of stimuli in this study. Pure tone stimuli were 100 msec in duration with 5 msec linear ramp rise-fall times. Tones were generated online using the same custom software that controlled sound delivery. Song stimuli consisted of a set of songs recorded from 7 individual male sparrows held under breeding condition in the laboratory. We used male songs because females of this species do not sing. We recorded songs using Syrinx software (John Burt, www.syrinxpc.com) and previously published protocols (Meitzen et al., 2007a, 2009b). Low frequency background noise was digitally filtered offline. We recorded one song from each bird, for a total of 7 songs.

Gambel's white-crowned sparrow songs typically consist of 5 syllables: a whistle, a warble, and three buzzes (Fig. 3.1A). The songs presented in this study were 2.15 +/- 0.19 seconds in duration (mean +/- STDEV) and spanned an average frequency range of 2.44 to 5.98 kHz. These values are similar to those previously published for a larger song set (Meitzen et al., 2009b).

The majority of song stimuli (1 though 4 in Fig. 3.1A) were recorded from captive males before 2007, and thus were unfamiliar to all of our experimental birds. Three songs (5 through 7 in Fig.

3.1A) were recorded from males that had overlapping periods of captivity with some of the experimental birds, and therefore may have been familiar. Though song familiarity can affect neurophysiological responses in more specialized auditory regions, such as NCM, field L does not display this characteristic (Theunissen et al., 2004). We therefore did not include song familiarity as a factor in our data analysis.

3.3.3.4 Data acquisition

We recorded the extracellular activity of well-isolated single units. Spikes were amplified 10,000X (ISO-80, World Precision Instruments and MA3, Tucker Davis Technologies), bandpass filtered 0.1-10 kHz with a 24dB/octave roll-off (Krohn-Hite model 3550), digitized at 24.4 samples/sec (RX6 multifunction processor, Tucker Davis Technologies), and monitored online via a digital oscilloscope and audio speaker. Custom data acquisition software displayed spike trains, isolated waveforms and raster plots in real time. We analyzed raw waveforms offline using custom MATLAB scripts (David Schneider and Sarah Woolley, Columbia University) to ensure that only well isolated single units were included in the dataset. Neurons were assessed to be well isolated by the following criteria: (1) a stable waveform shape, (2) a high (> 4) signal-to-noise ratio, and (3) the absence of any interspike intervals < 1 msec. The vast majority of recordings (71/77) met all three criteria. The remaining six recordings demonstrated the presence of two clearly separable waveforms with high signal-to-noise ratios. These waveforms were manually sorted offline; sorting efficacy was additionally verified by principal components analysis.

Band-limited white noise (0.25-8 kHz) at 80 dB SPL was used as a search stimulus. Once a unit was well isolated, we presented song and tone stimuli, with the order of presentation randomized across cells. For song trials, we chose one song exemplar at random and presented it from 90 to 10 dB SPL in 10 dB descending steps at a rate of 0.14/sec. We recorded five to ten trials at each intensity. For tone presentations, we initially estimated the unit's characteristic frequency (CF) and best threshold online. We then presented a range of frequencies around the CF, in increments approximately equal to 10% of the CF. Each frequency was presented from 90 to 10 dB SPL in 10 dB descending steps at a rate of 1.25/sec to construct the unit's full response area. We recorded five to ten trials for each frequency-intensity pair, with the order of frequency presentation randomized across trials.

It should be noted that the stimulus intensities used here (10-90 dB SPL) are similar to the sound amplitudes that would be experienced by free-living birds in the wild. Avian species are capable of singing at high intensities, with maximum values ranging from 74-105 dB SPL at 1m (Brackenbury, 1979; Brenowitz, 1982), though some species can generate song amplitudes as high as 111.5 dB SPL (e.g. the Screaming Piha (*Lipaugus vociferans*) Nemeth, 2004). Therefore, we consider the stimulus levels used here to be within a normal, ethologically relevant range.

3.3.3.5 Data analysis

3.3.3.5.1 Tone responses:

A unit was considered tone responsive if its average stimulus-evoked firing rate was significantly different (student's paired t-test, $p < 0.05$) than its average spontaneous firing rate (calculated

from the 100 msec immediately preceding tone onset). The vast majority (54/56) of tone responses were excitatory. The remaining two cells (one from a non-breeding female, one from a breeding female) gave what appeared to be post-inhibitory rebound responses, as evidenced by strong excitation immediately following tone offset. If these cells were truly exhibiting post-inhibitory rebound, their firing rates should be suppressed during tone presentation. The cells' spontaneous firing rates were already quite low (1.48 and 1.67 sp/s, respectively), however, making it difficult to detect a suppressive response. Because these potentially suppressive responses were so rare, we removed them from the tone analyses. Both of these cells did show suppressive responses to songs and were included in the song analyses (see *Song Responses* below).

To determine a unit's pure tone sensitivity, we measured the threshold for each stimulus frequency. Threshold was defined as the lowest intensity (dB SPL) to elicit a significant response. An additional criterion was that successively higher level stimuli must also elicit reliable responses. The CF was identified as the stimulus frequency with the lowest threshold. If multiple frequencies had the same (lowest) threshold, CF was defined as the stimulus with the greatest response strength at threshold. Here, we define response strength (RS) as the difference between the average stimulus evoked firing rate and the average spontaneous firing rate during the 100 msec immediately preceding tone onset, a window equal to the duration of the tone.

We measured the frequency bandwidth 10 dB above the neuron's best threshold as an indicator of frequency tuning. In addition, we made the following measurements of the responses to the

CF: First, we identified the maximum average evoked firing rate, and the stimulus intensity that elicited the maximum response (max dB). Second, we set a noise floor two standard deviations above the neuron's baseline rate. We then defined the neuron's firing rate range (sp/s) as the difference between the noise floor and the maximum evoked firing rate. Third, we calculated the neuron's dynamic range, or the range of stimulus intensities within which a neuron is sensitive to differences in intensity. The dynamic range (dB SPL) was calculated as the difference between the max dB and the threshold.

During the early phases of our studies it became clear that neuronal responses in field L could be either monotonically related to tone intensity at CF, or non-monotonic. Monotonic and non-monotonic neurons are thought to play different roles in auditory coding (Polley et al., 2006; Sadagopan and Wang, 2008; Watkins and Barbour, 2011), raising the possibility that breeding condition might modulate each neuronal population in a distinctive manner. We therefore chose to analyze monotonic and non-monotonic responses separately, as discussed below.

To objectively determine whether a cell should be considered monotonic or non-monotonic, we set a boundary halfway between the noise floor and the maximum average evoked firing rate. A neuron was considered non-monotonic if its average evoked firing rate dropped below this boundary at stimulus intensities above the dB level that evoked the maximum firing rate. If the cell maintained a high evoked firing rate, staying above this boundary, it was considered monotonic (Fig. 3.2).

To determine whether these categorizations truly reflected two separate populations of neurons, we calculated a monotonicity index (MI) for each cell. The MI ranges from 0 to 1, with increasing values indicative of increasing degrees of monotonicity. Similar measures of monotonicity have been used previously by other researchers (Sutter and Schreiner, 1995; Recanzone et al., 2000; de la Rocha et al., 2008; Watkins and Barbour, 2011). The MI was calculated for each cell as follows:

MI = Rate evoked at highest pure-tone amplitude presented/ maximum evoked rate of the neuron

In the majority of our cases (27/28 monotonic and 23/25 non-monotonic neurons), the highest pure-tone amplitude tested was 90 dB SPL. In the remaining 3 cases, the highest amplitude tested was 80 dB SPL.

One non-monotonic neuron recorded in a breeding female had particularly strong tone and song responses. To determine whether this cell was an outlier, we averaged tone and song-evoked |RS| values separately across stimulus level for each non-monotonic cell recorded under breeding condition. We used these average values to perform Dixon's *Q* test for outliers (Dixon, 1950). We found that the cell in question was an outlier at the 99th confidence interval (Rorabacher, 1991) for both tone and song-evoked responses. We therefore removed this cell from all analyses.

3.3.3.5.2 Song Responses

To determine whether a unit was responsive to song, we first established a noise floor two standard deviations above and below the neuron's spontaneous rate. For a unit to be considered song responsive, its evoked firing rate had to fulfill the following criteria at a minimum of two consecutive song intensities: i) surpass the noise floor and ii) be statistically different (student's paired t-test, $p < 0.05$) than the average spontaneous firing rate during the 2000 msec immediately preceding song onset, a window approximately equal to the duration of each song stimulus. We found that these criteria reliably included units that were considered responsive by an experienced observer, while minimizing false positives. Two neurons clearly responded to song, but only at the highest stimulus intensity tested, and therefore could not meet the response criteria. An observer experienced in single-unit physiology blinded to the experimental conditions examined raster and post-stimulus time histogram (PSTH) plots. A decision to include these cells in the analysis was made after this observer agreed that the neurons showed increased activity during song presentation.

A unit's song threshold (dB SPL) was defined as the lowest of at least two consecutive intensities to elicit a significant response. We then identified the maximum average evoked firing rate (for excitatory song responses), the minimum average evoked firing rate (for suppressive song responses), and the stimulus intensity that elicited the maximum or minimum firing rate (max or min dB, respectively). We calculated the song dynamic range (dB SPL) as the difference between max or min dB and the threshold. Finally, similar to tones, we used RS (sp/s) as a measure of response magnitude. Songs elicited both excitatory and suppressive responses (Fig.

3.6), however, which resulted in positive and negative RS values, respectively. In order to analyze all song responses as a whole, we used the absolute value of RS.

3.3.4 Electrode track reconstruction

Two injections of either 10% fluororuby (20/21 birds) or 10% BDA (1/21 birds) were made at the end of each electrode penetration to enable offline reconstruction of recording sites. Fluororuby was injected iontophoretically through the recording pipette by using a current source (BAB-501, Kation Scientific) set to +10μA for one minute, followed by +4μA (alternating 7 seconds on/off) for 8 minutes. BDA was injected with 5-10 rapid 40 msec pulses of nitrogen gas at 20 pounds per square inch using a picospritzer (Parker).

At the end of each recording session, birds were perfused transcardially with ice cold phosphate-buffered saline, followed by 4% paraformaldehyde. Brains were removed, postfixed in paraformaldehyde, cryoprotected in 30% sucrose, embedded in gelatin and postfixed in a 20% sucrose/10% neutral buffered formalin solution for 48 hours. Parasagittal 40 μm sections were cut on a freezing microtome and floated in 0.05M PB. Sections were mounted onto gelatin-subbed slides and processed for Nissl; alternates were air dried until fluorescent or BDA processing.

Sections containing fluororuby injections were cleared in xylene, coverslipped in DPX mounting medium (Electron Microscopy Sciences) and dried overnight. Sections containing BDA injections were incubated in 30% hydrogen peroxide in 100% methanol, rehydrated in phosphate

buffered saline (PBS), incubated in ABC (Vector Laboratories), and visualized using 3'3 diaminobenzidine (DAB, Sigma). All images were captured on a Olympus BH2 microscope fitted with a Qimaging camera and Qcapture software.

Only units that could be localized unambiguously to field L were included in our analyses. It should be noted here that differences in spectrotemporal tuning have been reported for the different subregions of the field L complex (Sen et al., 2001; Nagel and Doupe, 2008; Kim and Doupe, 2011), raising the possibility that E_2 has disparate effects on these different areas. There was insufficient statistical power to allow analysis by subregion, however, as our experimental design already consisted of multiple independent variables. We therefore did not separate our recording sites into anatomical subregions for our analysis.

3.3.5 Hormone measurement

Immediately before each recording session, we collected blood from the alar wing vein of each bird into a heparinized tube and centrifuged the sample at 4°C. Separated plasma was stored at -80°C until Enzyme-Linked Immunosorbent Assay (ELISA). Estradiol levels were measured using a kit (Cayman Chemicals) that had not previously been used with this species, so the assay was first validated as described below.

3.3.5.1 Assay validation

Multiple controls were used to assess the kit's validity. First, plasma samples were pooled from multiple sparrows and stripped of steroids by incubating with dextran-coated charcoal in assay

buffer (Sigma-Aldrich). This stripped plasma is expected to contain no, or very low levels of estradiol. Second, stripped plasma was spiked with E_2 to 3200 pg/ml and serially diluted. This serial dilution is expected to parallel the kit's standard curve. Third, raw (unstripped) plasma was divided into two samples, one of which was spiked with 1000 pg/ml. These samples are expected to differ in E_2 concentration by exactly 1000 pg/ml, and thus is a test of the kit's precision. Finally, to determine whether lipids or proteins endogenous to white-crowned sparrow plasma interfere with the assay, hormones were extracted from all of the samples outlined above, reconstituted in assay buffer, and assayed separately.

To extract hormones, anhydrous diethyl ether was added to each sample aliquot and vortexed for 1 min. The ether fraction was pipetted into a new test tube, and the extraction was repeated for the remaining plasma layer. Ether fractions were combined for each sample and evaporated under nitrogen gas. Dried, extracted hormone was resuspended in the kit assay buffer and samples were stored at 4°C until use.

Results from the validation assay were as expected: stripped plasma contained extremely low levels of estradiol, serial dilutions paralleled the kit's standard curve, and raw-spiked plasma differed from raw plasma by ~1000 pg/ml. No dramatic differences were observed between extracted samples assayed in buffer and those assayed in raw plasma, therefore, we did not extract hormone from experimental samples and instead assayed the raw plasma directly.

We ran 50 µl aliquots of each sample along with eight estrogen standards (6.6 - 4000 pg/ml) in a single assay following the kit's protocol. Some samples were lost during preparation; therefore, only 7 samples were assayed for each experimental group. Most samples and all of the kit standards were run in duplicate; however, 3 samples in each experimental group were run singly because of insufficient sample volume. Briefly, we incubated each sample with 50 µl of E_2 antiserum and 50 µl of an E_2-acetylcholinesterase conjugate for 1 hour. After emptying and washing the plate, we added 200 µl of enzymatic substrate (Ellman's reagent) to all sample wells. After a one hour incubation, we read the plate immediately at 405 nm on a Dynex MRX II microplate reader.

We plotted the optical densities of the kit standards as a function of known E_2 concentration and fit the points with a sigmoid 4PLC equation; sample hormone levels were extrapolated from this standard curve. Intra-assay variability was 6.50%.

3.3.6 Statistics

Monotonic and non-monotonic neurons were analyzed separately. To measure the effect of breeding condition on tone and song-evoked |RS| values, we set breeding condition as the between subjects variable and stimulus level as the within subject variable in two-way repeated-measures mixed-model ANOVAs. For some cells, we had an incomplete dataset, such that a given stimulus (tone or song) was only presented for a limited range of intensities. These missing values presented an obstacle for running a repeated measures ANOVA. We therefore performed each ANOVA twice: In one version, we included all the cells in the dataset and discarded any

stimulus level with missing values. In the other version, we discarded any cells that had missing values and included all the stimulus levels. Both of these versions gave similar results; therefore we report here only the results obtained when all cells were included in the ANOVAs.

We used a Mann-Whitney U test to compare E_2 levels across experimental conditions. All correlations (between song and tone thresholds or between hormone levels and firing rates) were assessed with Pearson's *r*. For the remainder of our analyses, we indicate which statistical tests were used in table legends, or in the results text, when appropriate. Unless otherwise stated, all values are reported as means +/- S.E.M.s. All statistical analyses were made using PASW Statistics 18.0 or Graphpad Prism.

3.4 Results

3.4.1 Plasma 17ß-estradiol (E_2) levels

Females housed under breeding (LD+E_2) condition had elevated levels of plasma E_2 compared with females housed under non-breeding (SD) condition (397.8 +/- 187.5 vs. 26.3 +/- 8.13 pg/ml, Mann-Whitney $U = 1.000$, $n_1 = n_2 = 7$, $p = 0.003$). Plasma E_2 levels in birds housed under breeding condition were similar to the physiological range reported by Wingfield and Farner (1978) for wild breeding female white-crowned sparrows (~300-500 pg/ml).

3.4.2. Auditory responses of field L neurons

We recorded from a total of 77 auditory-responsive cells histologically confirmed to be in field L (Fig. 3.1C-E). Of these, 30 auditory cells were recorded from 9 birds in breeding condition

and 47 cells were recorded from 12 birds in non-breeding condition (Table 3.1). For some cells, we were only able to record song responses (either because the cell was unresponsive to tones, or because we could not hold the isolation long enough to record a full tone response area). Similarly, in another subset of cells, we were only able to record tone responses. We were able to record both song and tone responses in a final subset of cells.

3.4.3 Tone responses

3.4.3.1 Tone responses can be monotonic or non-monotonic

Tone responsive neurons in field L can be categorized as monotonic or non-monotonic, based on the shape of their rate-level function. Monotonic neurons increase their firing rate with increasing stimulus intensities (Figs. 3.2A and C). Conversely, the firing rate of non-monotonic neurons increases up to some mid-level stimulus intensity before decreasing at higher intensities (Figs. 3.2B and D).

We calculated a monotonicity index (MI) for each neuron to determine whether monotonic and non-monotonic cells were two separate populations. The results of this analysis are shown in figure 3.2E. While there is a small amount of overlap between the two groups, the distributions clearly segregate from one another. Only 3/25 neurons classified as non-monotonic have MIs >0.70. Each of these neurons had classic “inverted V”-shaped rate-level functions, up through 80 dB SPL. At 90 dB SPL, each of these cells showed an increase in activity, such that their overall rate-level function was “N” shaped. This “N” shape accounted for the high MI values in these

cells. If the MI was instead calculated using 80 dB SPL as the maximum stimulus amplitude, each of these cells showed MI values < 0.70.

Similarly, only 2/28 cells that were classified as monotonic had MI values <0.70. Both of these cells showed rate-level functions that saturated at mid-level intensities, with a small decrease in firing rate at 90 dB SPL. This decrease, though not large enough for us to classify the cells as non-monotonic, accounts for the lower MI values.

When we compared the groups using a two-sample t-test, we found that monotonic neurons had significantly higher MIs than non-monotonic neurons (0.887 +/- 0.025 vs. 0.410 +/- 0.054, $t_{(51)}$ = 8.331, p<0.001). Together, these findings suggest that the monotonic and non-monotonic cells we report on here likely comprise two distinct populations of neurons.

Monotonic (n=28) and non-monotonic (n=25) cells were equally abundant in field L, and breeding condition had no effect on their relative proportions. Similarly, spike half-widths of monotonic and non-monotonic neurons remained stable across breeding conditions. These results are presented in more detail with their accompanying statistics in table 3.2.

The anatomical positions of monotonic and non-monotonic neurons did not differ across the anterior-posterior and dorsal-ventral extents of field L. Individual recording sites overlapped along both the rostral-caudal and dorsal-ventral axes (Fig. 3.3), and breeding condition had no effect on the spatial distribution of monotonic or non-monotonic neurons (Table 3.2).

3.4.3.2 Breeding condition does not affect CF distributions or frequency tuning

Tone-responsive neurons in the avian auditory forebrain are tuned to specific frequencies arranged in a topographic manner (Müller and Leppelsack, 1985; Wild et al., 1993). We investigated whether the CF distributions for monotonic and non-monotonic neurons differed between breeding conditions. Breeding condition had no effect on the distribution of characteristic frequencies in monotonic or non-monotonic neurons. We also quantified tuning precision by calculating frequency bandwidths 10 dB above each neuron's best threshold. No effect of breeding condition was observed on frequency bandwidths for monotonic or non-monotonic cells. Detailed results and accompanying statistics can be found in table 3.2.

3.4.3.3 Breeding condition increases spontaneous and maximum firing rates in monotonic neurons

Previous work has suggested that E_2 increases neuronal responsiveness in NCM, a secondary region of the songbird auditory forebrain that express estrogen receptors (Tremere et al., 2009; Maney and Pinaud, 2011; Tremere and Pinaud, 2011, Fig. 3.1B). To determine if E_2 has similar effects on field L neurons, a region that does not express steroid receptors, we calculated average spontaneous and maximum evoked firing rates from cells in birds under different breeding conditions (Fig. 3.4). E_2 treatment significantly increased spontaneous firing rates of monotonic neurons. Similarly, monotonic cells showed a trend toward an increase in maximum evoked firing rates at CF. Spontaneous and maximum firing rates increased by the same relative amount, however, such that the firing rate range of these cells remained constant across breeding and non-breeding conditions. Table 3.3 provides the statistical results of these comparisons.

Figure 3.4 also illustrates that E_2 had different effects on non-monotonic neurons. While breeding condition did not have a significant effect on spontaneous firing rates of non-monotonic neurons, E_2 treatment significantly decreased maximum evoked firing rates of these cells. This combination resulted in a significant decrease in the firing rate range of non-monotonic neurons. The associated statistics for these comparisons are listed in table 3.3.

3.4.3.4 Breeding condition increases tone-evoked response strength and sensitivity of monotonic neurons

The effects of E_2 on maximum evoked firing rates could be explained by an overall shift in evoked firing rates across stimulus levels, and/or a change in the shape of the rate-level function, both of which could give rise to changes in auditory thresholds and dynamic ranges. To address this issue, we calculated RS-level functions at CF for monotonic and non-monotonic neurons under different breeding conditions.

Figure 3.5A shows group RS data for monotonic neurons across stimulus level; accompanying statistical results are listed in table 3.4. Input-output functions had similar shapes across experimental conditions, peaking at 80 dB SPL under breeding condition and 90 dB SPL under non-breeding condition. The effect of sound intensity was significant. In addition, breeding condition significantly increased monotonic tone RS values across levels, by an average of 9.08 sp/s. The interaction between breeding condition and tone intensity on monotonic tone RS was also significant, such that the largest differences between the experimental groups occurred at mid-level intensities. Table 3.4 shows the accompanying statistics for this analysis.

The effect of breeding condition on overall response magnitude resulted in differences in auditory sensitivity. Breeding condition significantly lowered CF thresholds compared to non-breeding condition in monotonic cells (Fig. 3.5C). The E_2-induced decrease in threshold contributed to a slight, but non-significant increase in monotonic neuron dynamic range (Fig. 3.5E). The statistics for these comparisons can be found in table 3.3.

Figure 3.5B shows group RS data for non-monotonic neurons across stimulus level. As above, input-output functions for breeding and non-breeding groups had similar shapes, peaking at 60 dB SPL and 50 dB SPL, respectively, and the overall effect of sound level was significant. In contrast to the monotonic neurons, breeding condition significantly decreased tone RS values in non-monotonic neurons across stimulus levels by an average of 5.76 sp/s. The interaction term between level and breeding condition was not significant and no effect was found on CF threshold (Fig. 3.5D) or on dynamic ranges (Fig. 3.5F) in these cells. The results of these statistical analyses can be found in tables 3.3 and 3.4.

To summarize the preceding results, breeding condition increased spontaneous firing rates, maximum evoked firing rates, tone-evoked response strengths and pure-tone sensitivity in monotonic, but not non-monotonic neurons.

3.4.4 Song responses of field L neurons

3.4.4.1 Song responses can be excitatory or suppressive

Previous work has shown an effect of E_2 treatment on selectivity and discrimination of conspecific song stimuli in secondary auditory forebrain regions (Maney et al., 2006; Tremere et al., 2009; Remage-Healey et al., 2010; Sanford et al., 2010; Tremere and Pinaud, 2011; Remage-Healey et al., 2012; Remage-Healey and Joshi, 2012). All of these studies presented song at a single intensity level, however. Therefore, before determining whether E_2 affects field L song response properties, we first examined song-evoked rate-level functions in individual cells. We observed that while the majority (40/58) of responses to conspecific song were excitatory (Fig. 3.6A and C), increasing their rate as a function of song level, a substantial portion of them (18/58) were suppressive (Fig. 3.6B and D). Breeding condition did not influence the relative proportions of excitatory or suppressive song responses in field L (Table 3.5). To determine whether breeding condition affects song-evoked excitability, we calculated the maximum song-evoked |RS| for each cell; we found no effect of breeding condition (Table 3.5).

3.4.4.2 Breeding condition increases song-evoked response strength and dynamic range of cells with monotonic tone responses

We used the absolute value of response strength (|RS|) to analyze the change in neuronal firing rate for all song responses together. Song |RS| values increased as a function of song level in both breeding and non-breeding groups ($F_{(4,56)} = 14.46$, $p < 0.001$). E_2 treatment, however, did not significantly affect rate-level shapes or magnitudes ($F_{(1,56)} = 0.075$, $p = 0.785$), and no interaction between breeding condition and song level was observed ($F_{(4,56)} = 0.313$, $p = 0.870$).

As noted in table 3.5, breeding and non-breeding groups also had similar song thresholds and dynamic ranges.

Thus, our results show that when all neurons in our sample are considered, E_2 treatment has no effect on song responses. Given that E_2 treatment modulated tone responses in a selective manner, however, we analyzed song responses separately for different classes of neurons.

Tone and song thresholds were correlated within individual cells for both breeding ($r = 0.60$, $n = 15$, $p = 0.019$) and non-breeding ($r = 0.61$, $n = 19$, $p = 0.006$) groups (Fig. 3.7). Song thresholds were higher than tone thresholds. This finding is not surprising, given that tone thresholds were measured at CF, the unit's optimal tonal stimulus.

The correlation between song and tone thresholds led us to predict that E_2 treatment enhances song responses, but only in neurons with monotonic input-output functions in response to pure tone stimuli. To address this issue, we examined song-evoked |RS|-level functions separately for cells that had monotonic and non-monotonic tone input-output functions. For cells that had monotonic tone responses, there was a significant effect of sound intensity on average song-evoked |RS| values under both breeding and non-breeding conditions (Fig. 3.8A). E_2 treatment significantly increased song-evoked |RS| values in these cells by an average of 2.578 sp/s across levels. Importantly, there was a significant interaction between song intensity and breeding condition; while breeding condition had a small impact at even at the lowest intensity tested, this effect became more pronounced as song intensity increased. The greatest difference between

conditions was observed at 90 dB SPL. Because the greatest shift in the input-output function occurred at higher stimulus levels, there was no significant change in song threshold (Fig. 3.8C). In addition, there was a trend for breeding condition to increase song dynamic range in cells with monotonic tone responses (Fig. 3.8E), but this trend failed to achieve statistical significance. The results of these statistical analyses can be found in tables 3.3 and 3.4.

Average song-evoked |RS| values are plotted as a function of sound level for cells that had non-monotonic tone responses in figure 3.8B. In these cells, the effect of level was not significant. E_2 treatment did not significantly alter |RS| values across sound intensity, nor was there a significant interaction between song intensity and breeding condition (Table 3.4). Finally, breeding condition did not have a significant effect on song thresholds (Fig. 3.8D) or song dynamic ranges (Fig. 3.8F) in cells that had non-monotonic tone responses (see Table 3.3 for associated statistics).

In summary, breeding condition increased song-evoked response strengths and dynamic ranges in neurons with monotonic tone responses, but not neurons with non-monotonic tone responses.

3.4.5 Plasma E_2 concentrations predict firing rates and response strengths

The observations that breeding condition influenced auditory response properties in a select subset of field L neurons (Figs. 3.4, 3.5, 3.8) led us to ask whether plasma E_2 concentrations in individual birds correlate with single-unit firing rates or response strengths. To address this question, we compared the response properties of neurons from individual animals with the

circulating level of plasma E_2. As shown in figure 3.9, plasma E_2 concentrations were positively and significantly correlated with spontaneous firing rates ($r = 0.71$, $n = 18$, $p < 0.001$) and maximum evoked firing rates ($r = 0.66$, $n = 18$, $p = 0.003$) of monotonic neurons (Fig. 3.9A). Plasma E_2 concentrations did not correlate with either spontaneous or evoked firing rates in non-monotonic cells (Fig. 3.9B). Similarly, while systemic E_2 levels positively predicted both tone-evoked (Fig. 3.9C) and song-evoked (Fig. 3.9D) response strengths in cells with monotonic rate-level functions to pure tones, there was no correlation between E_2 and response strengths in cells with non-monotonic tone rate-level functions (Fig. 3.9E-F). The response strengths shown in Fig. 3.9C-F were all elicited at 50 dB SPL; we observed similar results at all other sound levels tested (data not shown).

Thus, spontaneous firing rates, maximum firing rates, and sound-evoked response strengths of monotonic, but not non-monotonic neurons, are all modulated by plasma E_2 in a dose-dependent manner.

3.5 Discussion

3.5.1 Hormonal regulation of auditory processing in the central nervous system

The influence of sex steroid hormones on central auditory processing has received considerable attention, particularly for its clinical relevance. The latency of auditory brainstem responses (ABRs) change across the menstrual cycle and after hormone replacement therapy in adult women (Al-Mana et al., 2008, 2010). In addition, sound localization is impaired in women with Turner's syndrome, a chromosomal abnormality that results in estrogen deficiency (Hederstierna

et al., 2009). Recent work in both humans and rodents has demonstrated that ERs are expressed widely in the mammalian auditory system, including auditory cortex (Charitidi et al., 2010; Stenberg et al., 2001; Tremere et al., 2011). Whether plasma hormones affect the response properties of single neurons in the mammalian auditory cortex, however, is currently unknown. One group has reported that mouse cortical multi-unit responses to pup isolation calls differ between mothers and virgins, but the relative contributions of hormonal state and pup care experience cannot be separated in these experiments, and these two variables may interact (Miranda and Liu, 2009). In the current study, we demonstrate that single-unit auditory function in the telencephalon of an avian species is modulated by circulating reproductive hormones in a dose-dependent manner. Together these findings highlight the need for detailed neurophysiological investigations of the mammalian auditory cortex under carefully controlled hormonal conditions.

The majority of work investigating hormonal modulation of central auditory function focuses on the rapid action of brain-derived E_2 to increase neuronal responsiveness in the songbird nucleus NCM (Pinaud and Tremere, 2012). NCM is a secondary nucleus downstream of field L and is specialized for conspecific song processing (Mello et al., 2004). In zebra finches, direct infusion of E_2 into NCM increases single-unit evoked firing rates both locally in NCM and downstream in HVC (Tremere et al., 2009; Remage-Healey et al., 2010; Tremere and Pinaud, 2011; Remage-Healey and Joshi, 2012). Here, we report that E_2 increases neuronal responsiveness in the primary auditory forebrain, indicating that the central effects of sex steroids are not limited to higher processing regions, but extend more generally within the auditory pathway. Surprisingly,

the influence of sex steroids on auditory thresholds has never been assessed at a single or multi-unit level in the telencephalon. We show that monotonic field L cells have lower pure-tone thresholds and expanded song dynamic ranges under breeding condition. These results indicate that hormones do not simply modulate specialized forebrain processing tasks, such as neural song selectivity or discrimination. Instead, E_2 also modulates fundamental aspects of auditory forebrain function across a wide range of stimulus intensities.

3.5.2 Cellular basis of E_2 modulation of field L neurons

In NCM, blockade of ERs decreases neuronal activity (Tremere et al., 2009; Tremere and Pinaud, 2011), suggesting that E_2 influences neuronal responses by binding directly to ERs. Field L does not express classical ERs, (Jeong et al., 2011; Maney and Pinaud, 2011), and expresses little to no GPR30 (a non-classical ER) in adulthood (Acharya and Veney, 2011), but demonstrates a clear sensitivity to E_2. Here, we discuss multiple possibilities for the cellular basis underlying estrogenic modulation of field L neurons.

One possibility is that E_2 directly modulates activity in an area upstream of field L that contains ERs. In songbirds, ERs are absent in the auditory thalamus and midbrain (Gahr et al., 1993; Gahr, 2001). While no systematic study has examined ER expression in the songbird auditory brainstem, ERα is expressed in three chicken brainstem nuclei: magnocellularis, angularis, and laminaris (Wang and Rubel, unpublished observations). Additionally, ERα is expressed in hair cells and support cells of the zebra finch inner ear (Noirot et al., 2009), and in the cochlear ganglion of Gambel's white-crowned sparrows (Wang, Brenowitz and Rubel, unpublished

observations). All of these auditory regions are possible candidates for direct estrogenic influence.

Similarly, field L activity may be modulated by descending input from efferent regions that express ERs. Field L's only known source of top-down input is from the caudolateral mesopallium (Vates et al., 1996; Reiner et al., 2004; Fig. 3.1B), a secondary auditory region that lacks ER expression (Gahr, 1990; Gahr et al., 1993; Metzdorf et al., 1999; Gahr, 2001). E_2 modulation could be initiated instead in brain regions that are indirectly connected with field L. NCM, which expresses ERs (Bernard et al., 1999; Gahr, 2001; Saldanha and Coomaralingam, 2005; Jeong et al., 2011; Maney and Pinaud, 2011), is reciprocally connected to field L via three synapses, which pass through the medial and lateral portions of the cadual mesopallium (Fig. 3.1B). Additionally, the cup of the robust nucleus of the arcopallium is auditory-responsive (Mello and Clayton, 1994) and may express ERs (Gahr et al., 1993). The cup sends projections to the shell of nucleus ovoidalis (Mello et al., 1998), which provides input into field L (Bonke et al., 1979; Vates et al., 1996). None of these pathways can be ruled out at this time.

Another possibility is that E_2 modulates field L activity via monaminergic signaling. The songbird auditory system receives catecholaminergic innervation and these inputs are sensitive to hormonal state (Maney and Pinaud, 2011). For example, sex steroids regulate catecholamine turnover in field L (Barclay and Harding, 1988, 1990). In female white-throated sparrows (a congener to the white-crowned sparrow), systemic E_2 increases the number of catecholaminergic cells in locus coeruleus (LeBlanc et al., 2007) and increases the density of monoaminergic fibers

in the auditory midbrain and forebrain (Matragrano et al., 2011, 2012). Furthermore, monoamines modulate songbird auditory forebrain physiology (Dave et al., 1998; Shea and Margoliash, 2003; Cardin and Schmidt, 2004) and behavioral responses to song playback (Appeltants et al., 2002; Riters and Pawlisch, 2007; Vyas et al., 2009; Pawlisch et al., 2011). Future experiments should test whether intact monoamine signaling is necessary to mediate the effects of systemic E_2 on field L neurons.

3.5.3 Dose-responsive effects of E_2 on central sensory physiology

Few studies have addressed whether the effects of circulating E_2 on central sensory physiology scale with hormone concentration in a graded manner or are exerted in an all-or-none fashion once hormone levels reach some critical level (Oshima and Gorbman 1969). Here we demonstrate that in monotonic neurons, firing rates and response strengths gradually increase with increasing plasma E_2. These findings suggest that individual auditory responsiveness is maximal when plasma E_2 is highest (during courtship and copulation, Wingfield and Farner, 1978) and is less sensitive at other times during the breeding season, when inter-sex communication may be less important. Given the metabolic cost of increased neural activity (Niven and Laughlin, 2008), a graded hormonal effect may serve to reduce unnecessary energy expenditure post-mating, when other behaviors associated with the breeding season (e.g. feeding young, molting) occur.

3.5.4 Cell-specific effect of E_2

We found that E_2 has robust effects on monotonic auditory function while leaving non-monotonic cell processing unchanged. While the precise roles of monotonic and non-monotonic cells in auditory coding are still a matter of speculation, several hypotheses have been proposed. One of these hypotheses, the level-tolerance model, suggests that non-monotonic neurons maintain sound source identity over a wide range of intensities, allowing the frequency content of a complex stimulus to be encoded by neuronal firing rates without the confounding influence of stimulus level (Sadagopan and Wang, 2008). If this model is true, then our findings suggest that E_2 may enhance sound responses in monotonic neurons to allow better signal detection in the breeding season, while the stability of non-monotonic cells might ensure that signal identity remains constant under variable listening conditions. Maintaining a consistent representation of sounds across seasons could be important for the accurate recognition of species or individuals within a flock.

3.5.5 Disparate effects of E_2 within auditory pathway

In a previous study, systemic E_2 treatment elevated ABR thresholds in female white-crowned sparrows (Caras et al., 2010). This result seems to contradict the findings presented here. To reconcile this apparent discrepancy, it is important to note a few important differences between the studies. First, the ABR is a population response, generated by electrical activity in the auditory nerve and brainstem (Hall, 2007). Because no particular pure-tone frequency will elicit an optimal response in all neurons contributing to the ABR, the threshold is actually a measurement of sensitivity to a sub-optimal stimulus. Conversely, in the current study, we

calculated threshold at an individual neuron's optimal stimulus: its CF. Furthermore, because the ABR is a pooled response recorded far-field (Jewett et al., 1970; Jewett and Williston, 1971), it is better described as a measure of neural synchrony, as opposed to firing rate. It is therefore difficult to compare the two measurements directly. Regardless of the methodological differences between the two studies, the possibility still remains that sex steroids have heterogeneous effects on separate portions of the ascending auditory system. This divergence could be explained by differences in hormone receptor expression patterns or mechanisms of hormonal action, as discussed above.

Notes:

This work is currently in press:

Caras ML, O'Brien M, Brenowitz E, Rubel EW (2012) Estradiol selectively enhances auditory function in avian forebrain neurons. J Neurosci *in press.*

I also performed similar experiments on male white-crowned sparrows. For additional information and unpublished results, see Appendix 3.1.

3.6 Tables and Figures

Table 3.1. Auditory responsive cells in field L Values are number of cells; numbers in parentheses indicate number of animals.

	Breeding	**Non-Breeding**
# Total responsive cells	**30* (9)**	**47 (12)**
# Total song responses	21 (8)	37 (11)
# Total tone responses	24 (9)	29 (10)
Only song response	**6 (5)**	**18 (9)**
Only tone response	**9 (7)**	**10 (5)**
Monotonic	3 (3)	9 (5)
Non-Monotonic	6 (5)	1 (1)
Both tone and song response	**15* (6)**	**19 (8)**
Monotonic	9 (6)	7 (5)
Non-Monotonic	6* (3)	12 (7)

*Denotes value excludes an outlier that was removed from the dataset. For explanation of response breakdown see Results.

Table 3.2. Properties of cells under breeding and non-breeding conditions. Values are means ± STDEVs unless otherwise noted. Spike halfwidth, 10 dB bandwidth, mean CF, and mean recording depth were assessed with one-way ANOVAs. The relative numbers of cells under each condition were assessed with Pearson's chi-square test.

	Breeding	**Non-Breeding**	**Effect of breeding condition**	
Monotonic neurons				
Spike Halfwidth (msec)	0.154 ± 0.045	0.154 ± 0.038	$F_{(1,26)} = 0.002$	$p = 0.968$
10 dB Bandwidth (kHz)	1.55 ± 0.78	1.65 ± 0.82	$F_{(1,26)} = 0.107$	$p = 0.746$
Mean CF (kHz)	3.93 ± 1.82	3.78 ± 2.15	$F_{(1,26)} = 0.037$	$p = 0.849$
Mean recording depth (mm)	2.377 ± 0.368	2.270 ± 0.388	$F_{(1,26)} = 0.548$	$p = 0.466$
Number (percent of monotonic cells)	12 (43%)	16 (57%)	$\chi^2_{(1,N=28)} = 0.571$	$p = 0.450$
Non-monotonic neurons				
Spike Halfwidth (msec)	0.167 ± 0.062	0.172 ± 0.052	$F_{(1,23)} = 0.044$	$p = 0.836$
10 dB Bandwidth (kHz)	1.30 ± 0.56	1.16 ± 0.49	$F_{(1,17)} = 0.308$	$p = 0.586$
Mean CF (kHz)	4.53 ± 2.00	4.53 ± 2.05	$F_{(1,23)} = 0.000$	$p = 0.994$
Mean recording depth	2.427 ± 0.421	2.338 ± 0.345	$F_{(1,23)} = 0.334$	$p = 0.569$
Number (percent of non-monotonic cells)	12 (48%)	13 (52)%	$\chi^2_{(1,N=25)} = 0.040$	$p = 0.841$

Table 3.3. Statistics for neurons under breeding and non-breeding conditions. Three separate MANOVAs were performed on each cell population (monotonic and non-monotonic): One encompassed spontaneous rate, maximum evoked rate and firing rate range. Another included CF threshold and CF dynamic range. The third included song threshold and song dynamic range. Individual F statistics and associated *p* values indicating the effect of breeding condition are reported here.

	Effect of breeding condition	
Monotonic neurons		
Spontaneous Rate (sp/s)	$F_{(1,26)} = 9.932$	$p = 0.004$
Maximum Evoked Rate (sp/s)	$F_{(1,26)} = 4.078$	$p = 0.054$
Firing Rate Range (sp/s)	$F_{(1,26)} = 2.274$	$p = 0.144$
CF Threshold (dB SPL)	$F_{(1,26)} = 4.788$	$p = 0.038$
CF Dynamic Range (dB SPL)	$F_{(1,26)} = 2.979$	$p = 0.096$
Song Threshold (dB SPL)	$F_{(1,14)} = 0.732$	$p = 0.407$
Song Dynamic Range (dB SPL)	$F_{(1,14)} = 4.212$	$p = 0.059$
Non-monotonic neurons		
Spontaneous Rate (sp/s)	$F_{(1,23)} = 1.388$	$p = 0.251$
Maximum Evoked Rate (sp/s)	$F_{(1,23)} = 5.001$	$p = 0.035$
Firing Rate Range (sp/s)	$F_{(1,23)} = 6.926$	$p = 0.015$
CF Threshold (dB SPL)	$F_{(1,23)} = 1.118$	$p = 0.301$
CF Dynamic Range (dB SPL)	$F_{(1,23)} = 1.135$	$p = 0.298$
Song Threshold (dB SPL)	$F_{(1,16)} = 0.482$	$p = 0.497$
Song Dynamic Range (dB SPL)	$F_{(1,16)} = 1.623$	$p = 0.221$

Table 3.4. Effects of breeding condition and sound level on tone RS and song |RS| values for monotonic and non-monotonic neurons. Four separate 2-way (condition x level) mixed model ANOVAs were performed. Breeding condition was the between subject measure; sound level was the repeated subject measure. The values listed in each row are the result of a single ANOVA.

	Effect of breeding condition	Effect of sound level	Breeding condition x level interaction
Monotonic			
Tone RS	$F_{(1,26)} = 6.082$ $p = 0.021$	$F_{(7,26)} = 28.14$ $p < 0.001$	$F_{(7,26)} = 2.329$ $p = 0.027$
Song |RS|	$F_{(1,14)} = 4.879$ $p = 0.044$	$F_{(5,14)} = 12.13$ $p < 0.001$	$F_{(5,14)} = 3.020$ $p = 0.016$
Non-Monotonic			
Tone RS	$F_{(1,23)} = 5.269$ $p = 0.031$	$F_{(7,23)} = 12.01$ $p < 0.001$	$F_{(7,23)} = 0.692$ $p = 0.679$
Song |RS|	$F_{(1,16)} = 1.087$ $p = 0.313$	$F_{(4,16)} = 2.039$ $p = 0.099$	$F_{(4,16)} = 1.175$ $p = 0.330$

Table 3.5. Effects of breeding condition on all song responses pooled together. Values are means ± STDEVs unless otherwise noted. The effect of breeding condition on the number of excitatory and suppressive song responses was assessed with Pearson's chi-square test. The effect of breeding condition on maximum song |RS| was assessed with a one-way ANOVA. Song threshold and dynamic range were analyzed together in a one-way MANOVA.

	Breeding	**Non-Breeding**	**Effect of breeding condition**	
Number of excitatory (E) and suppressive (S) song responses	E = 17, S= 4	E = 23, S = 14	$\chi^2_{(1,N=58)} = 2.210$	$p = 0.137$
Maximum song |RS| (sp/s)	5.15 ± 5.12	3.86 ± 4.15	$F_{(1,56)} = 1.090$	$p = 0.301$
Song Threshold (dB SPL)	56.7 ± 22.0	57.3 ± 20.2	$F_{(1,56)} = 0.012$	$p = 0.912$
Song Dynamic Range (dB SPL)	28.6 ± 23.1	21.6 ± 16.6	$F_{(1,56)} = 1.762$	$p = 0.190$

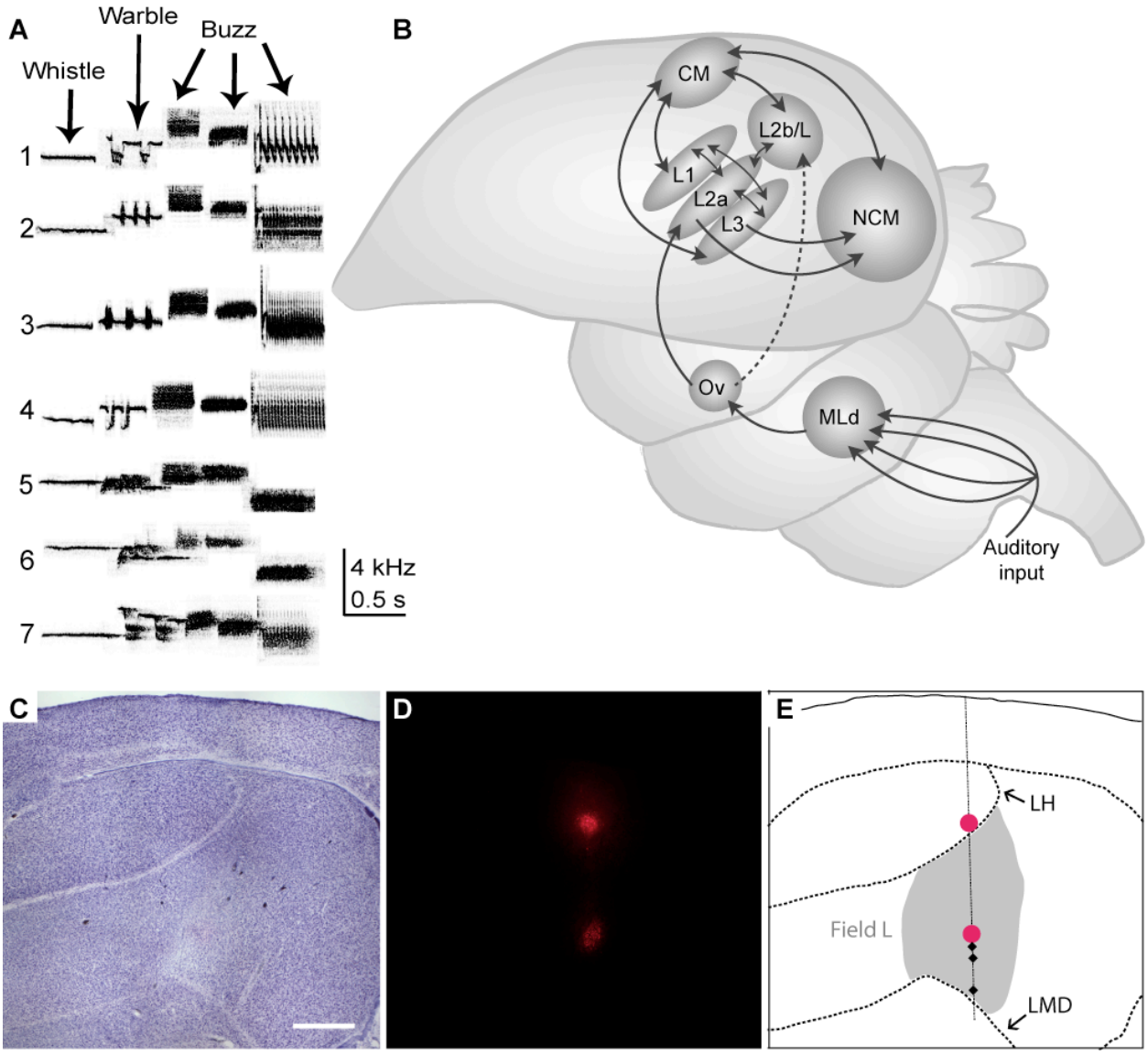

Figure 3.1. Experimental song stimuli, avian auditory schematic and histological reconstruction. A. Individual Gambel's white-crowned sparrow songs were recorded from seven wild-caught males and used as sound stimuli in this study. Typical white-crowned songs consist of five syllables: a whistle, a warble, and three buzzes. In each experiment, song presentation was randomized. **B.** Simplified sagittal schematic of the ascending avian auditory system. Field L, the primary recipient of auditory information coming from the thalamic nucleus ovoidalis (Ov), consists of an interconnected set of subregions (L1, L2a, L2b/L, L3), each of which make connections to secondary nuclei, such as the caudal mesopallium (CM) and the caudomedial nidopallium (NCM). MLd, mesencephalicus lateralis pars dorsalis. Rostral is left; dorsal is up. **C.** Parasagittal nissl stained section from a non-breeding female. **D.** An adjacent parasagittal section from the same non-breeding female shown in C. Two injections of fluororuby were used to reconstruct a single recording track. **E.** Schematic drawing of the section shown in C. Field L, (shaded grey), is bounded dorsally by the hyperpallial lamina (LH)

and ventrally by the dorsal medullary lamina (LMD). Magenta circles indicate injection sites. The dashed vertical line shows the reconstruction of a single electrode track that penetrated through field L. Black diamonds show the location of individual recording sites along the track. Sections were 40 μm thick. Scale bar = 500 μm. Rostral is left; dorsal is up.

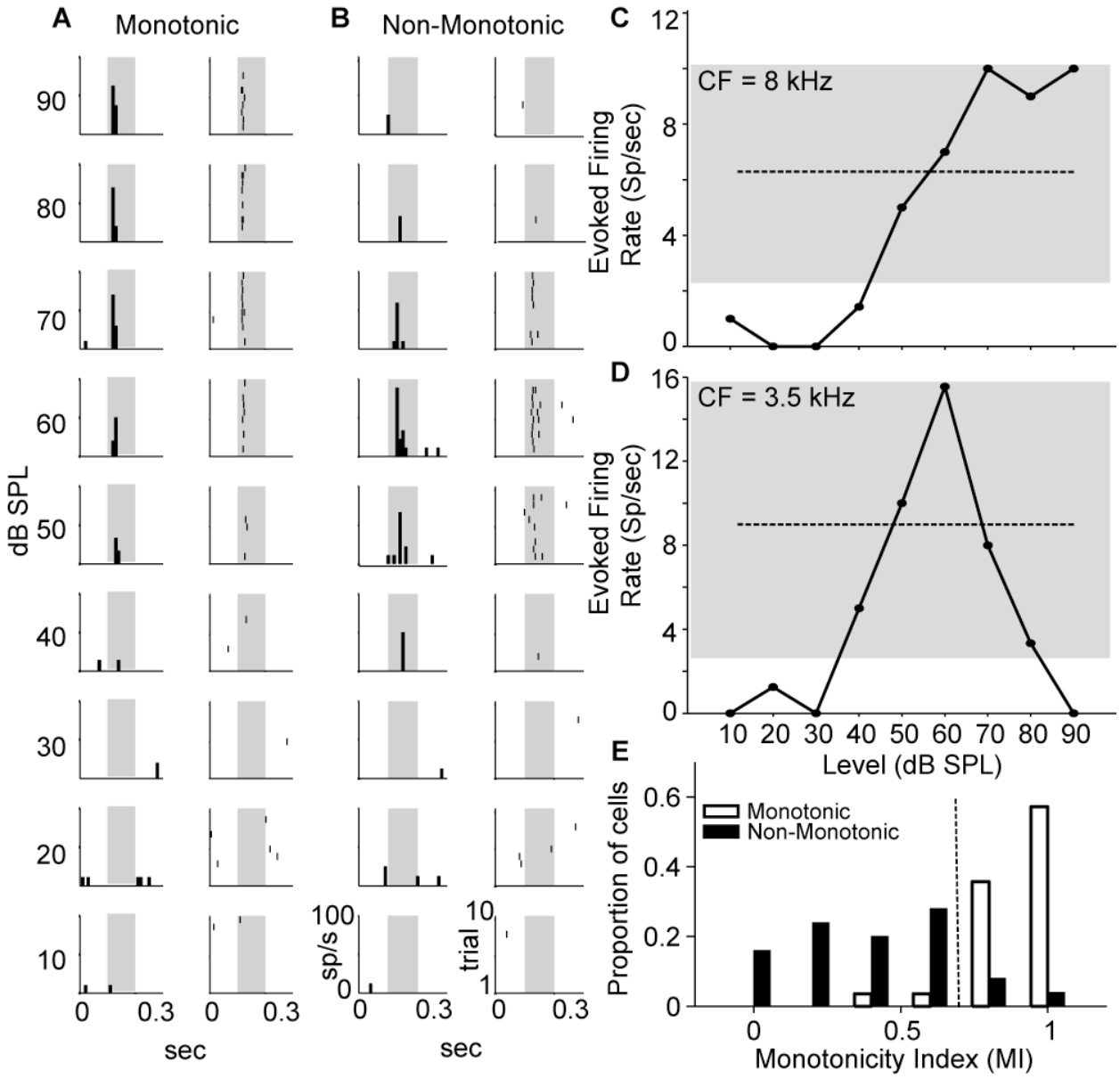

Figure 3.2. Field L contains monotonic and non-monotonic neurons. A. Representative PSTH (left) and raster plots (right) from an individual monotonic neuron in a non-breeding female. Plots were generated in response to ten presentations of the neuron's characteristic frequency (8 kHz) and are arranged in rows by decreasing tone intensity (indicated by dB SPL values on the left). The *x*-axis for each panel shows time (in seconds) as indicated on the bottom row of panels. The *y*-axis for each PSTH panel is the neuron's firing rate in spikes/second; the *y*-axis for each raster panel indicates the trial number. For clarity, only the bottom most panels in B have *y*-axis labels. Stimulus presentations are indicated by grey shaded regions. **B.** Representative raster and PSTH plots from an individual non-monotonic neuron in a breeding female. Characteristic frequency was 3.5 kHz. Plot conventions and labeling as in A. **C.** The rate-level function for the neuron shown in A. The grey shaded region highlights the neuron's firing rate range (sp/s). The dashed line is the halfway (50%) point between the neuron's

maximum firing rate and the noisefloor (2 STDEV above the spontaneous rate) and is the cutoff point for determining whether a neuron is monotonic or non-monotonic. This neuron's evoked firing rate increases with increasing tone intensity and reaches a maximum firing rate at 70 dB SPL. As this neuron's firing rate remained elevated at higher intensities, and never dropped below the 50% boundary, it was classified as monotonic. **D.** The rate-level function for the neuron shown in B. This neuron only increased its evoked firing rate to mid-level tone presentations (50-70 dB SPL). After reaching its maximum rate at 60 dB SPL, the neuron's firing rate drops below 50% of the firing rate range. This neuron was therefore classified as non-monotonic. Plot conventions as in C. **E.** Group histograms for monotonic (white) and non-monotonic (black) neurons showing the proportion of cells with various MIs. Increasing MI values represent increasing degrees of monotonicity. The majority of monotonic neurons have MI values > 0.70 (dotted vertical line), while the majority of non-monotonic neurons have MI values <0.70. The number of cells and the number of birds (in parentheses) are as follows: Monotonic neurons: 28 (16). Non-monotonic neurons: 25 (13).

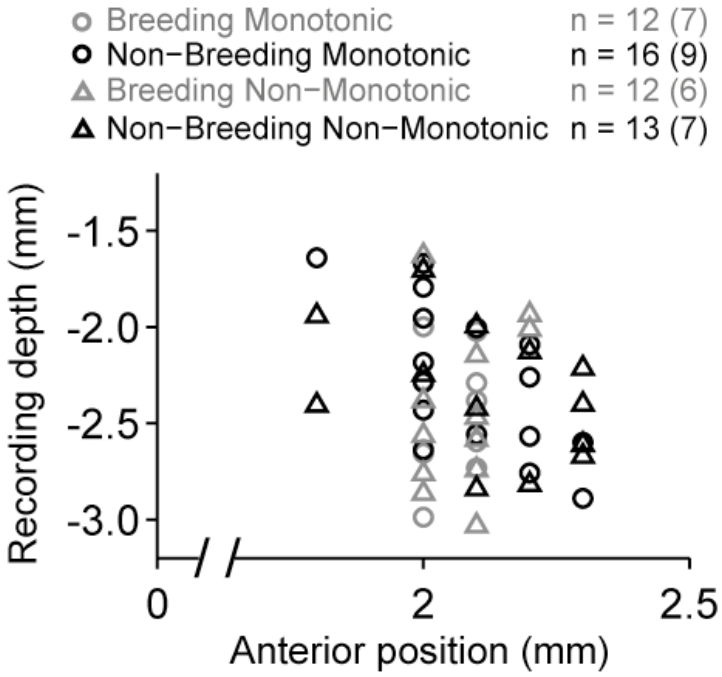

Figure 3.3. Breeding condition does not affect the spatial distribution of monotonic and non-monotonic neurons. The anatomical location of individual tone responsive neurons are plotted as a function of recording depth and anterior distance from the bifrucation of the midsagittal sinus. Breeding (grey) and non-breeding (black) monotonic (circles) and non-monotonic (triangles) neurons are evenly distributed across the anterior-posterior and dorsal-ventral extents of field L. Because the vast majority of neurons were recorded from the same medial-lateral position, all tone-responsive neurons are plotted within a single sagittal plane. Sample sizes for each group are the number of cells, followed by the number of birds in parentheses.

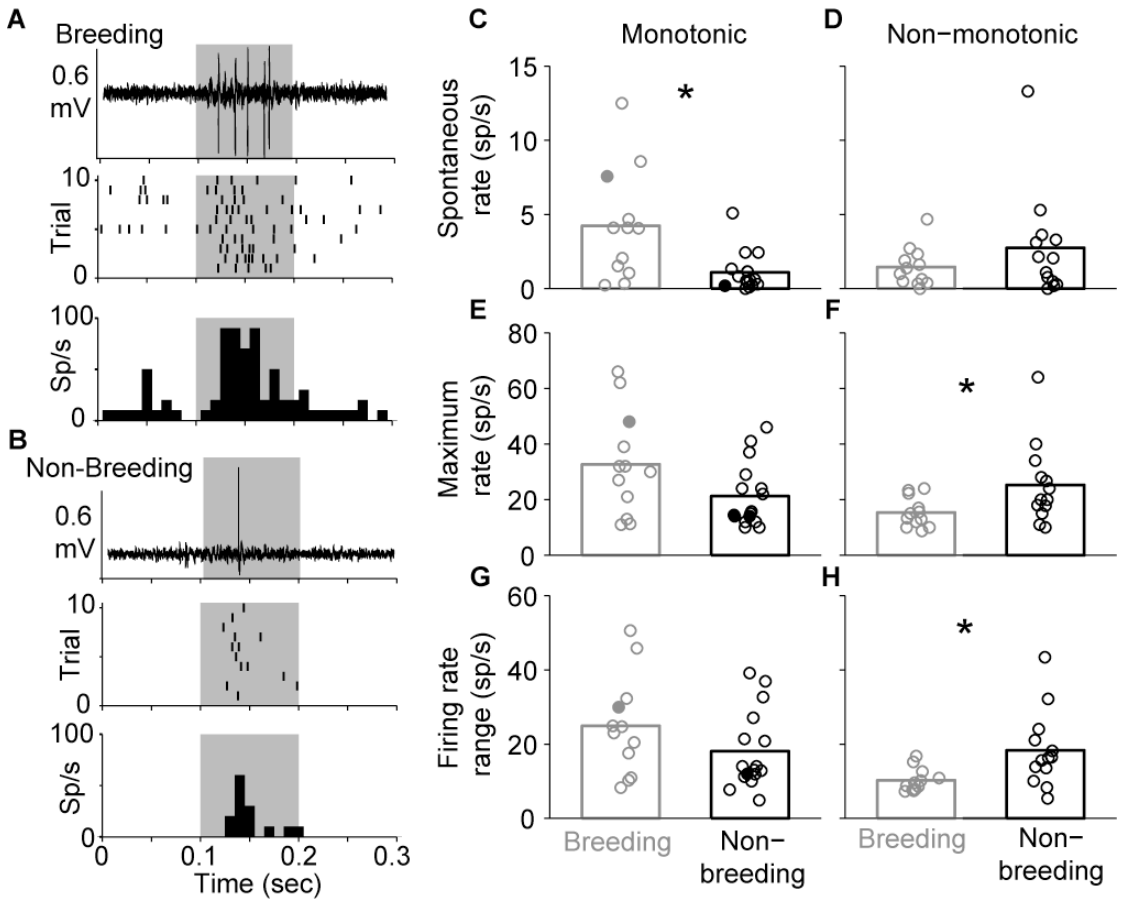

Figure 3.4. Breeding condition modulates activity in a cell-specific manner.
A. Representative raw trace (top), raster (middle) and PSTH (bottom) recorded from an individual monotonic neuron in a breeding female. Raster and PSTH plots were generated in response to ten presentations of the neuron's CF (2.2 kHz) at the stimulus intensity that elicited the neuron's maximum firing rate (80 dB SPL). The single raw trace shows the response to the first presentation of the CF (identical to the bottom row of the raster). Stimulus presentation is indicated by the grey shaded region. This neuron is indicated in panels C, E and G as the filled grey circle. **B.** Representative example from an individual monotonic neuron in a non-breeding female. CF was 1.6 kHz; the intensity that elicited the maximum rate was 70 dB SPL. Plot conventions as in A. This neuron is represented in panels C, E and G as the filled black circle. **C-D.** Breeding condition (grey) significantly increases spontaneous firing rates compared to non-breeding condition (black) in monotonic neurons (C), but does not significantly affect spontaneous firing rates in non-monotonic neurons (D). **E-F.** Breeding condition marginally increases CF-evoked maximum firing rates in monotonic neurons (E), but significantly decreases maximum firing rates in non-monotonic neurons (F). **G-H.** Breeding condition does not significantly affect CF-evoked firing rate ranges in monotonic neurons (G), but significantly decreases firing rate ranges in non-monotonic neurons (H). Bars in C-H are means; circles represent individual neurons. Asterisks indicate statistical significance ($p < 0.05$). The number of cells and the number of birds (in parentheses) are as follows: Monotonic neurons: breeding = 12 (7); non-breeding = 16 (9). Non-monotonic neurons: breeding = 12 (6); non-breeding = 13 (7).

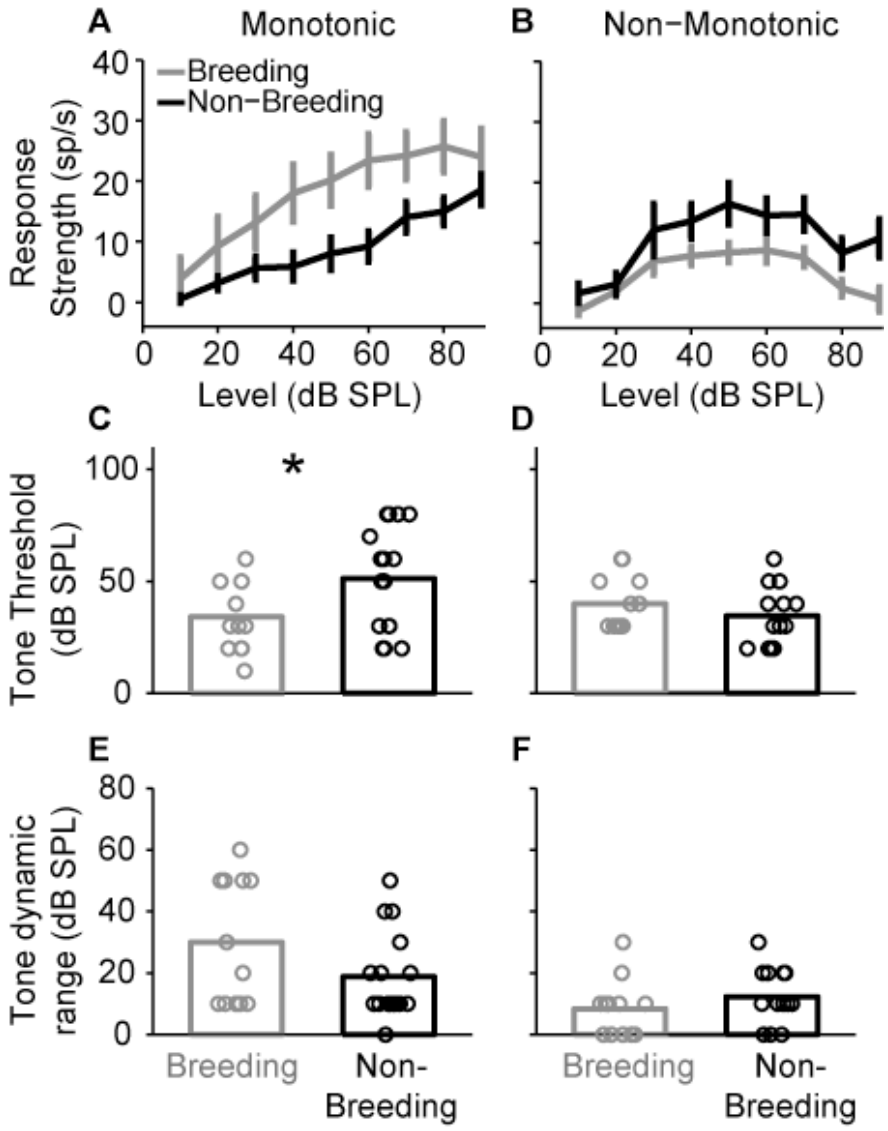

Figure 3.5. Breeding condition selectively increases tone-evoked response strength and sensitivity in monotonically driven neurons. A-B. Breeding condition (grey) significantly increases CF-evoked response strengths compared to non-breeding condition (black) in monotonic neurons (A), but decreases CF-evoked response strengths in non-monotonic neurons (B). **C-D.** Breeding condition selectively decreases CF-evoked thresholds in monotonic neurons (C), but does not significantly affect CF thresholds in non-monotonic neurons (D). **E-F.** Breeding condition does not significantly affect CF dynamic ranges in monotonic neurons (E), or non-monotonic neurons (F). Data in A and B are means +/- S.E.M.s. Bars in C-F are means; circles represent individual neurons. Asterisks indicate statistical significance ($p < 0.05$). The number of cells and the number of birds (in parentheses) are as follows: Monotonic neurons: breeding = 12 (7); non-breeding = 16 (9), except at 90 dB SPL in panel A, monotonic breeding = 11 (7). Sample sizes for non-monotonic neurons are: breeding = 12 (6); non-breeding = 13 (7), except at 90 dB SPL in panel B, non-monotonic breeding = 10 (5).

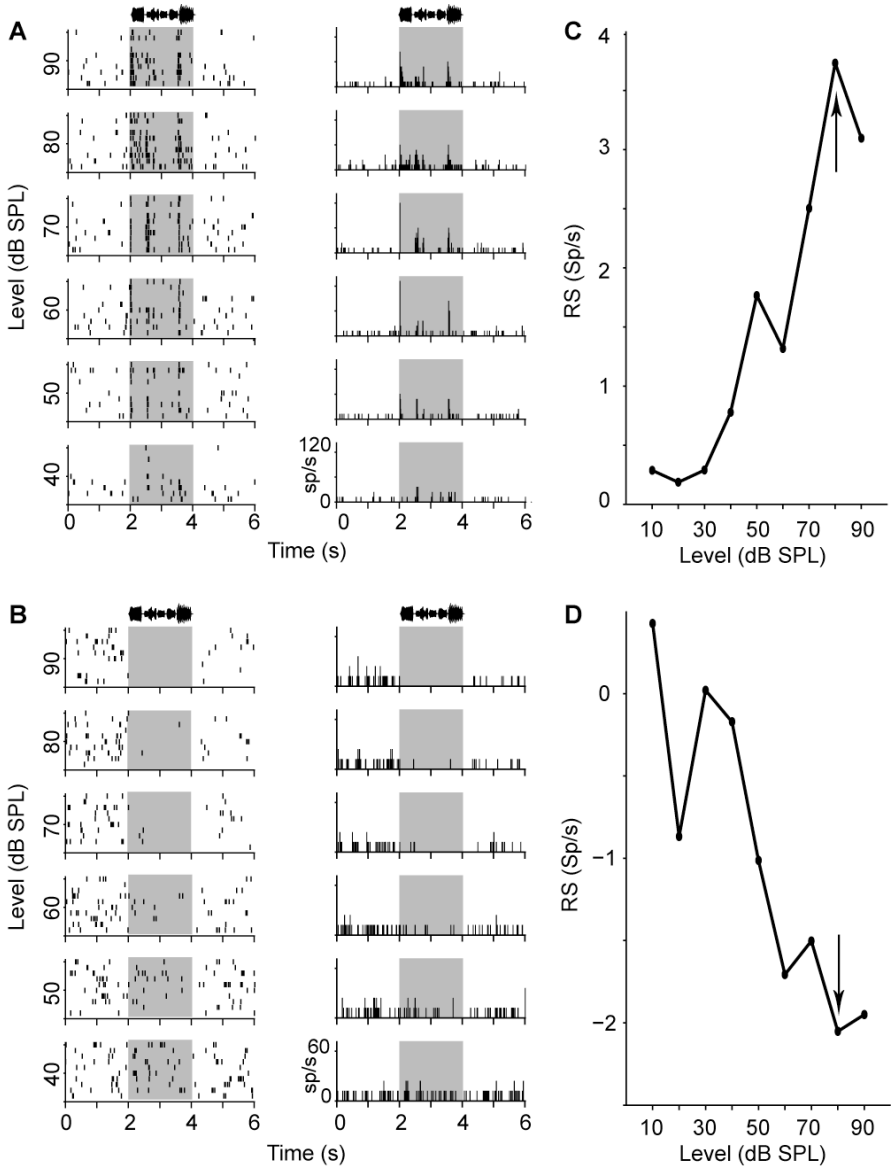

Figure 3.6. Neurons in field L can show suppressive song responses. A. Representative rasters (left) and PSTH plots (right) from a single cell in a breeding female that gave an excitatory song response are arranged in rows by decreasing stimulus intensity. To improve readability, only responses from 40-90dB SPL are shown. The same plot conventions as in figure 3.2 are used. The amplitude envelope of the song stimulus (song #1 in Fig. 3.1A) can be seen at the top of the raster and PSTH plots. This neuron's maximum response is indicated in C by an arrow. **B.** Representative rasters from a single cell in a non-breeding female that gave a suppressive song response. The song stimulus was song # 1 in Fig. 3.1A. This neuron's maximum response is indicated in D by an arrow. Plot conventions as in A. **C.** RS is plotted against song level for the neuron shown in A. As song intensity increased, RS increased above zero, indicative of a excitatory response. **D.** RS is plotted against song level for the neuron shown in B. As song intensity increased, RS decreased below zero, indicative of a suppressive response.

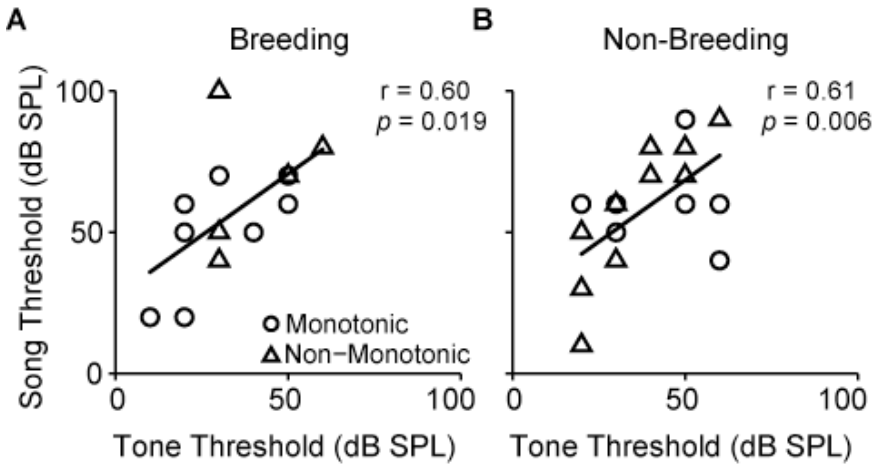

Figure 3.7. Song and tone thresholds are correlated within individual cells in both breeding and non-breeding condition. A. Song and CF thresholds from individual breeding cells are plotted against one another. Circles represent units with monotonic tone responses; triangles represent units with non-monotonic tone responses. Though song thresholds tend to be higher than those evoked by CF, thresholds are linearly correlated. **B.** Non-breeding condition song and tone thresholds are also linearly correlated. Plot conventions as in A. The number of cells and the number of birds (in parentheses) are as follows: Breeding monotonic = 9 (6); breeding non-monotonic = 6 (3); non-breeding monotonic = 7 (5); non-breeding non-monotonic = 12(7).

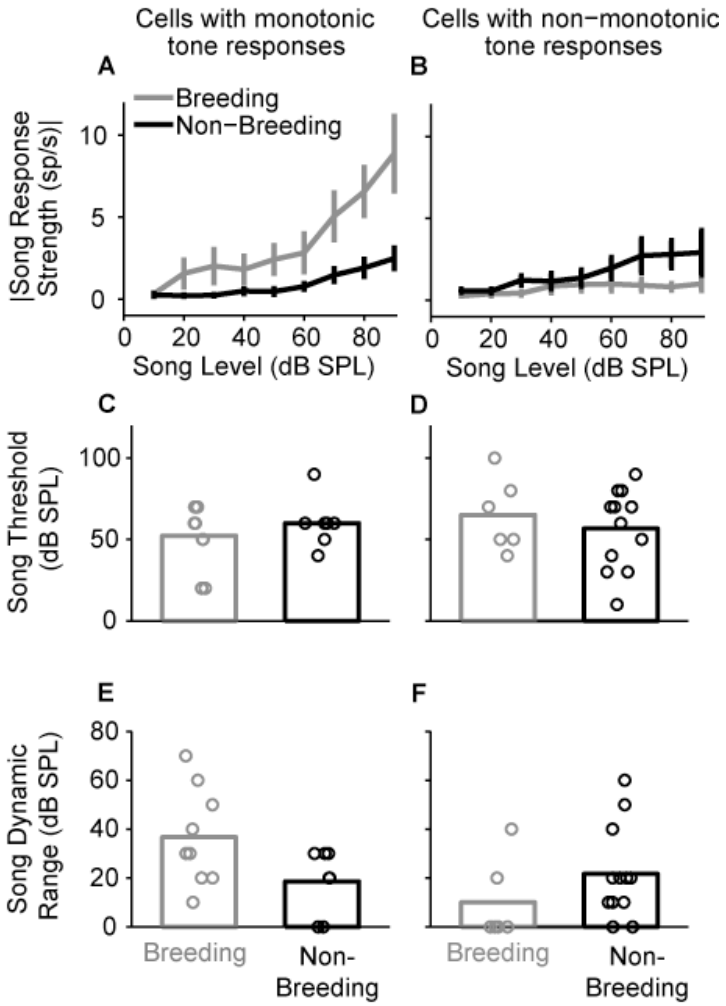

Figure 3.8. Breeding condition increases song response strengths and dynamic ranges in cells that have monotonic tone responses. A. Song |RS| values in cells that have monotonic tone responses are plotted as a function of song level. Breeding condition (grey) increases song |RS| values compared with non-breeding condition (black). **B.** Breeding condition does not significantly affect song |RS| values in cells that have non-monotonic tone responses. **C-D.** Breeding condition does not affect song thresholds in cells that have either monotonic (C) or non-monotonic (D) tone rate level functions. **E.** Breeding condition marginally increases song dynamic ranges in neurons with monotonic tone responses. **F.** Breeding condition does not significantly affect song dynamic ranges in neurons that have non-monotonic tone responses. Data in A and B are means +/- S.E.M.s. Bars in C-F are means; circles represent individual neurons. The number of cells and the number of birds (in parentheses) are as follows: Monotonic neurons: breeding = 9 (6), except at 10, 20 and 90 dB SPL in panel A, where the sample sizes are 6 (4), 7 (5), and 8 (5), respectively; non-breeding = 7 (5), except at 10 dB SPL in panel A, where the sample size was 5 (4). Non-monotonic neurons: breeding = 6 (4), except at 10 and 20 dB SPL in panel B, where the sample sizes are 1 (1) and 4 (3), respectively; non-breeding = 12 (7), except at 10, 80 and 90 dB SPL, where the sample sizes are 11 (6), 10 (6) and 9 (6), respectively.

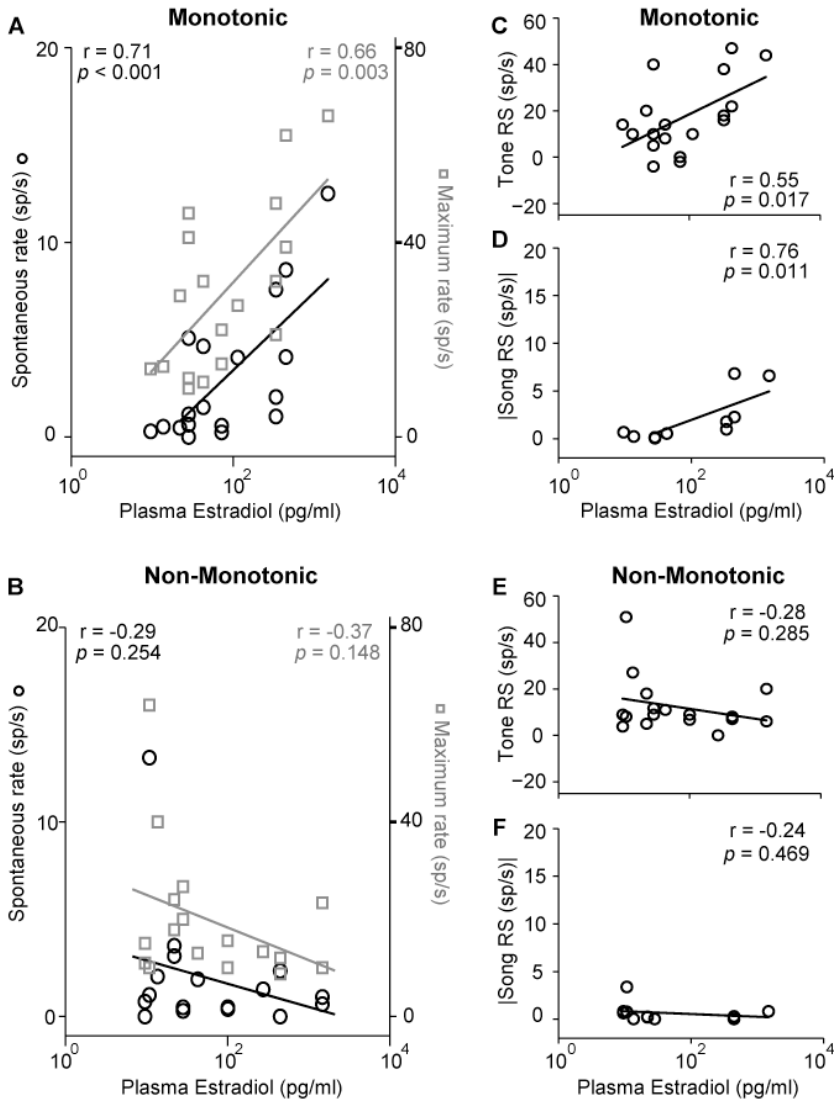

Figure 3.9. Plasma E_2 concentration predicts monotonic neuron firing rates and response strengths. A. Spontaneous (black circles, left axis) and maximum evoked firing rates (grey squares, right axis) for individual monotonic neurons are plotted as a function of circulating E_2 concentration. As plasma E_2 levels increase, spontaneous and maximum rates increase. Note that E_2 levels are plotted logarithmically along the x-axis; firing rates are plotted linearly along the y-axis. **B.** Circulating E_2 does not correlate with spontaneous or maximum evoked firing rates in non-monotonic neurons. Same plot conventions as in A. **C-D.** Individual tone-evoked (C) and song-evoked (D) response strengths increase with increasing levels plasma E_2 in monotonic neurons. **E-F.** E_2 levels do not predict individual tone-evoked (E) or song-evoked (F) response strengths in non-monotonic neurons. Song-evoked response strengths in D and F are absolute values. All responses in C-F were elicited at 50 dB SPL. Similar results were found for all other sound levels tested (data not shown). The number of cells and the number of birds (in parentheses) are as follows: Monotonic spontaneous rate, maximum rate, and tone RS = 18 (10). Non-monotonic spontaneous rate, maximum rate, and tone RS = 17 (10). Monotonic song RS = 10 (7). Non-monotonic song RS = 11 (8).

Chapter 4. Reproductive hormones modulate spike timing-based auditory intensity discrimination

4.1 Summary

In a vocal communication exchange, information is transmitted from a sender to a receiver. Given the fact that in many species, vocal intensity signals some aspect of social or reproductive status, it is of interest to understand the neural strategies underlying intensity discrimination, and to determine whether sex or hormonal state modulates discrimination coding across breeding seasons. We addressed this issue in a songbird, Gambel's white-crowned sparrow (*Zonotorichia leucophrys gambelii*), that demonstrates dramatic seasonal fluctuations in the levels of circulating sex steroid hormones. We recorded single-unit activity in the auditory forebrain of male and female white-crowned sparrows under different breeding conditions and compared two potential coding strategies: one based on spike counts, and one based on spike timing reliability. We report that overall, a spike timing-based strategy more accurately discriminates among vocal intensities than a spike count-based strategy. Additionally, we show that hormonal state selectively modulates spike timing-based discrimination in a sex and intensity specific manner, such that breeding females demonstrate increased discrimination accuracy for low and mid-level stimuli compared to non-breeding females. Our results suggest that spike timing reliability may provide a seasonally plastic neural substrate for the discrimination of incoming vocalization intensities.

4.2 Introduction

Sensory signals in the environment often overlap in time, spatial location, or underlying composition (e.g. intensity, vibrational frequency or chemical make-up). Nevertheless, animals are capable of determining the identity, location, and significance of one particular signal among many. Thus, the question of how objects are discriminated at the neural level is one that has attracted considerable attention, particularly in the context of vocal communication. Work in both mammals and songbirds have identified coding strategies that could be used to discriminate among different vocalizations (Huetz et al., 2006; Engineer et al., 2008; Billimoria et al., 2008; Huetz et al., 2009).

A less-studied, but related question is how the nervous system discriminates among vocalization *intensities*. Intensity discrimination is important for determining the size of the sender, the distance, and in the case of high frequency stimuli, the azimuthal location of a sound source (for review see Grothe et al., 2010). Additionally, if high amplitude vocalizations incur costs, such as increased energy expenditure (Eberhardt, 1994; Oberweger and Goller, 2001; Franz, 2003; Ward et al., 2003), predation risk (Mougeot and Bretagnolle, 2000), or social aggression (Brumm, 2004; Brumm and Ritschard, 2011), they may serve as honest indicators of male quality (Gil and Gahr, 2002). Accurate intensity discrimination might therefore contribute to female mate choice. Furthermore, vocal intensity may signal aggressive intent in a number of avian species, with “soft songs” indicative of social antagonism (Searcy and Beecher, 2009).

A goal of this study is to examine the neural strategies underlying discrimination of natural sound intensities. Traditional views of intensity coding have relied on measures of average firing rate. Neuronal firing rates often saturate at high intensities, however, which limits the dynamic range over which intensities can be discriminated. An alternate strategy could make use of absolute spike times or spike timing reliability; indeed, spike-timing based codes have proven successful in other auditory discrimination tasks (Schnupp et al., 2006; Narayan et al., 2006; Huetz et al., 2006; Wang et al., 2007; Engineer et al., 2008; Billimoria et al., 2008; Huetz et al., 2009). In addition, the fact that vocal intensity is so intertwined with mate choice and territorial defense raises the possibility that neural intensity discrimination strategies change across breeding conditions.

Here we address these issues in a seasonally-breeding songbird, Gambel's white-crowned sparrow (*Zonotrichia leucophrys gambelii*). In this species, both vocal motor (Meitzen et al., 2007a, 2007b, 2009a, 2009b) and auditory function (Caras et al., 2010; 2012) are modulated by circulating levels of sex steroid hormones, which fluctuate on a seasonal basis (Wingfield and Farner, 1978). We brought male and female white-crowned sparrows into either breeding or non-breeding condition in the laboratory and recorded single-unit activity in two established auditory regions: field L, the primary recipient of ascending auditory input from the thalamus, and the caudolateral mesopallium (CLM), a nucleus reciprocally connected to field L that displays auditory properties specialized for conspecific song processing. We also recorded auditory responses in an uncharacterized region just ventral to field L (see *Histology*, Table 4.1 and Fig 4.1). None of these brain regions are known to express sex steroid hormone receptors,

but auditory responses in field L are sensitive to plasma hormone levels (Caras et al., 2012). We report that a timing-based coding scheme achieves better overall intensity discrimination than a rate-based strategy, and that breeding condition alters timing-based, but not rate-based discrimination.

4.3 Materials and Methods

4.3.1 Subjects

Adult male (n = 15) and female (n = 18) Gambel's white-crowned sparrows were captured in eastern Washington state during autumn and spring migrations between 2007 and 2011. Birds were housed at the University of Washington in outdoor aviaries before being moved indoors. Once inside, all birds were housed in walk-in aviaries on a short-day photoperiod (SD, 8 hr light : 16 hr dark) for at least 10 weeks to ensure sensitivity to photoperiod and hormones (Wingfield et al., 1979). Food and water were freely available. All procedures were approved by the Institutional Animal Care and Use Committee at the University of Washington, Seattle.

4.3.2 Hormone and photoperiod manipulations

We manipulated light and hormone levels to mimic non-breeding and breeding conditions in the laboratory. To induce a non-breeding state, birds (males = 7, females = 10) were housed on a SD photoperiod. Under these conditions, gonads are regressed, plasma sex hormone levels are low, and neural morphology and physiology are typical of the non-breeding season (Middleton, 1965; Smith et al., 1995; Tramontin et al., 2000; Park et al., 2005; Meitzen et al., 2007a). To induce a breeding state, males (n = 8) and females (n = 8) were housed on a long day (LD; 20 hr light : 4

hr dark) photoperiod typical of their Alaskan breeding grounds. Additionally, because supplemental hormone is necessary to raise plasma hormone levels of laboratory-housed birds to physiological levels observed in the wild (Smith et al., 1995), these birds received subcutaneous hormone pellets made from SILASTIC tubing (i.d. 1.0mm; o.d. 2.0mm, length 12mm; VWR), filled with crystalline testosterone (T, males) or estradiol (E_2, females; Tramontin et al., 2003). Birds were exposed to these conditions for three weeks, a time period sufficient to induce morphological and physiological changes typical of the breeding season (Tramontin et al., 2000; Park et al., 2005; Meitzen et al., 2007a).

4.3.3 Electrophysiology

Methods for *in vivo* electrophysiology have been described previously (Caras et al., 2012). Briefly, birds were anesthetized with 25% urethane (6 µl/g body weight, Thermo Fisher Scientific) and were secured to a head holder that served as a stereotaxic device. A small craniotomy was made in the right hemisphere and a micropipette (5-19 MΩ impedance) filled with 10% fluororuby (10,000 MW tetramethylrhodamine dextran, Invitrogen) or 10% biontinylated detran amine (BDA 10,000 MW, Invitrogen) in 0.9% NaCl was advanced into the auditory lobule. Body temperature was maintained at 40-42 ^{o}C throughout the recording sessions (TC-1000 Temperature Controller, CWE Inc.). Up to three recording tracks were made in each bird.

Spikes were amplified 10,000X (ISO-80, World Precision Instruments and MA3, Tucker Davis Technologies), filtered 0.1-10 kHz (Krohn-Hite model 3550), digitized at 24.4 samples/sec (RX6

multifunction processor, Tucker Davis Technologies), and monitored online. Custom MATLAB scripts (David Schneider and Sarah Woolley, Columbia University) were used to analyze raw waveforms offline to ensure that only well-isolated single units were included in the dataset (Caras et al., 2012). The vast majority of recordings that were ultimately included in our analysis (69/73) met the criteria for single-units. The remaining 4 recordings demonstrated two separable waveforms with high signal-to-noise ratios. These waveforms were manually sorted offline and verified by principal components analysis.

Songbird auditory processing is lateralized, but depends on a number of factors, including species, anesthesia, brain region, analysis type, sex, and stimuli (Cynx et al., 1992; George et al., 2004, 2005; Avey et al., 2005; Hauber et al., 2007; Poirier et al., 2009; Phan and Vicario, 2010). Therefore, in order to avoid a potential lateralization confound, we chose to focus only on the right hemisphere for these experiments.

4.3.3.1 Stimulus delivery and calibration

The stimulus delivery system and calibration procedures have been used previously (Caras et al., 2010; 2012). A custom-made sound delivery tube enclosing a small speaker (Etymotics ER-2B) and microphone (Etymotics ER-10B) was positioned flush against the skull around the left external auditory meatus and sealed with Petroleum jelly. Custom scripts (Python) delivered stimuli through an RX6 multifunction processor (Tucker Davis Technologies).

For our initial experiments, we used a band-limited white-noise-generated calibration table of sound pressure levels (dB SPL re: 20 μPa) to determine root-mean squared sound pressure levels (RMS dB SPL) for song stimuli. In later experiments, we determined RMS dB SPL values separately for each song. The levels for earlier recordings were corrected for each song type presented. RMS intensities for song stimuli were reliable within ≤ 4.9 dB SPL.

4.3.3.2 Auditory stimuli

The auditory stimuli used in this study have been described elsewhere (Caras et al., 2012). Pure tones were 100 msec long; rise-fall times were 5 msec linear ramps. Songs were recorded (Syrinx, John Burt, www.syrinxpc.com) from 7 individual breeding-condition male Gambel's white-crowned sparrows. Each bird contributed one song to the stimulus set.

The majority of our song stimuli were unfamiliar to all of our experimental birds. Three songs, however, were recorded from males that had overlapping periods of captivity with some of the experimental birds, and therefore may have been familiar. Song familiarity can affect neurophysiological responses in CLM, but not field L (Theunissen et al., 2004). To address this issue, we treated all potential instances of familiarity as familiar; the remaining recordings were considered to be presentations of novel stimuli. Song familiarity did not affect spike timing-based or spike count-based percent correct values in CLM (independent sample t-tests, all $p > 0.05$, data not shown). Additionally, because we recorded auditory-responsive units in a previously uncharacterized area just ventral to L (see *Histology*), we also assessed the effect of song familiarity in that region. Again, song familiarity had no effect on percent correct values

(all $p > 0.05$, data not shown). We therefore did not include song familiarity as a factor in our data analysis.

4.3.3.3 Data acquisition

Data acquisition procedures have been used previously (Caras et al., 2012). Briefly, band-limited white noise (0.25-8 kHz) at 80 dB SPL was used as a search stimulus. Once a cell was isolated, one song, chosen at random, was presented at a rate of 0.14/sec.

Because we wished to examine neural coding of intensity discrimination, we presented stimuli at a wide range of amplitudes (-10 to 110 RMS dB SPL). Within that range, however, each cell was only presented with 9 different (but consecutive) intensities. Songs were presented in 10 dB descending steps, with ten trials at each intensity. We note here that many avian species are capable of generating high-amplitude vocalizations; maximum values from 74 to 111.5 dB SPL have been reported at a distance of 1 m (Brackenbury, 1979; Brenowitz, 1982; Nemeth, 2004). Therefore, we consider the stimulus intensities used in these experiments to be within a normal, behaviorally relevant range.

4.3.4 Data Analysis

4.3.4.1 Inclusion criteria

One of the goals of this study was to examine the neural strategies underlying intensity discrimination. When defining our inclusion criteria, therefore, we purposely avoided using quantitative measures that rely on *a piori* knowledge of the nature of a cell's response. Instead,

we chose a qualitative approach, as described below. Similar approaches have been used by previous researchers (Huetz et al., 2009).

We recorded activity from 289 isolated single units in 39 birds. Because of the nature of our spike timing reliability measurement (see *Pattern Classifier* below), we initially restricted our analysis to 91 cells that demonstrated spiking activity in every recorded trial. The activity of these 91 cells were examined offline by three trained observers blind to experimental treatment. For every cell, each observer was provided with stimulus-evoked rasters and/or PSTHs at nine different stimulus intensities. Observers were asked to determine whether each cell was "responsive" to the stimulus presented; excitatory, suppressive, and/or time-locked firing at any stimulus intensity could qualify as a response. Furthermore, if a cell was considered responsive, observers were asked to estimate the cell's threshold, defined as the lowest stimulus intensity to elicit a response.

Of the 91 cells examined, 14 were determined by at least two observers to be unresponsive and were removed from the analysis. Of the remaining 77 cells, 9 generated substantially different threshold estimates from each observer, or were considered unresponsive by one observer, but not the others. To resolve these discrepancies, two additional trained, blind observers were asked to examine the activity of these cells. Two of the cells were ultimately categorized as unresponsive and were removed from the analysis. Finally, of the remaining 75 cells, all except 2 were localized to CLM, field L, or a region just ventral to L (see *Histology* below); these 2 cells were therefore also removed, yielding a total of 73 neurons from 33 birds that were included in

our analyses. A final breakdown of the number of cells and birds by sex and breeding condition can be found in table 4.1.

Some of the neurons included in our analysis were used in a previous study (Caras et al., 2012). That work focused on the role of E_2 on basic auditory function in field L of female white-crowned sparrows, and was restricted to rate-based analyses. Intensity discrimination was not addressed, nor was the potential influence of spike timing.

4.3.4.2 Threshold estimates

As explained above, we used a blind observer approach to estimate cell thresholds. Of the 73 cells included in our analysis, 27 elicited identical threshold estimates from all three blind observers. In instances when one observer was in disagreement, threshold was taken as the estimate provided by the other two observers (36 cells). In 5 cases, each observer identified a different threshold; however, each of these estimates differed by only 10 dB SPL (as, for instance, if each observer estimated 30, 40 and 50 dB SPL, respectively). In these cases, the middle threshold (40 dB SPL in the previous example) was taken as threshold, with the rationale that the middle estimate represents the value that the observers were converging on. Finally, in 7 cells, each threshold estimate differed by more than 10 dB SPL. In these cases, two additional observers provided estimates that were used to resolve the discrepancies.

4.3.4.3 Pattern Classifier

We analyzed the ability of cells to discriminate among different intensities by adopting a spike train pattern classifier (Machens et al., 2003; Narayan et al., 2006; Wang et al., 2007; Billimoria et al., 2008; Fig. 4.2). The classifier was applied to each cell individually as follows. A template spike train was randomly chosen from one of the 10 trials for each stimulus intensity. The remaining spike trains were assigned to the stimulus intensity with the closest template based on two metrics: the "spike count" metric and the "spike timing" metric. These metrics are described in more detail below. We repeated this procedure 100 times; at the beginning of each repetition, we randomly selected a new set of template spike trains. Intensity discrimination was quantified as the percent of correctly assigned spike trains. Chance performance was 11.11% because a spike train could be assigned to 1 of 9 different intensities.

The "spike count" metric first counted the total number of action potentials in each spike train (both templates and non-templates). The metric then calculated the absolute difference in the number of spikes between each remaining spike train and each template. Spike trains were assigned to intensities by minimizing this absolute difference (Fig. 4.2).

The "spike timing" metric uses an established correlation-based measure of spike timing reliability, R_{corr} (Schreiber et al., 2003; Wang et al., 2007). First, the metric established a gaussian filter of mean 0 and SD σ; this filter was used to smooth all of the cell's spike trains. The temporal similarity of two smoothed spike trains, $\vec{s_i}$ and $\vec{s_j}$ is calculated as follows:

$$R_{\text{corr}} = \frac{\vec{s_i} \bullet \vec{s_j}}{|\vec{s_i}|\,|\vec{s_j}|},$$

R_{corr} is a normalized measure ranging from -1 to 1. A value of 1 indicates a perfect correlation between the pair of spike trains being compared; -1 indicates perfect anti-correlation, and 0 indicates no relationship. Spike trains were assigned to the stimulus intensity whose template gave the maximum value of R_{corr} between it and the spike train.

The temporal resolution of the R_{corr} analysis is controlled by σ. An optimal σ is small enough to capture the dynamics of spiking activity on a fine time scale, but large enough to allow for negligible amounts of jitter in the spike times. We did not know *a priori* what the optimal σ was, and it was possible that it was different for each cell. Therefore, for each set of templates, we made spike train assignments after smoothing the trains with gaussian filters of differing widths. The width varied from 3 to 600 msec in intervals of 3.

The output of each metric was the percentage of correctly assigned spike trains. The spike count metric generated 100 of these estimates, one for each repetition of the classifier. These were averaged to obtain and mean and standard deviation of the percent correct. The spike timing metric output 100 of these estimates for each σ tested. An average and stdev were calculated for each σ. The σ that generated the highest average percent correct was considered the optimal σ; all of the spike timing data reported here were generated at each cell's optimal σ unless otherwise stated.

The intensity discrimination measures described above were applied to stimulus-evoked spike trains. As a control, we also applied these measures to spontaneously generated spike trains. For these analyses, the gaussian filter width was set to the optimal σ identified for the stimulus-evoked spike trains.

R_{corr} cannot be calculated between two spike trains if one of them contains no spikes. We originally considered setting up the classifier so that only non-empty spike trains could be selected as templates, and all empty remaining spike trains would not be analyzed. This strategy would allow us to include cells that did not fire at least one action potential in every stimulus-evoked trial in our analysis. The absence of spiking, however, while meaningless in a spike timing context, is meaningful when considering spike counts. That is, while an R_{corr} value cannot be calculated if one spike train is empty, a spike count value (zero) can be calculated. Thus, analyzing only non-empty spike trains could potentially bias the output of the spike count metric. Therefore, as mentioned above (*Inclusion criteria*), we restricted our analysis to cells that had at least one spike in every stimulus-evoked trial, which allowed us to calculate both R_{corr} and spike count values for every potential pair of spike trains.

4.3.5 Histology

Histological and electrode track reconstruction procedures have been described previously (Caras et al., 2012). Briefly, electrode tracks were marked by two injections using either iontophoresis (10% fluororuby, 32/33 birds, BAB-501 Iontophoresis pump, Kation Scientific) or pressure injection (10% BDA , 1/33 birds, Parker Picospritzer).

At the end of each recording session, birds were perfused (phosphate-buffered saline, followed by 4% paraformaldehyde), brains were postfixed, cryoprotected, embedded in gelatin and postfixed again to let the gelatin become firm. Parasagittal 40 μm sections were cut on a freezing microtome, mounted onto gelatin-subbed slides and processed for Nissl; alternates were air dried until fluorescent or BDA processing.

Sections containing fluororuby were cleared, coverslipped and dried overnight. Sections containing BDA were incubated in 30% hydrogen peroxide in 100% methanol, rehydrated in phosphate buffered saline, and visualized using the ABC-DAB method (Vector Laboratories, Sigma). All images were captured on a Olympus BH2 microscope fitted with a Qimaging camera and Qcapture software.

Of the 73 cells in our analysis, 53 of them were localized to either CLM or field L. Ten cells were on the border between CLM and L and could not be definitively localized to one region or another. The remaining 10 cells were in a region just ventral of field L. Four of these fell just below the dorsal medullary lamina (the most ventral boundary of field L); the remaining 6 were deeper, spanning a region ~100-400 μm below the lamina (Table 4.1, Fig 4.1). The cells in this region did not differ significantly in intensity discrimination compared to cells in the other three areas (CLM, CLM/L border, and L, all $p > 0.05$) and were therefore included in our analyses.

Our main findings highlight sex and breeding condition differences in discrimination performance as a function of stimulus intensity (see *Results*). We wished to determine whether

our group effects were related to the anatomical location of our recording sites. Thus, we performed a 2-way mixed model (location x intensity) on spike timing and spike count-based percent correct values. There was no effect of location on percent correct values for either metric, nor were there any interactions between location and intensity (all $p > 0.05$). In addition, we performed chi-square analyses to determine whether anatomical locations were represented equally across all experimental groups. We found no significant group differences in the number of cells from each location (all $p > 0.05$). Therefore, we concluded that our group effects were unrelated to the anatomical location of our recording sites and we did not include location as a factor in any further analyses.

Finally, we note that field L is a heterogeneous complex made up of different subregions that demonstrate differences in spectrotemporal tuning (Sen et al., 2001; Nagel and Doupe, 2008; Kim and Doupe, 2011). It is therefore possible that intensity discrimination and/or the effect of breeding condition differs among these sub nuclei. Previous investigations of song discrimination using similar computational methods to those described here have treated field L as a single entity (Narayan et al., 2006; Wang et al., 2007; Billimoria et al., 2008). Our primary reason for choosing to follow the same approach is the fact that due to the multi-dimensional nature of our experimental design, we lacked sufficient statistical power to separate responses into further subcategories.

4.3.6 Hormone measurement

We collected blood from the alar wing vein of each bird into a heparinized tube and centrifuged the sample at 4°C immediately before each recording session. We stored separated plasma at -80°C until Enzyme-Linked Immunosorbent Assay (ELISA). Plasma E_2 levels were assayed using a kit from Cayman Chemicals. All of the E_2 levels reported here were originally measured for a previous study (Caras et al., 2012). Plasma T levels were assayed using a standard kit from Enzo Life Sciences (formerly Assay Designs) that successfully was used with white-crowned sparrow plasma in a previous study (Caras et al., 2010).

Briefly, aliquots of each sample were run with kit standards following each kit's protocol. Each steroid was measured in a single assay. Some female samples were lost during preparation; therefore, only 6/8 breeding female samples and 5/10 non-breeding female samples were assayed. Most samples and all of the kit standards were run in duplicate; however, 3 breeding female and 2 non-breeding female samples were run singly because of insufficient sample volume. Because T levels in breeding males can exceed the highest range of the T kit's detectability (2 ng/ml), we made a 1:20 dilution of each breeding male sample with assay buffer. After incubating samples with with antiserum and a steroid-enzyme conjugate, wells were emptied and washed, and substrate was added to all sample wells. Plates were read immediately at 405 nm on a Dynex MRX II microplate reader.

We plotted the optical densities of the kit standards as a function of known hormone concentration and fit the points with a sigmoid 4PLC equation; sample hormone levels were extrapolated from this standard curve. Intra-assay variability was 6.50% (E_2) and 9.94% (T).

4.3.7 Statistics

We used a Mann-Whitney U test to compare E_2 and T levels across experimental conditions. Paired t-tests were used to compare the overall percent of correctly assigned spike trains between the spike timing and spike count classifier. One-sample t-tests were used to compare classifier performance to chance. Cumulative distribution plots were assessed using Kolmogorov-Smirnov two-sample tests. All correlations were assessed with Pearson's *r*. A 2-way MANOVA was used to assess the effect of recording location and song familiarity on timing-based and count-based intensity discrimination.

To make these comparisons at individual stimulus levels, we used a two-way repeated-measures ANOVA (with stimulus level and classifier type as within subject conditions). For some cells, we had an incomplete dataset, such that a given stimulus was only presented for a limited range of intensities. These missing values presented an obstacle for running a repeated measures ANOVA. We therefore aimed to include as many stimulus levels as possible while still including the majority of our cells. When an effect of classifier type was present, we performed individual paired t-tests at all stimulus levels (including those that were originally excluded from the ANOVA) for which we had sufficient sample sizes. We report Bonferroni adjusted *p* values.

Unless otherwise stated, all values are reported as means +/- S.E.M.s. All statistical analyses were made using PASW Statistics 18.0 or Graphpad Prism.

4.4 Results

4.4.1 Plasma hormone levels

Females housed under breeding condition had higher levels of plasma E_2 than their non-breeding housed counterparts (Table 4.2). These levels are similar to the physiological range reported for wild breeding female white-crowned sparrows (~300-500 pg/ml E_2; Wingfield and Farner, 1978). Breeding condition also elevated T levels in our male birds (Table 4.2), though the breeding levels we report here are slightly higher than what has been observed in wild breeding males (4-10 ng/ml T; Wingfield and Farner, 1978).

4.4.2 Output for a single representative cell demonstrates successful intensity discrimination using both spike timing and spike count-based neural strategies

We analyzed the intensity discrimination of 73 single-units using spike count-based and spike timing-based pattern classifiers (Table 4.1). For each cell, both classifiers were run 100 times to obtain an average percent of correctly assigned spike trains based on spike counts, and an average value based on spike times. To determine whether 100 repetitions were sufficient for our analysis, we plotted the mean and standard deviation of the percent correct as a function of the number of classifier repetitions. Figure 4.3 shows the output of classifier for a single cell that demonstrated above chance performance with both classifiers. As shown in panel B mean percent correct values reach stability before 100 repetitions. This convergence was observed for

values obtained using spike counts, as well as spike timing-based values using different gaussian filter widths (σ). Similarly, the standard deviation of the percent correct also stabilizes before reaching 100 repetitions (Fig 4.3C). After verifying that all cells in our analysis demonstrated this convergence (data not shown), we concluded that 100 repetitions were sufficient.

Before comparing timing and count-based intensity discrimination capabilities, we first needed to determine the optimal gaussian σ for each cell. Figure 4.3D shows the percent of correctly assigned spike trains using the spike timing-based classifier as a function of σ for the single representative cell discussed above. As σ increases, the percent correct value drops to chance performance, albeit in a non-linear manner. All of the cells in our analysis showed this general trend of decreased performance for wider widths (not shown). We defined the optimal σ for each cell as the value that gave the highest percent of correctly assigned spike trains; in this example, the optimal σ was 18 msec (Fig. 4.3D).

We used the optimal σ for each cell to compare spike timing and spike-count based methods of intensity discrimination (Fig 4.3E). Our example cell performed significantly better than chance for both spike timing ($t_{99} = 51.0$, $p < 0.001$), and spike count-based classifiers ($t_{99} = 58.7$, $p < 0.001$). In addition, for this cell, the spike count-based classifier slightly, but significantly, outperformed the spike timing-based classifier by an average of 5.60% ($t_{99} = -6.61$, $p < 0.001$).

The overall percent correct value, while useful, does not give us any information about how each classifier performs at individual stimulus intensities. Therefore, we created confusion matrices

for each cell, plotting the proportion of all spike trains for a given stimulus level (*y*-axis) assigned to each stimulus level (*x*-axis) by the spike timing (Fig. 4.3F) and spike count-based classifier (Fig 4.3G). Perfect performance would be indicated by a red diagonal line running from the upper-left to the lower right of each plot. For the spike timing classifier, our example cell showed above chance performance at the majority of stimulus levels, with performance reaching a maximum at 90 dB SPL. The spike count metric, on the other hand, showed peak performance at mid-level sound intensities (40-50 dB SPL). These results indicate that this cell is able to use both spike timing reliability and spike counts to discriminate sound intensities over a wide range; however, depending on the stimulus intensity, one strategy may be more accurate than the other.

4.4.3 A spike timing-based strategy achieves better intensity discrimination than a spike count-based strategy

To compare neural strategies for intensity discrimination, for each cell, we plotted the percent of correctly assigned song-evoked spike trains for the spike timing metric against the percent correct for the spike count metric (Fig. 4.4A). The majority of cells fall above the unity line, indicating superior intensity discrimination when spike timing-based classification is used. Averaged across all cells, the spike timing metric yielded a higher percent of correctly assigned spike trains than the spike count metric ($23.42 \pm 0.998\%$ vs. $16.95 \pm 0.780\%$; $t_{72} = 7.178$, $p < 0.001$). Similarly, the cumulative distributions of song-evoked percent correct values shows a difference between classifiers; the spike timing-based distribution shows a significant shift to the right, towards higher values ($D = 0.4110$, $p < 0.001$, Fig. 4.4B).

We wanted to be sure that classifier performance was actually related to song-evoked spiking activity, rather than spontaneously generated changes in spiking activity or timing correlations. To address this issue, we ran the classifier a second time for each cell. In this analysis, σ was set to the optimal value as previously determined using song-evoked spike trains. We then ran the classifier on the spike trains generated in the 2 sec immediately preceding stimulus onset (a duration approximately equal to each of our song stimuli). As these spike trains were spontaneously generated, and should show no systematic differences across stimulus intensities, we would expect the classifier to perform no better than chance. In fact, percent correct values for spontaneously-generated spike trains tightly cluster at chance level (11.11%, Fig. 4.4C). Average performance across cells did not differ between spike timing and spike-count based assignments (11.07 ± 0.133 vs. 11.45 ± 0.166%, respectively, $p > 0.05$). Similarly, the cumulative distributions of percent correct values for spontaneously generated spike trains overlap and are centered around chance performance. Again, no difference between classifiers was observed ($D = 0.1644$, $p > 0.05$, Fig. 4.4D).

Once it was clear that spike timing-based classification yields superior intensity discrimination, we wished to determine whether this advantage was present for all stimulus levels tested, or whether a strong bias at one or two stimulus intensities was responsible for our finding. We therefore compared percent correct values for both metrics at individual stimulus intensities (Fig. 4.4E). A 2-way repeated measures ANOVA (stimulus intensity x classifier metric) revealed a significant effect of stimulus intensity, such that the percent correct increased with the stimulus intensity for both classifier metrics ($F_{(7,413)} = 31.289$, $p < 0.001$). This result is likely due to the

fact that many cells were simply not responsive at lower stimulus intensities. We would expect the percent of correctly assigned spike trains to increase as the stimulus intensity increased, and more cells began responding. Also apparent in figure 4.4E is a significant effect of classifier metric. The spike timing metric yielded better performance at the majority of stimulus intensities tested ($F_{(1,413)} = 34.533$, $p < 0.001$). The degree of this advantage, however, did depend on stimulus intensity, such that there was a significant interaction between intensity and metric ($F_{(7,413)} = 2.395$, $p < 0.05$). The disparity between the two metrics increased with increasing stimulus intensities, up to 80 dB SPL, for which the largest disparity (9.25%) occurred.

The spike timing-based percent correct values we report here were calculated using each neuron's optimal temporal resolution (σ). As shown in figure 4.4F, the distribution of optimal values was skewed towards lower values. Though values spanned a wide range (3 - 375 msec), the median optimal σ for the population of cells was 18 msec, similar to values previously reported (Schnupp et al., 2006; Narayan et al., 2006). To determine whether the optimal σ was related to the percent of correctly assigned spike trains using the spike timing metric, we plotted individual percent correct values against each neuron's optimal σ (Fig. 4.4G). Optimal σ values were not correlated with spike timing-based percent correct values ($r = -0.167$, $p = 0.159$).

4.4.4 Intensity discrimination depends on sex and breeding condition

The results presented above indicate that on average, both spike timing and spike count information can be used to discriminate stimulus intensities, but spike timing yields enhanced discrimination. These data were collected from males and females under breeding and non-

breeding conditions, leading us to wonder whether sex or hormonal state might influence intensity discrimination. We addressed this issue by performing a 3-way (sex x breeding condition x metric) mixed model ANOVA. Spike timing-based classification results in higher percent correct values ($F_{(1,69)} = 46.660$, $p < 0.001$; Fig. 4.4A-B). Neither sex nor breeding condition impacted percent correct values, however, nor were there any interactions between sex, breeding condition, or classifier metric (all $p > 0.05$, data not shown).

Though the overall percent of correctly assigned spike trains was unaffected by sex or breeding condition, there may be intensity-specific effects that our analysis did not capture. To address this issue, we analyzed the effect of sex and breeding condition on the percent of correctly assigned spike trains at individual stimulus intensities. Additionally, because we have already described a significant interaction between stimulus intensity and metric type (Fig. 4.4F), we chose to analyze the effects of sex and breeding condition separately on each metric type. The results of these analyses are described in detail below.

4.4.4.1 Effect of sex, breeding condition and intensity on spike-timing based discrimination

To visualize how sex, breeding condition, and stimulus intensity might affect spike timing-based discrimination, we created confusion matrices for each experimental group, as shown in figure 4.5. As described previously, each confusion matrix is a color-coded heat map representing the proportions of spike train assignments. In each matrix, the rows represent actual stimulus intensities; the columns represent assigned stimulus intensities. The sum of the proportions in each row total 1. So, for example, in figure 4.5A, the dark red square in the bottom right-hand

corner indicates that ~45% of spike trains that were elicited by a 100 dB SPL stimulus were correctly assigned to the 100 dB SPL template. Unlike the confusion matrices presented in figure 4.3F-G, which represent the spike train assignments for a single cell, the matrices presented in figure 4.5 are created from all the spike train assignments that were made across all cells in each experimental group.

We measured the differences among experimental groups using a 3-way (sex x breeding condition x stimulus intensity) mixed model ANOVA. First, there was a significant effect of stimulus intensity, such that discrimination performance increased with increasing stimulus intensities ($F_{(7,392)} = 20.13$, $p < 0.001$). This result is most easily seen for the non-breeding females in figure 4.5A; the color of the diagonal gradually changes from cyan to red, indicative of improving performance. Across all groups, the percent correct increased from 15.05 ± 1.15% at 20 dB SPL to 36.02 ± 2.84% at 90 dB SPL. Next, we examined the effect of sex on spike timing discrimination performance. Males and females had similar performance overall, with no significant differences between the groups (21.41 ± 1.91 vs. 24.70 ± 1.95%, respectively; $p > 0.05$). We then looked for an effect of breeding condition. On average, percent correct values trended towards higher values under breeding condition compared to non-breeding condition (25.62 ± 1.87 vs. 20.48 ± 1.99%), though this difference was not statistically significant ($p = 0.065$). There was a significant interaction among sex, breeding condition and stimulus intensity, however, such that at lower stimulus intensities (20-60 dB SPL), breeding females outperformed every other experimental group by as much as 12% ($F_{(1.56)} = 5.657$, $p < 0.05$). As the stimulus intensity increased, the performance of the breeding females leveled off, while the performance

of the other groups continued to improve. Thus, at higher stimulus intensities, non-breeding females were the best performers, with 41.9% correct at 90 dB SPL.

4.4.4.2 Effect of sex, breeding condition and intensity on spike-count based discrimination

To explore the effect of sex, breeding condition, and stimulus intensity on spike count-based discrimination, we created confusion matrices for each experimental group as described previously, and assessed differences among the groups using a 3-way (sex x breeding condition x stimulus intensity) mixed model ANOVA (Fig. 4.6). Again, discrimination performance increased with increasing intensity ($F_{(7,392)} = 17.82$, $p < 0.001$). Unlike with spike timing-discrimination, where performance began improving at low or mid-level intensities (Fig 4.5), average spike count-based discrimination performance only began showing substantial improvement at 80-90 dB SPL (Fig 4.6). On average, males and females showed similar spike count-based discrimination (15.71 ± 1.30 vs. 16.49 ± 1.32%, respectively, $p > 0.05$). Similarly, breeding condition did not affect spike count-based performance values, nor were there any interactions between sex, condition, or intensity (all $p > 0.05$).

4.4.4.3 Sex and breeding condition do not affect thresholds or optimal σ values

We report above that breeding condition increases spike timing-based discrimination performance for low and mid-level stimuli, in particular for females, but also perhaps weakly for males (Fig 4.5). One possible explanation for this finding may be that breeding birds have lower song thresholds than non-breeding birds. We addressed this issue by comparing thresholds among our experimental groups. Males and females had similar thresholds across breeding

conditions (Table 4.3). A 2-way ANOVA revealed no significant effects of sex, breeding condition, nor was there a significant interaction (all $p > 0.05$).

Similarly, because sex and breeding condition affected spike-timing, but not spike count based discrimination, we wondered whether these variables might also modulate optimal neuronal time resolutions. To address this issue, we compared optimal σ values across each of our experimental groups. Males and females in breeding and non-breeding condition all had similar optimal σ values (Table 4.3). A 2-way ANOVA revealed no significant effects of sex, breeding condition, nor was there a significant interaction (all $p > 0.05$).

To summarize, we have reported the following: 1) Spike timing-based discrimination is superior to spike count based discrimination across the majority of stimulus intensities (Fig. 4.4). 2) Breeding females show increased spike timing-based discrimination at low and mid-level stimuli, and a similar trend is found in males (Fig 4.5). 3) These effects are not due to differences in thresholds or optimal time resolutions (Table 4.3). 4) Sex and breeding condition do not affect spike count-based discrimination at any intensity (Fig 4.6).

4.5 Discussion

4.5.1 Spike timing and auditory discrimination

Understanding how spike timing contributes to sensory discrimination is fundamental for linking neural activity with perception. Recently, researchers have begun investigating this issue in telencephalic structures known to be important for the perception and discrimination of

behaviorally relevant sounds, such as conspecific vocalizations. Specifically, studies in auditory cortex (and its non-mammalian analogues) have asked how the discrimination of two or more vocalizations depends on the temporal resolution of individual cortical responses (Schnupp et al., 2006; Narayan et al., 2006; Huetz et al., 2006; Wang et al., 2007; Engineer et al., 2008; Billimoria et al., 2008; Huetz et al., 2009). Overwhelmingly, the data point towards higher discrimination accuracy at shorter time scales; 10-20 msec have been reported as optimal (Schnupp et al., 2006; Narayan et al., 2006). Here we found that single neurons in the avian forebrain are capable of using spike timing reliability to accurately discriminate the sound level of a complex signal. Furthermore, we report that a similar temporal resolution, 18 msec, is optimal for the discrimination of sound intensity. Our results suggest that the contribution of spike timing is not limited to the discrimination of sounds that differ in terms of spectral or temporal properties, but also extends to sounds whose spectro-temporal features remain constant, but vary in mean intensity.

4.5.2 Sex steroid hormones and auditory discrimination

A growing body of literature has begun to elucidate the role of circulating and brain-derived sex steroid hormones in basic auditory function (for reviews see Maney and Pinaud, 2011; Pinaud and Tremere, 2012, and Chapter 1 of this text), though the impact of these hormones on auditory discrimination remains poorly understood. To date, only two other studies have addressed this issue from a neural coding perspective. One study, which focused on the zebra finch caudomedial nidopallium (NCM), used a linear decoder to analyze the ability of single neurons to discriminate among 4 different conspecific songs during manipulation of local E_2 levels

(Tremere and Pinaud, 2011). The authors reported enhanced discrimination accuracy after E_2 infusion, and decreased accuracy after either estrogen receptor blockade or aromatase inhibition. Furthermore, they report that even after normalizing spike trains to account for hormone-dependent changes in evoked activity, their pharmacological manipulations had similar, albeit smaller, effects on discrimination. Their results suggest that endogenous E_2 enhances song discrimination in part by shaping fine temporal processing, though the precise role of spike timing was not measured. In the second study, Liu and Schreiner (2007) recorded multi-unit responses from the auditory cortex of female mice that were either recent mothers, or naive regarding pup care. The authors found that when recordings were analyzed with a 2 msec resolution, the responses of mothers conveyed more information at earlier latencies for pup call detection and discrimination compared to responses of naive females. It should be noted, however, that in this study, hormone levels were not assessed; furthermore, the relative role of sex steroids and pup-care experience cannot be separated, and likely interact (Miranda and Liu, 2009).

Here, we expand on these findings by directly assessing the contribution of fine temporal processing to auditory discrimination under different hormonal conditions. Specifically, we report that sex steroid hormones modulate spike timing-based discrimination of auditory forebrain neurons in a sex and intensity specific manner, such that breeding condition increases the range of intensities over which accurate discrimination can be achieved. Our results, which are based on recordings in CLM, field L, and an area located just ventral to L, indicate that hormonal modulation of auditory discrimination is not limited to NCM, but may be a general

feature of the avian auditory forebrain. Furthermore, our findings indicate that in addition to neurosteroids, plasma hormones are also capable of modulating discrimination accuracy. Collectively, these findings suggest that sex steroid hormones shape single unit responses at a high temporal resolution to enhance the discrimination of vocal stimuli and vocal intensities.

4.5.3 Cellular and hormonal mechanisms

The cellular and hormonal mechanisms underlying the findings we report here are unknown, and many questions remain unanswered. First, we report that the effect of breeding condition on spike timing-mediated discrimination is sex-dependent. However, T, which was administered to males, can be aromatized *in vivo* into E_2, which was administered to females. Additional studies utilizing a combination of hormonal manipulations are needed to determine whether androgenic and/or estrogenic metabolites are responsible for the effects we observed in males.

Further investigations are also needed to gain a better understanding of the cellular mechanisms by which hormones alter intensity discrimination in CLM and field L, two brain areas known to lack both classical (Gahr, 1990; Gahr et al., 1993; Metzdorf et al., 1999; Jeong et al., 2011) and non-classical (Acharya and Veney, 2011) steroid receptors in adult songbirds. One possibility to be explored is the direct action of hormones receptors in the auditory periphery (Noirot et al., 2009) or brainstem (see Figure 1.2 in this work). Similarly, efferent modulation from NCM, which connects to the caudal mesopallium, is a likely candidate mechanism, for reasons discussed extensively above (Tremere and Pinaud, 2011). Additional evidence suggests that sex

steroids may modulate auditory forebrain function via monoaminergic signaling (for review see Maney and Pinaud, 2011). None of these potential mechanisms can be excluded at this time.

4.5.4 Behavioral relevance

One obvious issue that arises from this study is the functional significance of the data. Specifically, do sex steroid hormones modulate behavioral discrimination capabilities? Though we did not perform the necessary experiments to answer that question directly here, we can draw on existing literature from songbirds and other animal models.

First, in a series of companion papers, Cynx et al. reported that zebra finches trained in an operant paradigm to discriminate among songs achieved 75% discrimination accuracy more quickly when they were trained and tested under long-day photoperiods (Cynx and Nottebohm, 1992a; Cynx et al., 1992); a follow up study suggested that this effect may be mediated by circulating T (Cynx and Nottebohm, 1992b). In a separate series of experiments, two independent groups demonstrated that disrupting estrogenic signaling in NCM, either through aromatase inhibition or estrogen receptor blockade, abolishes the native behavioral preferences of male zebra finches for the song of their tutor or their own song, compared to the song of another conspecific (Remage-Healey et al., 2010; Tremere and Pinaud, 2011). Finally, Vyas et al. (2008) reported that female zebra finches demonstrate differential behavioral responses to the playback of conspecific songs only after E_2 treatment.

While these studies are promising, an interpretation of their results should proceed with caution. Many of these experiments do not allow for a separation of auditory discrimination and preference. Further, in the one set of studies that does allow us to make this distinction, the impact of hormones and/or photoperiod on discrimination accuracy was not assessed; only the number of trials to reach training criterion was reported (Cynx and Nottebohm, 1992a, 1992b; Cynx et al., 1992). Nevertheless, these results suggest that the hormonal modulation of neural discrimination may have a behavioral correlate. Future work could address this issue directly by using a go-no-go paradigm to assess song and intensity discrimination accuracy of birds under different hormonal conditions.

4.6 Tables and Figures

Table 4.1 Breakdown of cells included in analysis. Values are number of cells and number of birds (in parentheses). Note that the number of birds indicated in the right-most column is not a simple sum of the number of birds in each preceding column because units from each anatomical location may have been recorded in the same bird.

	CLM	CLM/L Border	Field L	Ventral to L	Totals
Breeding females	3(3)	3(2)	12(7)	4(3)	22(8)
Non-breeding females	4(3)	2(2)	11(8)	1(1)	18(10)
Breeding males	6(5)	2(1)	9(6)	3(2)	20(8)
Non-breeding males	2(2)	3(3)	6(5)	2(2)	13(7)
Totals	15(13)	10(8)	38(26)	10(8)	73(33)

Table 4.2 Plasma hormone levels (mean ± SEM)

	Non-Breeding	Breeding	U[a]	*p*
Plasma testosterone (ng/ml)	0.391 ± 0.110 (n=7)	21.84 ± 4.23 (n=8)	0.00	<0.01
Plasma estradiol (pg/ml)	16.91 ± 3.65 (n=6)	447.45 ± 214.00 (n=5)	0.00	<0.01

[a]Mann-Whitney U test (two-tailed)

Table 4.3. Threshold and optimal σ values for each experimental group (means ± SEMs)

	Females		Males	
	Breeding	**Non-Breeding**	**Breeding**	**Non-Breeding**
Threshold (dB SPL)	49.09 ± 5.66	52.78 ± 4.63	41.50 ± 3.93	48.46 ± 5.04
Optimal σ (msec)	34.36 ± 14.73	79.83 ± 28.30	58.05 ± 19.66	39.46 ± 10.74

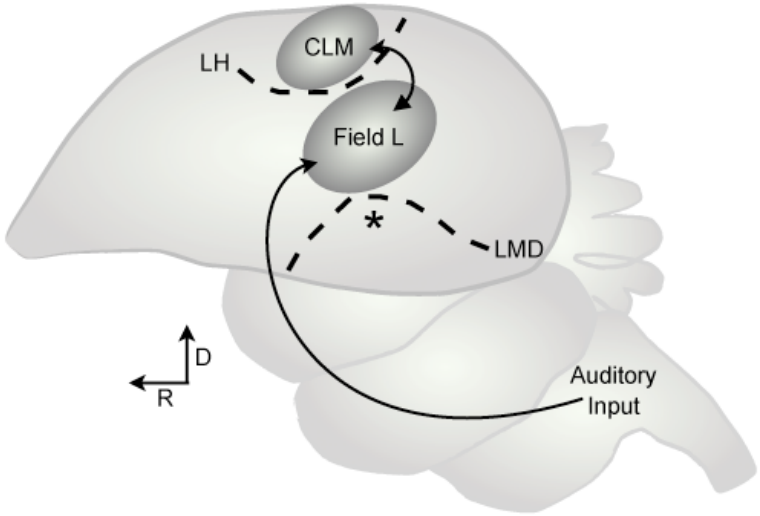

Figure 4.1. Simplified sagittal schematic of the avian auditory system. Auditory responses were recorded in the caudolateral mesopallium (CLM), the field L complex, and an area just ventral to L (marked by an asterisk). Field L is the primary recipient of ascending auditory information from the thalamus. CLM and Field L are separated by the hyperpallial lamina (LH) and are reciprocally connected. The dorsal medullary lamina (LMD) separates field L from the ventral area where we recorded units. The origin of the auditory input into this region is unknown.

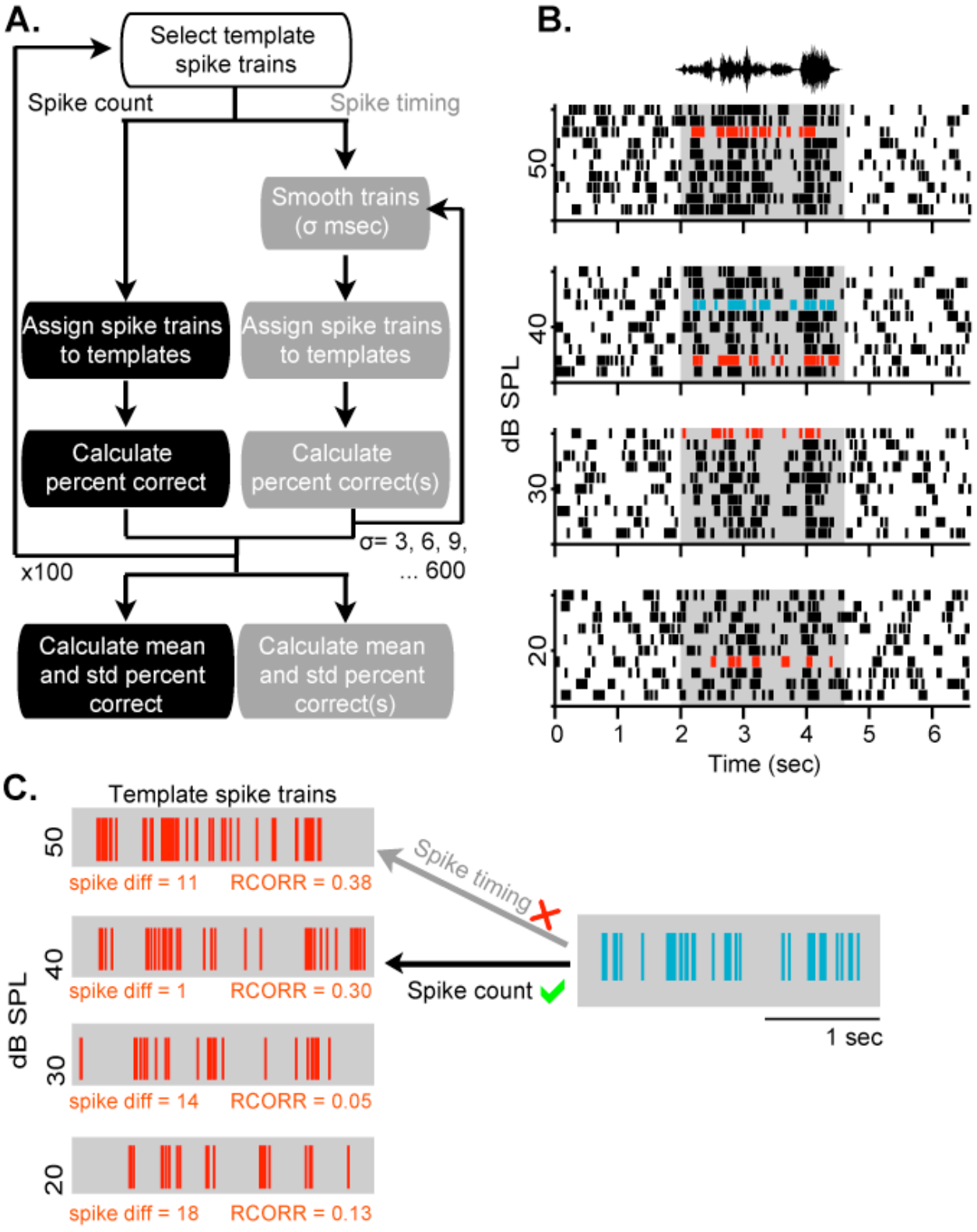

Figure 4.2. Pattern classifier schematic and demonstration of spike train assignments
A. A flow chart depicting each step the pattern classifier performs when analyzing data from a single cell. After randomly selecting one "template" spike train from each stimulus intensity

(examples highlighted in red in panel B), the classifier branches into two paths. The "spike count" path (left, black) counts the number of action potentials in each spike train and each template. This path assigns each train to a template by minimizing the absolute difference in the number of spikes. The "spike timing" path (right, grey) establishes a gaussian window with a given stdev (σ) in msec, smooths the spike trains with this gaussian and calculates an RCORR value between each remaining (non-template) spike train and each template. This path assigns each spike train to a template by maximizing the value of RCORR. This path starts by setting σ to 3 msec and repeats 200 times; in each loop, σ increases by 3 msec. After calculating the percent of spike trains that were assigned to the correct dB SPL for each path, the classifier loops back to the beginning, randomly selects an entirely new set of template spike trains, and assigns the spike trains again. This process is repeated 100X. Finally, an overall mean and stdev percent correct is calculated for each path. **B.** Representative raster plots from a single unit recorded in a breeding female are arranged by decreasing song intensity (as indicated by the dB SPL values on the left). In each subplot, time (in sec) is on the *x*-axis and each row of tick marks shows the spike times for a single stimulus presentation. The song (#6) stimulus waveform is shown above the rasters; the grey shaded region indicates the time during which the stimulus was presented. Spike trains highlighted in red are randomly selected template trains (enlarged in panel C). The spike train highlighted in cyan is an example train that is used in panel C to demonstrate how the classifier assigns individual trains to templates. For simplicity, only responses from 20-50 dB SPL are shown here. **C.** One template spike train (red) was randomly chosen for each dB SPL (panel B) and enlarged here. The absolute difference in the number of spikes between the cyan spike train and each template train is shown under each template on the left ("spike diff"). The cyan spike train, which was elicited by a 40 dB SPL stimulus (panel B) only differed by the 40 dB SPL template by 1 spike. Therefore, the spike count metric correctly assigned the cyan spike train to the 40 dB SPL template. The spike timing reliability calculated between the cyan spike train and each template is shown under each template on the right ("RCORR"). These values were calculated at the neuron's optimal σ (9 msec). The highest RCORR calculated in this example was 0.38; therefore, the spike timing metric incorrectly assigned the cyan spike train to the 50 dB SPL template.

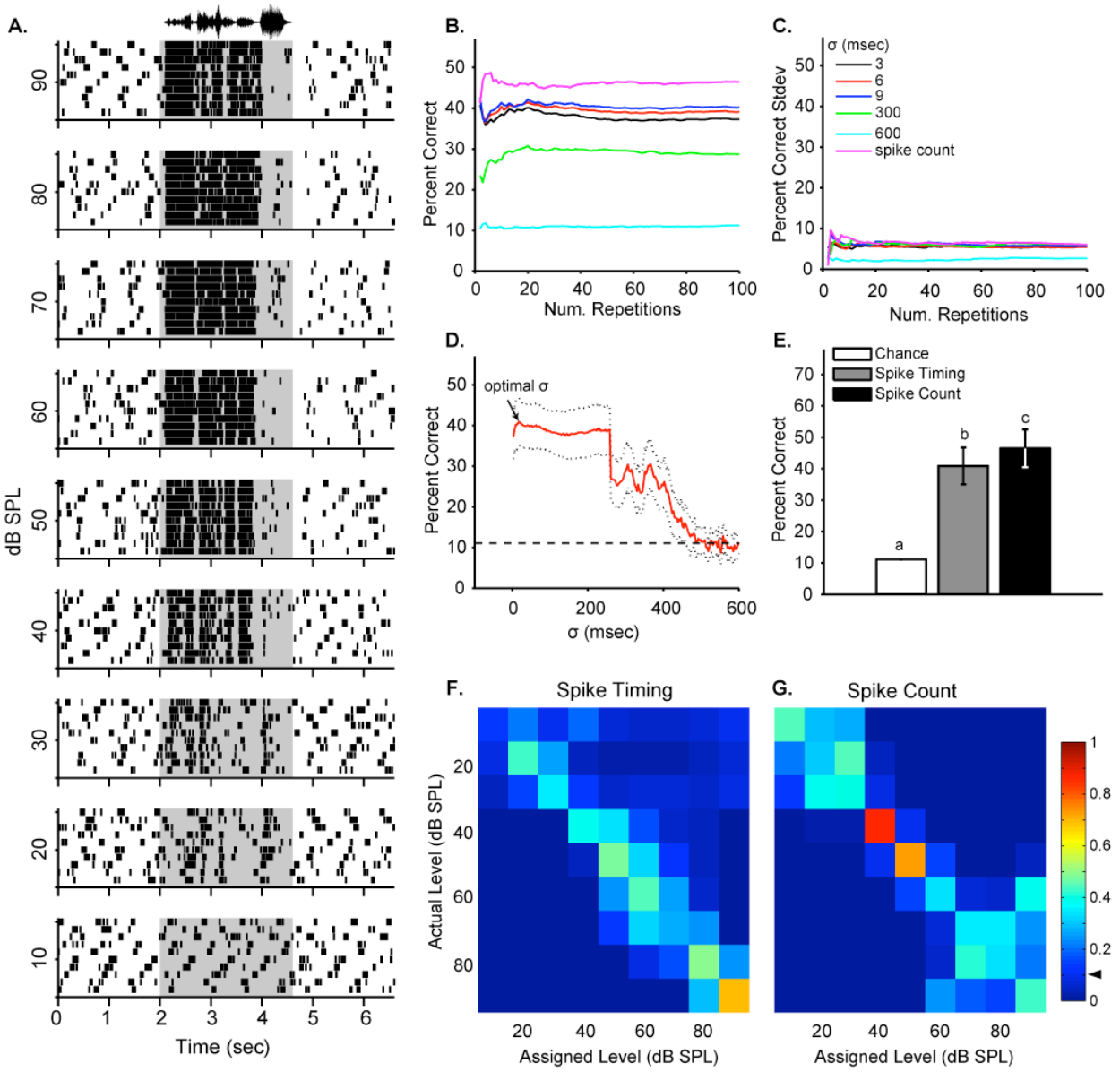

Figure 4.3 Pattern classifier results for a single cell.

A. Representative raster plots from a single unit recorded in a breeding male are arranged by decreasing song intensity (as indicated by the dB SPL values on the left). In each subplot, time (in sec) is on the *x*-axis and each row of tick marks shows the spike times for a single stimulus presentation. The song (#6) stimulus waveform is shown above the rasters; the grey shaded region indicates the time during which the stimulus was presented. Panels B-G show the output of the classifier for this single cell. **B.** The mean percent correct is plotted as a function of the number of overall repetitions performed by the pattern classifier for various values of σ (for the spike timing metric) and separately for the spike count metric. The mean percent correct leveled off well before the classifier has performed 100 repetitions. Together with panel C, this indicates that our choice of 100 repetitions is valid. For legend, see panel C. **C**. The STDEV of the percent correct is plotted as a function of the number of overall repetitions performed by the pattern

classifier for various values of sigma (for the spike timing metric), and separately for the spike count metric. The stdev of the percent correct has leveled off by the time the classifier has performed 30 repetitions. **D**. The mean percent correct calculated by the "spike timing" metric (red line) is plotted against increasing values of σ. Dashed black lines are +/- 1 STDEV of the percent correct. The optimal σ is the value that gave the highest percent correct; in this example, the optimal σ was 18 msec. **E.** The mean percent correct for the spike count metric (black bar) and the spike timing metric (grey bar) are plotted and compared to chance output (white bar). Error bars are +/- 1 STDEV. The spike timing mean was calculated at the optimal σ as indicated in panel B. This cell showed strong performance with both the spike timing and spike count metric. Lowercase letters above the bars indicate groups that are statistically different from one another. The spike timing and spike count metrics were each compared to chance level using one-sample t-tests; spike count and spike timing metrics were compared to each other using a 2-sample paired t-test. Statistics are as follows: spike timing vs. chance ($t(99) = 51.0$, $p < 0.001$); spike count vs. chance ($t(99) = 58.7$, $p < 0.001$), spike timing vs spike count ($t(99) = -6.61$, $p < 0.001$). **F.** Confusion matrix output for the spike timing metric. Actual stimulus levels are on the *y*-axis; levels assigned by the classifier are on the *x*-axis. Within each row of the matrix, each small square indicates the proportion of spike trains assigned to each level for a single actual level. Proportions range from 0 to 1 and are color coded, as shown in the color bar in panel G. As an example, the yellow square in the bottom right corner of the matrix indicates that ~70% of spike trains that were actually elicited by a 90 dB SPL stimulus were correctly assigned to the 90 dB SPL template. The cyan square to the immediate left, on the other hand, indicates that the remaining ~30% of spike trains actually elicited by a 90 dB SPL stimulus were incorrectly assigned to the 80 dB SPL template. Perfect classifier performance would be represented by a diagonal line of red squares. At almost all stimulus levels, the spike timing classifier correctly assigned spike trains above what would be expected by chance (indicated on color bar in panel G with black pointer). The spike timing classifier's performance increases with stimulus intensity, such that maximal performance is achieved for spike trains elicited by a 90 dB SPL stimulus. **G.** Confusion matrix output for the spike count metric. Plot conventions as in panel F. Again, at most stimulus levels the classifier correctly assigned spike trains above what would be expected by chance. Unlike the spike timing metric, however, the spike count metric performance is best at mid-level stimulus intensities, with maximal performance achieved for spike trains elicited by 40 dB SPL. The drop off in performance at higher levels is likely due to firing rate saturation, which would limit the ability of the classifier to discriminate among intensities.

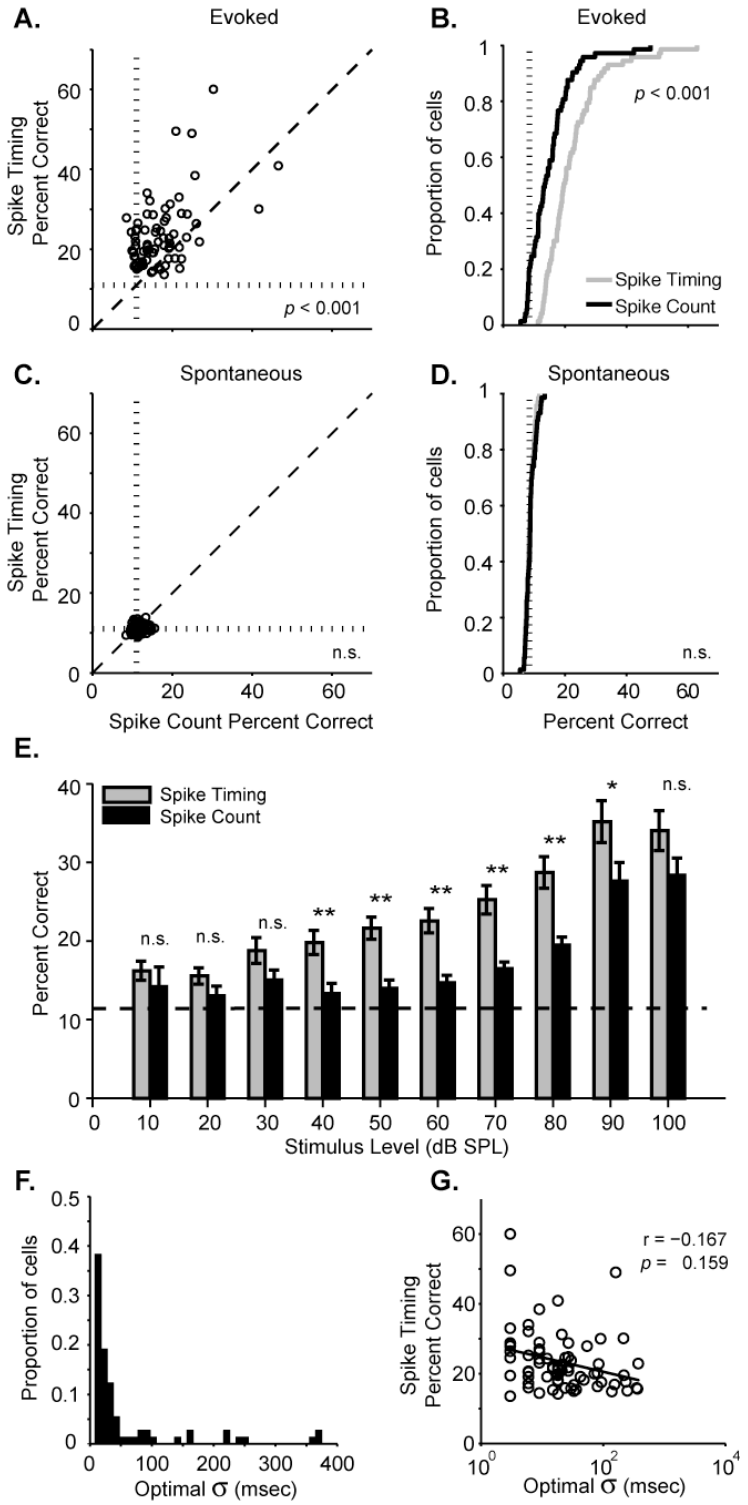

Figure 4.4 A spike timing-based strategy achieves better intensity discrimination than a spike count-based strategy A. The percent of correctly assigned song-evoked spike trains using the spike timing classifier (*y*-axis) is plotted against the percent correct using the spike count classifier (*x*-axis) for all individual cells included in the analysis. Chance performance is

indicated by the vertical and horizontal hash marks. The dashed diagonal line represents unity. The majority of cells fall above the unity line, indicating better intensity discrimination for spike timing-based classification. Except as noted for panel E, the sample size for this figure was 73 cells from 33 birds. **B.** A cumulative distribution of percent correct values for spike timing (grey) and spike count-based (black) classifiers for song-evoked spike trains. The spike timing distribution is shifted to the right,towards higher percent correct values, compared with the spike count distribution. **C.** The percent of correctly assigned spontaneously generated spike trains using spike timing and spike count classifiers. Plot conventions as in A. All cells cluster at chance performance for both spike timing and spike count strategies. **D.** A cumulative distribution of percent correct values for spike timing (grey) and spike count (black) classifiers for spontaneously generated spike trains. Plot conventions as in B. Both distributions overlap and are centered around chance performance. **E.** The average percent of correctly assigned spike trains at for spike timing (grey) and spike count-based (black) strategies are compared for individual stimulus levels. Spike timing-based classification correctly assigns significantly more spike trains than spike-count based classification at almost all stimulus intensities. Chance performance is indicated by the horizontal dashed line. Note that only those intensities for which we had sufficient sample sizes are presented here. Bars are means (across cells) +/- S.E.M. $*p<0.05$, $**p<0.01$. n.s. = not significant. All p values were Bonferroni adjusted for multiple comparisons. Sample sizes (number of cells, followed by number of birds in parentheses) are as follows: 10 dB SPL = 42(19), 20 dB SPL = 68(32), 30-70 dB SPL = 73(33), 80 dB SPL = 72(33), 90 dB SPL = 65(32), 100 dB SPL = 31(16). **F.** The distribution of optimal gaussian σ values spans a wide range, but is skewed towards lower values. **G.** The percent of correctly assigned spike trains using the spike-timing based classification does not correlate with the optimal gaussian σ. Each circle represents one cell. Note that for clarity, the x-axis is on a log scale.

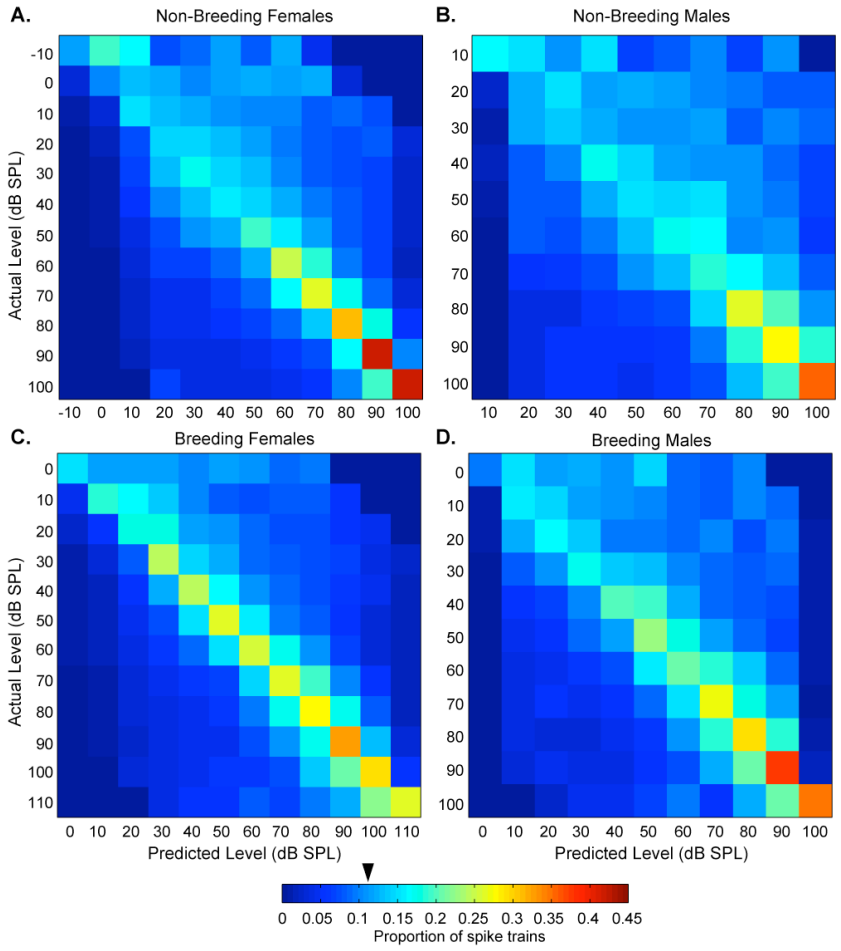

Figure 4.5 Spike timing-based discrimination of dB SPL intensities depends on sex, breeding condition, and intensity. A-D. Spike timing-based confusion matrix created from all non-breeding female (**A**), non-breeding male (**B**), breeding female (**C**) and breeding male (**D**) spike trains. For each matrix, actual stimulus levels are on the *y*-axis; levels assigned by the classifier are on the *x*-axis. Within each row of the matrix, each small square indicates the proportion of spike trains assigned to each level; each row sums to 1. While possible proportions range from 0 to 1, the color bar ranges from 0 to 0.45 to allow differences to be seen more easily. Chance performance is indicated on the color bar at the bottom of the figure with a black pointer. Note that each cell was presented with 9 different intensities, but the absolute intensities may have differed from cell to cell (e.g 10-90 dB SPL vs 20-100 dB SPL). Thus, the number of squares may differ among matrices, depending on which intensities were presented to cells in each experimental group. The number of cells, followed by the number of birds (in parentheses) are as follows. Non-breeding females: -10 dB = 1(1), 0 dB = 3(2), 10 dB = 12(6), 20-70 dB = 18 (10), 80 dB = 17(10), 90 dB = 15(9), 100 dB = 6(4). Breeding females: 0 dB = 4(2), 10 dB = 10 (4), 20 dB = 18(8), 30-80 dB = 22(8), 90 dB = 18(8), 100 dB = 12(4), 110 dB = 4(3). Non-breeding males: 10 dB = 2(2), 20-90 dB = 13(7), 100 dB = 11(6). Breeding males: 0 dB = 1(1), 10 dB = 18(7), 20 dB = 19(7), 30-80 dB = 20(8), 90 dB = 19(8), 100 dB = 2(2).

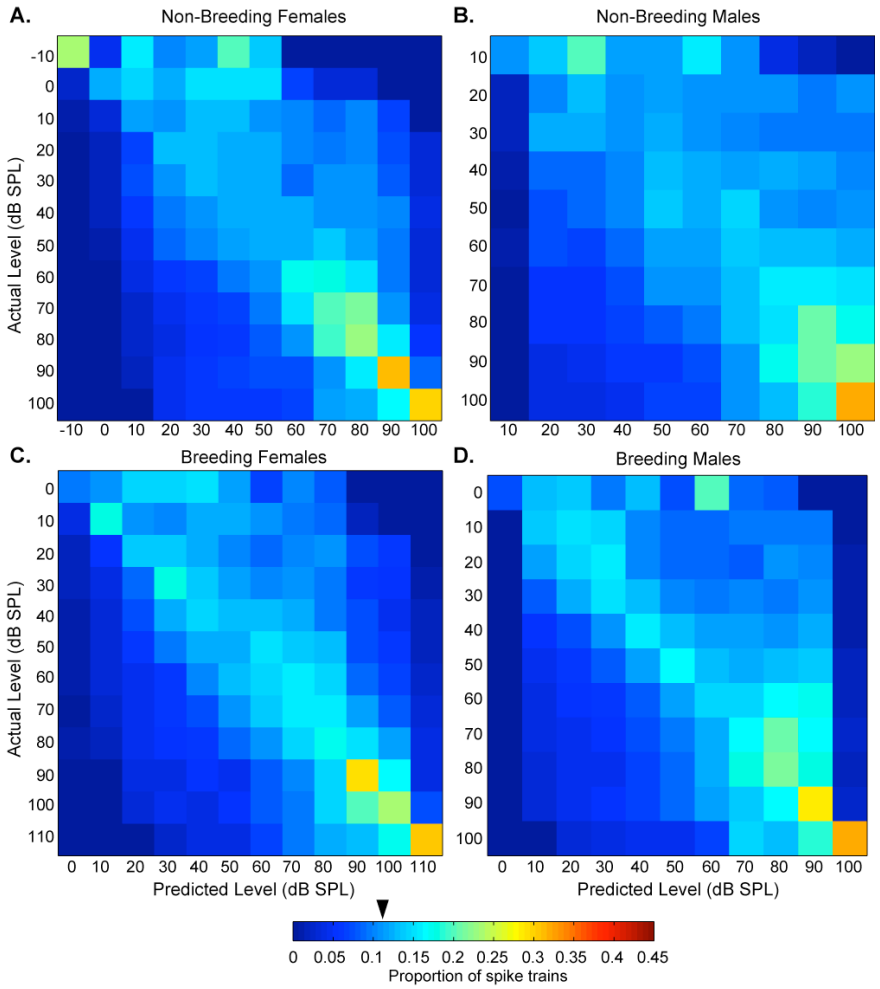

Figure 4.6 Spike count-based discrimination of dB SPL intensities does not depend on sex, breeding condition, or intensity. A-D. Spike count-based confusion matrix created from all non-breeding female (**A**), non-breeding male (**B**), breeding female (**C**) and breeding male (**D**) spike trains. All plot conventions and sample sizes are the same as in figure 4.5.

Chapter 5. Summary and Future Directions

This dissertation explored the role of two sex steroid hormones, testosterone and estradiol, on auditory processing in a seasonally-breeding songbird, Gambel's white-crowned sparrow. In the preceding chapters, I demonstrated that systemic administration of these hormones affects auditory function in a disparate manner along the ascending auditory pathway. Below, I summarize these results in more detail and highlight some questions raised by my studies. Finally, I leave the reader with additional directions for future research.

5.1 Effects of sex steroid hormones on the auditory brainstem and periphery

My investigation began at the level of the auditory periphery and brainstem. In Chapter 2, I demonstrated that increased levels of circulating testosterone or estradiol, typical of the breeding season, increased auditory brainstem response (ABR) thresholds and prolonged ABR peak latencies in male and female white-crowned sparrows.

These results were surprising in a number of ways. While some evidence suggests that testosterone may negatively affect peripheral auditory function (McFadden et al., 2006; Snihur and Hampson, 2012), estrogen is typically thought of as protective (Coleman et al., 1994; Meltser et al., 2008; Nakamagoe et. al, 2010, 2011). How is it that in my study, testosterone and estradiol had statistically identical effects on ABR thresholds and latencies? This question is answered relatively easily by remembering that aromatase is capable of converting testosterone into estradiol *in vivo*, raising the possibility that the effects I observed were mediated by estradiol in both males and females. Future studies could explore this issue directly by utilizing various

combinations of hormonal manipulations, including the non-aromatizable androgen dihydrotestosterone.

Even if estradiol was solely responsible for the results described in Chapter 2, how do we explain that my hormonal manipulations *impaired* ABR processing? An answer to this question may lie in the fact that much of the evidence supporting estrogenic protection of the auditory periphery and brainstem comes from research on the mammalian system. Unlike mammals, birds are capable of regenerating inner ear hair cells after acoustic trauma (Corwin and Cotanche, 1988; Ryals and Rubel, 1988). Thus, perhaps in avian species, the need for auditory "protection" is reduced, and estrogen instead plays some other modulatory role.

5.2 Effect of estradiol on the auditory forebrain

I continued my investigation by recording single-unit activity in field L, the avian analogue of the mammalian primary auditory cortex. The results of this study, detailed in Chapter 3, revealed that systemic administration of estradiol enhanced auditory function in a select population of forebrain neurons: those with monotonic responses to pure tone stimuli. Specifically, I demonstrated that breeding condition increased monotonic neuron firing rates, auditory response strengths and pure tone sensitivity, and expanded the range of intensities over which neurons were sensitive to differences in song amplitude. Furthermore, my results indicated that the activity of monotonic neurons in individual birds strongly correlated with the concentration of circulating estradiol. These effects were not observed in non-monotonic neurons, which overlap anatomically with monotonic cells.

One of the most pressing questions raised by this study is the following: *How do we reconcile estradiol-mediated enhancement of auditory forebrain function with the estradiol-mediated impairment in auditory brainstem function observed in Chapter 2?* To answer this question, one must remember that there are fundamental differences between the methods used in each study. In Chapter 3, we measured firing-rate based indicators of auditory function at the single cell level, at each neuron's characteristic frequency. The ABR, which was used in Chapter 2, is more accurately understood as a measure of neural synchrony, not firing rate. Thus, a comparison between the two studies is difficult to interpret. To resolve these apparent discrepancies, one could obtain single-unit recordings of individual auditory nerve fibers under different breeding conditions. The results of such a study, coupled with additional single-unit recordings in the midbrain nucleus MLd, and the thalamic nucleus Ov would allow us to gain a better understanding of how sex steroid hormones modulate processing along the ascending auditory pathway.

In addition, the findings described in Chapter 3 highlight the need for more detailed studies of sex steroid hormones on auditory forebrain function. The vast majority of work exploring this issue has come from studies on one secondary forebrain region in the zebra finch auditory system: the caudomedial nidopallium (NCM; Pinaud and Tremere, 2012). These studies have demonstrated that locally synthesized estradiol increases single unit firing rates (Tremere et al., 2009; Remage-Healey et al., 2010; Tremere and Pinaud, 2011). Many questions are left unanswered. For instance, does circulating estradiol, which in Chapter 3 was shown to affect the function of field L neurons, also affect the function of NCM neurons? Perhaps more

interestingly, one could also ask whether brain-derived estradiol affects processing in field L. Though field L neurons do not express estrogen receptors, a recent study by Remage-Healey and Joshi (2012) demonstrated that the effects of estrogen receptor binding in NCM are not limited to the confines of that nucleus. Future studies addressing these questions are warranted.

5.3 Effects of sex steroid hormones on intensity discrimination

I concluded my investigation by using a computational approach to examine the effects of both estradiol and testosterone on the ability of single units recorded in the auditory forebrain to discriminate among a range of song intensities. Chapter 4 compared two neural coding strategies that may underly intensity discrimination: one based purely on spike counts, and one based solely on spike timing reliability. I found that overall, spike timing-based intensity discrimination was more accurate than spike count-based discrimination. Furthermore, while overall discrimination accuracy did not differ between sexes or as a function of breeding condition for either coding strategy, there was an intensity-specific effect. Specifically, breeding condition broadened the range of intensities over which accurate spike timing-based discrimination occurred.

While this study adds to the growing body of evidence supporting a role for spike timing in auditory forebrain discrimination (Schnupp et al., 2006; Narayan et al., 2006; Huetz et al., 2006; Wang et al., 2007; Engineer et al., 2008; Billimoria et al., 2008; Huetz et al., 2009; Tremere and Pinaud, 2011), it also raises a number of questions. First, I assessed the effect of sex steroids on intensity discrimination in a heterogeneous population of forebrain neurons. It is unknown,

however, whether these effects are the result of selective hormonal modulation on a subset of these neurons, as might be predicted from the results in Chapter 3. Further analysis comparing spike timing-based intensity discrimination between monotonic and non-monotonic neurons is needed. Second, it is unknown whether sex steroids increase overall spike timing reliability, or whether they simply alter spike timing across intensities such that intensity discrimination is more easily achieved. A simple examination of how the R*corr* metric changes with stimulus intensities would address this issue. Finally, these results (along with those of Tremere and Pinaud, 2011, and Liu and Schreiner, 2007) suggest that hormones modulate spike-timing based discrimination in the auditory forebrain. One issue not addressed by these studies is whether sex steroids modulate spike timing reliability in the auditory thalamus, midbrain or brainstem. This issue is particularly intriguing given the fact that in Chapter 2, I demonstrated an effect of sex steroid hormones on ABR thresholds and latencies, and as noted above, the ABR truly measures neural synchrony. Future studies should explore this issue further.

5.4 Additional future directions

The previous sections have focused on the direct questions raised as a result of my studies. Here, I discuss broader potential avenues for future research.

5.4.2 Do other steroids affect auditory function?

5.4.2.1 Glucocorticoids

Androgen and estrogen receptors are not the only steroid receptors expressed in the auditory system. Glucocorticoid receptors (GR) are expressed in the mammalian inner ear (Rarey et al.,

1993; Shimazaki et al., 2002) and inferior colliculus (Mazurek et al., 2010), and are thought to mediate protection against acoustic trauma (Meltser and Canlon, 2011). Corticosterone, the primary GR ligand in many species, regulates auditory fear learning (Dagnino-Subiabre et al., 2012), and likely mediates stress-induced auditory brainstem hypersensitivity (Mazurek et al., 2010). Whether glucocorticoids modulate auditory cortical function or perception, however, is unknown. Levels of corticosterone fluctuate seasonally in Gambel's white-crowned sparrows, similar to testosterone and estradiol (Wingfield and Farner, 1978). Thus, the white-crowned sparrow may prove useful in future studies exploring the role of glucocorticoids on auditory processing.

5.4.2.2 Progesterone

Progesterone, another reproductive steroid, may also regulate auditory processing. Unlike estrogen, which is implicated in cellular protection, recent findings in humans (Guimaraes et al., 2006) and mice (Price et al., 2009) suggest that progesterone has detrimental effects on auditory function. Though it is unknown whether progesterone-specific receptors are expressed in the inner ear or central auditory system (Al-Mana 2008), progesterone can bind to glucocorticoid receptors (Xu et al., 1990). Careful hormonal manipulations are needed to determine how different types of steroid hormones modulate processing along the ascending auditory pathway.

5.4.3 Do sex steroid hormones affect auditory perception?

Though this dissertation contributes to a growing body of evidence supporting a modulatory role for sex steroid hormones on auditory physiology, it remains unclear whether these hormones actually impact auditory perception. In humans, pure tone audiometric thresholds may fluctuate across the menstrual cycle (Cox, 1980; Swanson and Dengerink, 1988), though in these studies, ovulatory state was estimated indirectly via basal body temperature, not serum hormone levels. Hormonal state is thought to mediate differential behavioral responses to salient auditory stimuli in a number of animal taxa (Arch and Naris, 2009; Sisneros, 2009b; Maney and Pinaud, 2011). However, in general, these studies have relied on behavioral outputs such as phonotaxis, copulatory signal displays, and percentage of time spent near a playback speaker. These measurements do not allow us to distinguish hormonal effects on auditory detection or discrimination, per se, from hormonal effects on preference or motivation. Surprisingly, carefully controlled experiments addressing this issue are lacking. Future studies should use a combination of behavioral assays, including an operant conditioning paradigm, to gain a clearer picture of how sex steroid hormones modulate auditory perception.

BIBLIOGRAPHY

Acharya KD, Veney SL (2011) Characterization of the G-protein coupled membrane bound estrogen receptor GPR30 in the zebra finch brain reveals a sex difference in gene and protein expression. Dev Neurobiol. doi: 10.1002/dneu.22004

Achor LJ, Starr A (1980) Auditory brain stem responses in the cat. I. Intracranial and extracranial recordings. Electroencephalogr Clin Neurophysiol 48:154-173

Akdogan O, Ozkan S (2006) Otoacoustic emissions in children with otitis media with effusion. Int J Pediatr Otorhinolaryngol 70:1941-1944

Al-Mana D, Ceranic B, Djahanbakhch O, Luxon LM (2008) Hormones and the auditory system: a review of physiology and pathophysiology. Neuroscience 153:881-900

Al-Mana D, Ceranic B, Djahanbakhch O, Luxon LM (2010) Alteration in auditory function during the ovarian cycle. Hear Res 268:114-122

Appeltants D, Del Negro C, Balthazart J (2002) Noradrenergic control of auditory information processing in female canaries. Behav Brain Res 133:221-235

Arch VS, Narins PM (2009) Sexual hearing: the influence of sex hormones on acoustic communication in frogs. Hear Res 252:15-20

Avey MT, Phillmore LS, MacDougall-Shackleton SA (2005) Immediate early gene expression following exposure to acoustic and visual components of courtship in zebra finches. Behav Brain Res 165:247-253

Baptista LF, Morton ML (1981) Interspecific song acquisition by a white-crowned sparrow. Auk 98:383-385

Baptista LF, Petrinovich L (1986) Song development in the white-crowned sparrow: Social factors and sex differences. Anim Behav 34: 1359-1371

Barclay SR, Harding CF (1988) Androstenedione modulation of monoamine levels and turnover in hypothalamic and vocal control nuclei in the male zebra finch: steroid effects on brain monoamines. Brain Res 459:333-343

Barclay SR, Harding CF (1990) Differential modulation of monoamine levels and turnover rates by estrogen and/or androgen in hypothalamic and vocal control nuclei of male zebra finches. Brain Res 523:251-262

Bass AH (2008) Steroid-dependent plasticity of vocal motor systems: novel insights from teleost fish. Brain Res Rev 57:299-308

Bergevin C, Freeman DM, Saunders JC, Shera CA (2008) Otoacoustic emissions in humans, birds, lizards, and frogs: evidence for multiple generation mechanisms. J Comp Physiol A Neuroethol Sens Neural Behav Physiol 194:665-683

Bernard DJ, Bentley GE, Balthazart J, Turek FW, Ball GF (1999) Androgen receptor, estrogen receptor alpha, and estrogen receptor beta show distinct patterns of expression in forebrain song control nuclei of European starlings. Endocrinology 140:4633-4643

Billimoria CP, Kraus BJ, Narayan R, Maddox RK, Sen K (2008) Invariance and sensitivity to intensity in neural discrimination of natural sounds. J Neurosci 28:6304-6308

Bonke D, Scheich H, Langner G (1979) Responsiveness of units in the auditory neostriatum of the Guinea Fowl (Numida meleagris) to species-specific calls and synthetic stimuli. J Comp Physiol 132:243-255

Borg E, Engstrom B (1983) Hearing thresholds in the rabbit. A behavioral and electrophysiological study. Acta oto-laryngologica 95:19-26

Brackenbury JH (1979) Power capabilities of the avian sound-producing system. J Exp Biol 78:163-166

Brenowitz EA (1981) 'Territorial song' as a flocking signal in red-winged blackbirds. Anim Behav 29:641-642

Brenowitz EA (1982) The active space of red-winged blackbird song. J Comp Physiol A Neuroethol Sens Neural Behav Physiol 147:511-522

Brenowitz EA (1991) Altered perception of species-specific song by female birds after lesions of a forebrain nucleus. Science 251(4991):303-305

Brenowitz EA (2004) Plasticity of the adult avian song control system. Ann N Y Acad Sci 1016:560-585

Brenowitz EA (2008) Plasticity of the song control system in adult birds. In: Neuroscience of birdsong (Zeigler P, Marler P, eds), pp332. New York: Cambridge University Press

Brenowitz EA, Baptista LF, Lent K, Wingfield JC (1998) Seasonal plasticity of the song control system in wild Nuttall's white-crowned sparrows. J Neurobiol 34:69-82

Brenowitz EA, Beecher MD (2005) Song learning in birds: diversity and plasticity, opportunities and challenges. Trends Neurosci 28:127-132

Brenowitz EA, Nalls B, Wingfield JC, Kroodsma DE (1991) Seasonal changes in avian song nuclei without seasonal changes in song repertoire. J Neurosci 11:1367-1374

Brittan-Powell EF, Dooling RJ, Gleich O (2002) Auditory brainstem responses in adult budgerigars (Melopsittacus undulatus). J Acoust Soc Am 112:999-1008

Brittan-Powell EF, Lohr B, Hahn DC, Dooling RJ (2005) Auditory brainstem responses in the Eastern Screech Owl: an estimate of auditory thresholds. J Acoust Soc Am 118:314-321

Brown-Borg HM, Beck MM, Jones TA (1987) Origins of peripheral and brainstem auditory responses in the White Leghorn chick. Comp Biochem Physiol A Comp Physiol 88:391-396

Brumm H (2004) Male–male vocal interactions and the adjustment of song amplitude in a territorial bird. Anim Behav 67:281-286

Brumm H, Ritschard M (2011) Song amplitude affects territorial aggression of male receivers in chaffinches. Behav Ecol 22:310-316

Buchwald JS, Huang C (1975) Far-field acoustic response: origins in the cat. Science 189:382-384

Burkard R, Jones S, Jones T (1994) Conventional and cross-correlation brain-stem auditory evoked responses in the white leghorn chick: rate manipulations. J Acoust Soc Am 95:2136-2144

Burkard R, McGee J, Walsh EJ (1996) Effects of stimulus rate on the feline brain-stem auditory evoked response during development. I. Peak latencies. J Acoust Soc Am 100:978-990

Capsius B, Leppelsack H (1999) Response patterns and their relationship to frequency analysis in auditory forebrain centers of a songbird. Hear Res 136:91-99

Caras ML, Brenowitz E, Rubel EW (2010) Peripheral auditory processing changes seasonally in Gambel's white-crowned sparrow. J Comp Physiol A Neuroethol Sens Neural Behav Physiol 196:581-599

Caras ML, O'Brien M, Brenowitz EB, Rubel EW (2012) Estradiol selectively enhances auditory function in avian forebrain neurons. Journal of Neuroscience. *In press*

Cardin JA, Schmidt MF (2004) Noradrenergic inputs mediate state dependence of auditory responses in the avian song system. J Neurosci 24:7745-7753

Cardwell JR, Stacey NE, Tan ESP, McAdam DSO, Lang SLC (1995) Androgen increases olfactory response to a vertebrate sex pheremone. J Comp Physiol A Neuroethol Sens Neural Behav Physiol 176:55-61

Catchpole CK, Slater PJB (1995) Bird Song: Biological themes and variations. Cambridge, Great Britain: University Press

Charitidi K, Canlon B (2010) Estrogen receptors in the central auditory system of male and female mice. Neuroscience 165:923-933

Charitidi K, Frisina RD, Vasilyeva ON, Zhu X, Canlon B (2010) Expression patterns of estrogen receptors in the central auditory system change in prepubertal and aged mice. Neuroscience 170:1270-1281

Chow RW, Handelsman DJ, Ng MK (2010) Minireview: rapid actions of sex steroids in the endothelium. Endocrinology 151:2411-2422

Coats AC (1978) Human auditory nerve action potentials and brain stem evoked responses. Arch Otolaryngol 104:709-717

Coats AC, Martin JL (1977) Human auditory nerve action potentials and brain stem evoked responses: effects of audiogram shape and lesion location. Arch Otolaryngol 103:605-622

Coffin AB, Mohr RA, Sisneros JA (2012) Saccular-specific hair cell addition correlates with reproductive state-dependent changes in the auditory saccular sensitivity of a vocal fish. J Neurosci 32:1366-1376.

Coleman JR, Campbell D, Cooper WA, Welsh MG, Moyer J (1994) Auditory brainstem responses after ovariectomy and estrogen replacement in rat. Hear Res 80:209-215

Conlee JW, Parks TN (1986) Origin of ascending auditory projections to the nucleus mesencephalicus lateralis pars dorsalis in the chicken. Brain Res 367:96-113

Cortopassi AJ, Mewaldt LR (1965) The Circumannual Distribution of White-Crowned Sparrows. Bird- Banding 36:141-169

Corwin JT, Bullock TH, Schweitzer J (1982) The auditory brain stem response in five vertebrate classes. Electroencephalogr Clin Neurophysiol 54:629-641

Corwin JT, Cotanche DA (1988) Regeneration of sensory hair cells after acoustic trauma. Science 240:1772-1774

Cox JR (1980) Hormonal influence on auditory function. Ear Hear 1:219-222

Craft RM (2007) Modulation of pain by estrogens. Pain 132 Suppl 1:S3-12

Cynx J, Nottebohm F (1992a) Role of gender, season, and familiarity in discrimination of conspecific song by zebra finches (Taeniopygia guttata). Proc Natl Acad Sci U S A 89:1368-1371

Cynx J, Nottebohm F (1992b) Testosterone facilitates some conspecific song discriminations in castrated zebra finches (Taeniopygia guttata). Proc Natl Acad Sci U S A 89:1376-1378

Cynx J, Williams H, Nottebohm F (1992) Hemispheric differences in avian song discrimination. Proc Natl Acad Sci U S A 89:1372-1375

Dagnino-Subiabre A, Pérez MA, Terreros G, Cheng MY, House P, Sapolsky R (2012) Corticosterone treatment impairs auditory fear learning and the dendritic morphology of the rat inferior colliculus. Hear Res. http://dx.doi.org/10.1016/j.heares.2012.09.008

Dallos P (2008) Cochlear amplification, outer hair cells and prestin. Curr Opin Neurobiol 18:370-376

Dallos P, Wu X, Cheatham MA, Gao J, Zheng J, Anderson CT, Jia S, Wang X, Cheng WH, Sengupta S, He DZ, Zuo J (2008) Prestin-based outer hair cell motility is necessary for mammalian cochlear amplification. Neuron 58:333-339

Dave AS, Yu AC, Margoliash D (1998) Behavioral state modulation of auditory activity in a vocal motor system. Science 282:2250-2254

De Groof G, Verhoye M, Poirier C, Leemans A, Eens M, Darras VM, Van der Linden A (2009) Structural changes between seasons in the songbird auditory forebrain. J Neurosci 29:13557-13565

de la Rocha J, Marchetti C, Schiff M, Reyes AD (2008) Linking the response properties of cells in auditory cortex with network architecture: cotuning versus lateral inhibition. J Neurosci 28:9151-9163

Del Negro C, Edeline JM (2002) Sex and season influence the proportion of thin spike cells in the canary HVc. Neuroreport 13:2005-2009

Del Negro C, Kreutzer M, Gahr M (2000) Sexually stimulating signals of canary (Serinus canaria) songs: evidence for a female-specific auditory representation in the HVc nucleus during the breeding season. Behav Neurosci 114:526-542

Del Negro C, Lehongre K, Edeline JM (2005) Selectivity of canary HVC neurons for the bird's own song: modulation by photoperiodic conditions. J Neurosci 25:4952-4963

Despland PA, Galambos R (1980) The auditory brainstem response (ABR) is a useful diagnostic tool in the intensive care nursery. Pediatric research 14:154-158

DeWolfe BB, Kaska DD, Peyton LJ (1974) Prominent variations in the songs of gambel's white crowned sparrows. Bird-Banding 45:224-252

Dixon WJ (1950) Analysis of extreme values. Ann Math Statist 21:488-506

Dooling RJ, Lohr B, Dent ML (2000) Hearing in Birds and Reptiles. In: Dooling RJ, Popper AN, Fay RR (eds) Comparative Hearing: Birds and Reptiles. Springer-Verlag, New York, pp 308-359

Eberhardt LS (1994) Oxygen consumption during singing by male Carolina wrens (Thryothorus ludovicianus). The Auk 111:124-130

Engineer CT, Perez CA, Chen YH, Carraway RS, Reed AC, Shetake JA, Jakkamsetti V, Chang KQ, Kilgard MP (2008) Cortical activity patterns predict speech discrimination ability. Nat Neurosci 11:603-608

Evrard HC (2006) Estrogen synthesis in the spinal dorsal horn: a new central mechanism for the hormonal regulation of pain. Am J Physiol Regul Integr Comp Physiol 291:R291-R299

Finsterer J (2010) Perspectives of Kennedy's disease. J Neurol Sci 298:1-10

Forlano PM, Deitcher DL, Bass AH (2005) Distribution of estrogen receptor alpha mRNA in the brain and inner ear of a vocal fish with comparisons to sites of aromatase expression. J Comp Neurol 483:91-113

Fortune ES, Margoliash D (1992) Cytoarchitectonic organization and morphology of cells of the field L complex in male zebra finches (Taenopygia guttata). J Comp Neurol 325:388-404

Franz M (2003) Respiratory patterns and oxygen consumption in singing zebra finches. J Exp Biol 206:967-978

Fusani L, Hutchison JB, Gahr M (2001) Testosterone regulates the activity and expression of aromatase in the canary neostriatum. J Neurobiol 49:1-8

Fusani L, Van't Hof T, Hutchison JB, Gahr M (2000) Seasonal expression of androgen receptors, estrogen receptors, and aromatase in the canary brain in relation to circulating androgens and estrogens. J Neurobiol 43:254-268

Gahr M (1990) Localization of androgen receptors and estrogen receptors in the same cells of the songbird brain. Proc Natl Acad Sci U S A 87:9445-9448

Gahr M (2001) Distribution of sex steroid hormone receptors in the avian brain: functional implications for neural sex differences and sexual behaviors. Microsc Res Tech 55:1-11

Gahr M, Güttinger HR, Kroodsma DE (1993) Estrogen receptors in the avian brain: survey reveals general distribution and forebrain areas unique to songbirds. J Comp Neurol 327:112-122

Gelinas D, Callard GV (1997) Immunolocalization of aromatase- and androgen receptor-positive neurons in the goldfish brain. Gen Comp Endocrinol 106:155-168

George I, Cousillas H, Richard JP, Hausberger M (2005) State-dependent hemispheric specialization in the songbird brain. J Comp Neurol 488:48-60

George I, Vernier B, Richard JP, Hausberger M, Cousillas H (2004) Hemispheric specialization in the primary auditory area of awake and anesthetized starlings (Sturnus vulgaris). Behav Neurosci 118:597-610

Gil D, Gahr M (2002) The honesty of bird song: multiple constraints for multiple traits. Trends Ecol Evol 17:133-141

Goense JB, Feng AS (2005) Seasonal changes in frequency tuning and temporal processing in single neurons in the frog auditory midbrain. J Neurobiol 65:22-36

Grace JA, Amin N, Singh NC, Theunissen FE (2003) Selectivity for conspecific song in the zebra finch auditory forebrain. J Neurophysiol 89:472-487

Grothe B, Pecka M, McAlpine D (2010) Mechanisms of sound localization in mammals. Physiol Rev 90:983-1012

Guimaraes P, Frisina ST, Mapes F, Tadros SF, Frisina DR, Frisina RD (2006) Progestin negatively affects hearing in aged women. Proc Natl Acad Sci U S A 103:14246-14249

Guimaraes P, Zhu X, Cannon T, Kim S, Frisina RD (2004) Sex differences in distortion product otoacoustic emissions as a function of age in CBA mice. Hear Res 192:83-89

Hall JW (1992) Handbook of Auditory Evoked Responses. Allyn and Bacon, Needham Heights, MA

Hall JW (2007) New Handbook of Auditory Evoked Responses. Allyn and Bacon, Boston, MA

Harris FP (1990) Distortion-product otoacoustic emissions in humans with high frequency sensorineural hearing loss. J Speech Hear Res 33:594-600

Hauber ME, Cassey P, Woolley SM, Theunissen FE (2007) Neurophysiological response selectivity for conspecific songs over synthetic sounds in the auditory forebrain of non-singing female songbirds. J Comp Physiol A Neuroethol Sens Neural Behav Physiol 193:765-774

Hederstierna C, Hultcrantz M, Rosenhall U (2009) Estrogen and hearing from a clinical point of view; characteristics of auditory function in women with Turner syndrome. Hear Res 252:3-8

Henry KS, Lucas JR (2009) Vocally correlated seasonal auditory variation in the house sparrow (Passer domesticus). J Exp Biol 212:3817-3822

Huetz C, Del Negro C, Lebas N, Tarroux P, Edeline JM (2006) Contribution of spike timing to the information transmitted by HVC neurons. Eur J Neurosci 24:1091-1108

Huetz C, Philibert B, Edeline JM (2009) A spike-timing code for discriminating conspecific vocalizations in the thalamocortical system of anesthetized and awake guinea pigs. J Neurosci 29:334-350

Hultcrantz M, Simonoska R, Stenberg AE (2006) Estrogen and hearing: a summary of recent investigations. Acta oto-laryngologica 126:10-14

Jeong JK, Burrows K, Tremere LA, Pinaud R (2011) Neurochemical organization and experience dependent activation of estrogen-associated circuits in the songbird auditory forebrain. Eur J Neurosci 34:283-291

Jerger J, Mauldin L (1978) Prediction of sensorineural hearing level from the brain stem evoked response. Arch Otolaryngol 104:456-461

Jewett DL, Romano MN, Williston JS (1970) Human auditory evoked potentials: possible brain stem components detected on the scalp. Science 167:1517-1518

Jewett DL, Williston JS (1971) Auditory-evoked far fields averaged from the scalp of humans. Brain 94:681-696

Karten HJ (1967) The organization of the ascending auditory pathway in the pigeon (Columba livia). I. Diencephalic projections of the inferior colliculus (nucleus mesencephali lateralis, pars dorsalis). Brain Res 6:409-427

Katayama A (1985) Postnatal development of auditory function in the chicken revealed by auditory brain-stem responses (ABRs). Electroencephal Clin Neurophysiol 62:388-398

Kelly MJ, Rønnekleiv OK (2009) Control of CNS neuronal excitability by estrogens via membrane- initiated signaling. Mol Cell Endocrinol 308:17-25

Kemp DT (1978) Stimulated acoustic emissions from within the human auditory system. J Acoust Soc Am 64:1386-1391

Kemp DT (2002) Otoacoustic emissions, their origin in cochlear function, and use. Br Med Bull 63:223-241

Kettembeil S, Manley GA, Siegl E (1995) Distortion-product otoacoustic emissions and their anaesthesia sensitivity in the European starling and the chicken. Hear Res 86:47-62

Kim G, Doupe A (2011) Organized representation of spectrotemporal features in songbird auditory forebrain. J Neurosci 31:16977-16990

Krützfeldt NO, Logerot P, Kubke MF, Wild JM (2010a) Connections of the auditory brainstem in a songbird, Taeniopygia guttata. I. Projections of nucleus angularis and nucleus laminaris to the auditory torus. J Comp Neurol 518:2109-2134

Krützfeldt NO, Logerot P, Kubke MF, Wild JM (2010b) Connections of the auditory brainstem in a songbird, Taeniopygia guttata. II. Projections of nucleus angularis and nucleus laminaris to the superior olive and lateral lemniscal nuclei. J Comp Neurol 518:2135-2148

LeBlanc MM, Goode CT, MacDougall-Shackleton EA, Maney DL (2007) Estradiol modulates brainstem catecholaminergic cell groups and projections to the auditory forebrain in a female songbird. Brain Res 1171:93-103

Leppelsack HJ, Vogt M (1976) Responses of Auditory Neurons in the Forebrain of a Songbird to Stimulation with Species-specific Sounds. J Comp Physiol A Neuroethol Sens Neural Behav Physiol 107:263-274

Liberman MC, Tartaglini E, Fleming JC, Neufeld EJ (2006) Deletion of SLC19A2, the high

affinity thiamine transporter, causes selective inner hair cell loss and an auditory neuropathy phenotype. J Assoc Res Otolaryngol 7:211-217

Liu RC, Schreiner CE (2007) Auditory cortical detection and discrimination correlates with communicative significance. PLoS Biol 5:e173

Lonsbury-Martin BL, Cutler WM, Martin GK (1991) Evidence for the influence of aging on distortion-product otoacoustic emissions in humans. J Acoust Soc Am 89:1749-1759

Lucas JR, Freeberg TM, Krishnan A, Long GR (2002) A comparative study of avian auditory brainstem responses: correlations with phylogeny and vocal complexity, and seasonal effects. J Comp Physiol A Neuroethol Sens Neural Behav Physiol 188:981-992

Lucas JR, Freeberg TM, Long GR, Krishnan A (2007) Seasonal variation in avian auditory evoked responses to tones: a comparative analysis of Carolina chickadees, tufted titmice, and white-breasted nuthatches. J Comp Physiol A Neuroethol Sens Neural Behav Physiol 193:201-215

Luu-The V, Labrie F (2010) The intracrine sex steroid biosynthesis pathways. Prog Brain Res 181:177-192

Machens CK, Schütze H, Franz A, Kolesnikova O, Stemmler MB, Ronacher B, Herz AV (2003) Single auditory neurons rapidly discriminate conspecific communication signals. Nat Neurosci 6:341-342

Maney DL, Cho E, Goode CT (2006) Estrogen-dependent selectivity of genomic responses to birdsong. Eur J Neurosci 23:1523-1529

Maney D, Pinaud R (2011) Estradiol-dependent modulation of auditory processing and selectivity in songbirds. Front Neuroendocrinol 32:287-302

Margoliash D (1983) Acoustic parameters underlying the responses of song-specific neurons in the white-crowned sparrow. J Neurosci 3:1039-1057

Marler P, Peters S, Ball GF, Dufty AM, Jr., Wingfield JC (1988) The role of sex steroids in the acquisition and production of birdsong. Nature 336:770-772

Marler P, Tamura M (1964) Culturally Transmitted Patterns of Vocal Behavior in Sparrows. Science 146:1483-1486

Matragrano LL, Sanford SE, Salvante KG, Beaulieu M, Sockman KW, Maney DL (2012) Estradiol-dependent modulation of serotonergic markers in auditory areas of a seasonally breeding songbird. Behav Neurosci 126:110-122

Matragrano LL, Sanford SE, Salvante KG, Sockman KW, Maney DL (2011) Estradiol-dependent catecholaminergic innervation of auditory areas in a seasonally breeding songbird. Eur J Neurosci 34:416-425

Mazurek B, Haupt H, Joachim R, Klapp BF, Stöver T, Szczepek AJ (2010) Stress induces transient auditory hypersensitivity in rats. Hear Res 259:55-63

McClintock M (1971) Menstrual Synchrony and Suppression. Nature 229:244

McEwen BS (1991) Non-genomic and genomic effects of steroids on neural activity. Trends Pharmacol Sci 12:141-147

McFadden D (1998) Sex differences in the auditory system. Dev Neuropsychol 14:261-298

McFadden D (2009) Masculinization of the mammalian cochlea. Hear Res 252:37-48

McFadden D, Pasanen EG, Raper J, Lange HS, Wallen K (2006) Sex differences in otoacoustic emissions measured in rhesus monkeys (Macaca mulatta). Horm Behav 50:274-284

Meitzen J, Moore IT, Lent K, Brenowitz EA, Perkel DJ (2007a) Steroid hormones act transsynaptically within the forebrain to regulate neuronal phenotype and song stereotypy. J Neurosci 27:12045-12057

Meitzen J, Perkel DJ, Brenowitz EA (2007b) Seasonal changes in intrinsic electrophysiological activity of song control neurons in wild song sparrows. J Comp Physiol A Neuroethol Sens Neural Behav Physiol 193:677-683

Meitzen J, Thompson CK (2008) Seasonal-like growth and regression of the avian song control system: neural and behavioral plasticity in adult male Gambel's white-crowned sparrows. Gen Comp Endocrinol 157:259-265

Meitzen J, Thompson CK, Choi H, Perkel DJ, Brenowitz EA (2009b) Time course of changes in Gambel's white-crowned sparrow song behavior following transitions in breeding condition. Horm Behav 55:217-227

Meitzen J, Weaver AL, Brenowitz EA, Perkel DJ (2009a) Plastic and stable electrophysiological properties of adult avian forebrain song-control neurons across changing breeding conditions. J Neurosci 29:6558-6567

Mello CV, Clayton DF (1994) Song-induced ZENK gene expression in auditory pathways of songbird brain and its relation to the song control system. J Neurosci 14:6652-6666

Mello CV, Pinaud R, Ribeiro S (1998) Noradrenergic system of the zebra finch brain: immunocytochemical study of dopamine-beta-hydroxylase. J Comp Neurol 400:207-228

Mello CV, Velho TA, Pinaud R (2004) Song-induced gene expression: a window on song auditory processing and perception. Ann N Y Acad Sci 1016:263-281

Meltser I, Canlon B (2011) Protecting the auditory system with glucocorticoids. Hear Res 281:47-55

Meltser I, Tahera Y, Simpson E, Hultcrantz M, Charitidi K, Gustafsson JA, Canlon B (2008) Estrogen receptor beta protects against acoustic trauma in mice. J Clin Invest 118:1563-1570

Metzdorf R, Gahr M, Fusani L (1999) Distribution of aromatase, estrogen receptor, and androgen receptor mRNA in the forebrain of songbirds and nonsongbirds. J Comp Neurol 407:115-129

Middleton J (1965) Testicular Responses of House Sparrows and White-Crowned Sparrows to Short Daily Photoperiods with Low Intensities of Light. Physiol Zool 38:255-266

Miranda JA, Liu RC (2009) Dissecting natural sensory plasticity: hormones and experience in a maternal context. Hear Res 252:21-28

Miranda JA, Wilczynski W (2009a) Female reproductive state influences the auditory midbrain response. J Comp Physiol A Neuroethol Sens Neural Behav Physiol 195:341-349

Miranda JA, Wilczynski W (2009b) Sex differences and androgen influences on midbrain auditory thresholds in the green tree-frog, Hyla cinera. Hearing research doi: 10.1016/j.heares 2009.04.004

Mitsushima D, Takase K, Funabashi T, Kimura F (2009) Gonadal steroids maintain 24 h acetylcholine release in the hippocampus: organizational and activational effects in behaving rats. J Neurosci 29:3808-3815

Moller AR, Jannetta PJ (1981) Compound action potentials recorded intracranially from the auditory nerve in man. Experimental neurology 74:862-874

Moller AR, Jannetta PJ (1983) Interpretation of brainstem auditory evoked potentials: results from intracranial recordings in humans. Scand Audiol 12:125-133

Moller AR, Jannetta PJ, Moller MB (1981) Neural generators of brainstem evoked potentials.

Results from human intracranial recordings. Ann Otol Rhinol Laryngol 90:591-596

Moore MC (1982) Hormonal response of free-living male white-crowned sparrows to experimental manipulation of female sexual behavior. Horm Behav 16:323-329

Moore IT, Wingfield JC, Brenowitz EA (2004) Plasticity of the avian song control system in response to localized environmental cues in an equatorial songbird. J Neurosci 24:10182-10185

Mougeot F, Bretagnolle V (2000) Predation as a cost of sexual communication in nocturnal seabirds: an experimental approach using acoustic signals. Anim Behav 60:647-656

Müller CM, Leppelsack HJ (1985) Feature extraction and tonotopic organization in the avian auditory forebrain. Exp Brain Res 59:587-599

Nagel KI, Doupe J (2008) Organizing principles of spectro-temporal encoding in the avian primary auditory area field L. Neuron 58:938-955

Nakamagoe M, Tabuchi K, Nishimura B, Hara A (2011) Effects of neuroactive steroids on cochlear hair cell death induced by gentamicin. Steroids 76:1443-1450

Nakamagoe M, Tabuchi K, Uemaetomari I, Nishimura B, Hara A (2010) Estradiol protects the cochlea against gentamicin ototoxicity through inhibition of the JNK pathway. Hear Res 261:67-74

Narayan R, Graña G, Sen K (2006) Distinct time scales in cortical discrimination of natural sounds in songbirds. J Neurophysiol 96:252-258

Nehls HB (1981) Familiar Birds of the Northwest. Portland Audubon Society, Portland

Nemeth E (2004) Measuring the sound pressure level of the song of the Screaming Piha Lipaugus vociferans: One of the loudest birds in the world. Bioacoustics 14:225-228

Niven JE, Laughlin SB (2008) Energy limitation as a selective pressure on the evolution of sensory systems. J Exp Biol 211:1792-1804

Noirot IC, Adler HJ, Cornil CA, Harada N, Dooling RJ, Balthazart J, Ball GF (2009) Presence of aromatase and estrogen receptor alpha in the inner ear of zebra finches. Hear Res 252:49-55

Nottebohm F (1981) A brain for all seasons: cyclical anatomical changes in song control nuclei of the canary brain. Science 214:1368-1370

Oberweger K, Goller F (2001) The metabolic cost of birdsong production. J Exp Biol

204:3379-3388

Okanoya K, Dooling RJ (1988) Hearing in the swamp sparrow (Melospiza georgiana) and the song sparrow (Melospiza melodia). Anim Behav 36:726-732

Oshima K, Gorbman A (1969) Effect of estradiol on NaCl-evoked olfactory bulbar potentials in goldfish: dose--response relationships. Gen Comp Endocrinol 13:92-97

Pak MW, Ng MH, Leung CB, van Hasselt CA (2000) Cochlear deafness in a Chinese family with Fechtner's syndrome. Am J Otol 21:345-350

Park KH, Meitzen J, Moore IT, Brenowitz EA, Perkel DJ (2005) Seasonal-like plasticity of spontaneous firing rate in a songbird pre-motor nucleus. J Neurobiol 64:181-191

Pawlisch BA, Stevenson SA, Riters LV (2011) α_1-Noradrenegic receptor antagonism disrupts female songbird responses to male song. Neurosci Lett 496:20-24

Phan ML, Vicario DS (2010) Hemispheric differences in processing of vocalizations depend on early experience. Proc Natl Acad Sci U S A 107:2301-2306

Phillmore LS, Veysey AS, Roach SP (2011) Zenk expression in auditory regions changes with breeding condition in male Black-capped chickadees (Poecile atricapillus). Behav Brain Res 225:464-472

Pinaud R, Tremere LA (2012) Control of central auditory processing by a brain-generated oestrogen. Nat Rev Neurosci 13:521-527

Poirier C, Boumans T, Verhoye M, Balthazart J, Van der Linden A (2009) Own-song recognition in the songbird auditory pathway: selectivity and lateralization. J Neurosci 29:2252-2258

Polley DB, Steinberg EE, Merzenich MM (2006) Perceptual learning directs auditory cortical map reorganization through top-down influences. J Neurosci 26:4970-4982

Ponton CW, Moore JK, Eggermont JJ (1996) Auditory brain stem response generation by parallel pathways: differential maturation of axonal conduction time and synaptic transmission. Ear and hearing 17:402-410

Price K, Zhu X, Guimaraes PF, Vasilyeva ON, Frisina RD (2009) Hormone replacement therapy diminishes hearing in peri-menopausal mice. Hear Res 252:29-36

Probst R, Lonsbury-Martin BL, Martin GK (1991) A review of otoacoustic emissions. The Journal of the Acoustical Society of America 89:2027-2067

Rarey KE, Curtis LM, ten Cate WJ (1993) Tissue specific levels of glucocorticoid receptor within the rat inner ear. Hear Res 64:205-210

Recanzone GH, Guard DC, Phan ML (2000) Frequency and intensity response properties of single neurons in the auditory cortex of the behaving macaque monkey. J Neurophysiol 83:2315-2331

Reiner A, Perkel DJ, Mello CV, Jarvis ED (2004) Songbirds and the revised avian brain nomenclature. Ann N Y Acad Sci 1016:77-108

Remage-Healey L, Coleman MJ, Oyama RK, Schlinger BA (2010) Brain estrogens rapidly strengthen auditory encoding and guide song preference in a songbird. Proc Natl Acad Sci U S A 107:3852-3857

Remage-Healey L, Dong SM, Chao A, Schlinger BA (2012) Sex-specific, rapid neuroestrogen fluctuations and neurophysiological actions in the songbird auditory forebrain. J Neurophysiol 107:1621-1631

Remage-Healey L, Joshi NR (2012) Changing Neuroestrogens Within the Auditory Forebrain Rapidly Transform Stimulus Selectivity in a Downstream Sensorimotor Nucleus. J Neurosci 32:8231-8241

Remage-Healey L, Maidment NT, Schlinger BA (2008) Forebrain steroid levels fluctuate rapidly during social interactions. Nat Neurosci 11:1327-1334

Riters LV, Baillien M, Eens M, Pinxten R, Foidart A, Ball GF, Balthazart J (2001) Seasonal variation in androgen-metabolizing enzymes in the diencephalon and telencephalon of the male European starling (Sturnus vulgaris). J Neuroendocrinol 13:985-997

Riters LV, Pawlisch BA (2007) Evidence that norepinephrine influences responses to male courtship song and activity within song control regions and the ventromedial nucleus of the hypothalamus in female European starlings. Brain Res 1149:127-140

Rohmann KN, Bass AH (2011) Seasonal plasticity of auditory hair cell frequency sensitivity correlates with plasma steroid levels in vocal fish. J Exp Biol 214:1931-1942

Rorabacher DB (1991) Statistical treatment for rejection of deviant values: critical values of Dixon's "Q" parameter and related subrange ratios at the 95% confidence level. Anal Chem 63:139-146

Rosenhamer HJ, Lindstrom B, Lundborg T (1981) On the use of click-evoked electric brainstem responses in audiological diagnosis. IV. Interaural latency differences (wave V) in cochlear hearing loss. Scand Audiol 10:67-73

Ryals BM, Rubel EW (1988) Hair cell regeneration after acoustic trauma in adult Coturnix quail. Science 240:1774-1776

Sadagopan S, Wang X (2008) Level invariant representation of sounds by populations of neurons in primary auditory cortex. J Neurosci 28:3415-3426

Saldanha CJ, Coomaralingam L (2005) Overlap and co-expression of estrogen synthetic and responsive neurons in the songbird brain--a double-label immunocytochemical study. Gen Comp Endocrinol 141:66-75

Sanford SE, Lange HS, Maney DL (2009) Topography of estradiol-modulated genomic responses in the songbird auditory forebrain. Dev Neurobiol 70:73-86

Schank JC (2001) Measurement and cycle variability: reexamining the case for ovarian-cycle synchrony in primates. Behav processes 56:131-146

Schlinger BA, Remage-Healey L (2012) Neurosteroidogenesis: insights from studies of songbirds. J Neuroendocrinol 24:16-21

Schnupp JW, Hall TM, Kokelaar RF, Ahmed B (2006) Plasticity of temporal pattern codes for vocalization stimuli in primary auditory cortex. J Neurosci 26:4785-4795

Schreiber S, Fellous JM, Whitmer D, Tiesinga P, Sejnowski TJ (2003) A new correlation-based measure of spike timing reliability. Neurocomputing 52:925-931

Schumacher M, Balthazart J (1986) Testosterone-induced brain aromatase is sexually dimorphic. Brain research 370:285-293

Searcy WA, Beecher MD (2009) Song as an aggressive signal in songbirds. Anim Behav 78:1281-1292

Sen K, Theunissen FE, Doupe AJ (2001) Feature analysis of natural sounds in the songbird auditory forebrain. J Neurophysiol 86:1445-1458

Shea SD, Margoliash D (2003) Basal forebrain cholinergic modulation of auditory activity in the zebra finch song system. Neuron 40:1213-1226

Shimazaki T, Ichimiya I, Suzuki M, Mogi G (2002) Localization of glucocorticoid receptors in the murine inner ear. Ann Otol Rhinol Laryngol 111:1133-1138

Sisneros JA (2009a) Seasonal plasticity of auditory saccular sensitivity in the vocal plainfin midshipman fish, Porichthys notatus. J Neurophysiol 102:1121-1131

Sisneros JA (2009b) Steroid-dependent auditory plasticity for the enhancement of acoustic communication: recent insights from a vocal teleost fish. Hear Res 252:9-14

Sisneros JA, Bass AH (2003) Seasonal plasticity of peripheral auditory frequency sensitivity. J Neurosci 23:1049-1058

Sisneros JA, Forlano PM, Deitcher DL, Bass AH (2004) Steroid-dependent auditory plasticity leads to adaptive coupling of sender and receiver. Science 305:404-407

Sisneros JA, Tricas TC (2000) Androgen-induced changes in the response dynamics of ampullary electrosensory primary afferent neurons. J Neurosci 20:8586-8595

Smith GT (1996) Seasonal plasticity in the song nuclei of wild rufous-sided towhees. Brain Res 734:79-85

Smith GT, Brenowitz EA, Beecher MD, Wingfield JC (1997) Seasonal changes in testosterone, neural attributes of song control nuclei, and song structure in wild songbirds. J Neurosci 17:6001-6010

Smith GT, Brenowitz EA, Wingfield JC (1997) Roles of photoperiod and testosterone in seasonal plasticity of the avian song control system. J Neurobiol 32:426-442

Smith GT, Brenowitz EA, Wingfield JC, Baptista LF (1995) Seasonal changes in song nuclei and song behavior in Gambel's white-crowned sparrows. J Neurobiol 28:114-125

Snihur AW, Hampson E (2012) Click-evoked otoacoustic emissions: response amplitude is associated with circulating testosterone levels in men. Behav Neurosci 126:325-331

Soha JA, Marler P (2000) A species-specific acoustic cue for selective song learning in the white-crowned sparrow. Anim Behav 60:297-306

Sohmer H, Feinmesser M, Szabo G (1974) Sources of electrocochleographic responses as studied in patients with brain damage. Electroencephalo Clin Neurophysiol 37:663-669

Soma KK, Hartman VN, Wingfield JC, Brenowitz EA (1999) Seasonal changes in androgen receptor immunoreactivity in the song nucleus HVc of a wild bird. J Comp Neurol 409:224-236

Soma KK, Schlinger BA, Wingfield JC, Saldanha CJ (2003) Brain aromatase, 5 alpha-reductase, and 5 beta-reductase change seasonally in wild male song sparrows: relationship to aggressive and sexual behavior. J Neurobiol 56:209-221

Soma KK, Tramontin AD, Featherstone J, Brenowitz EA (2004) Estrogen contributes to seasonal plasticity of the adult avian song control system. J Neurobiol 58:413-422

Starr A, Hamilton AE (1976) Correlation between confirmed sites of neurological lesions and abnormalities of far-field auditory brainstem responses. Electroencephal Clini Neurophysiol 41:595-608

Steimer T, Hutchison JB (1981) Androgen increases formation of behaviourally effective oestrogen in dove brain. Nature 292:345-347

Stenberg AE, Wang H, Fish J, 3rd, Schrott-Fischer A, Sahlin L, Hultcrantz M (2001) Estrogen receptors in the normal adult and developing human inner ear and in Turner's syndrome. Hear Res 157:87-92

Stenberg AE, Wang H, Sahlin L, Hultcrantz M (1999) Mapping of estrogen receptors alpha and beta in the inner ear of mouse and rat. Hear Res 136:29-34

Stevens SS, Poulton EC (1956) The estimation of loudness by unpracticed observers. J Exp Psychol 51:71-78

Sutter ML, Schreiner CE (1995) Topography of intensity tuning in cat primary auditory cortex:singleneuron versus multiple-neuron recordings. J Neurophysiol 73:190-204

Swanson SJ, Dengerink HA (1988) Changes in pure-tone thresholds and temporary threshold shifts as a function of menstrual cycle and oral contraceptives. J Speech Hear Res 31:569-574

Swett MB, Breuner CW (2008) Interaction of testosterone, corticosterone and corticosterone binding globulin in the white-throated sparrow (Zonotrichia albicollis). Comp Biochem Physiol A Mol Integr Physiol 151:226-231

Terleph TA, Lu K, Vicario DS (2008) Response properties of the auditory telencephalon in songbirds change with recent experience and season. PLoS ONE 3:e2854

Theunissen FE, Amin N, Shaevitz SS, Woolley SM, Fremouw T, Hauber ME (2004) Song selectivity in the song system and in the auditory forebrain. Ann N Y Acad Sci 1016:222-245

Tramontin AD, Hartman VN, Brenowitz EA (2000) Breeding conditions induce rapid and sequential growth in adult avian song control circuits: a model of seasonal plasticity in the brain. J Neurosci 20:854-861

Tremere LA, Jeong JK, Pinaud R (2009) Estradiol shapes auditory processing in the adult brain by regulating inhibitory transmission and plasticity-associated gene expression. J Neurosci 29:5949-5963

Tramontin AD, Wingfield JC, Brenowitz EA (2003) Androgens and estrogens induce seasonal like growth of song nuclei in the adult songbird brain. J Neurobiol 57:130-140

Tremere LA, Burrows K, Jeong JK, Pinaud R (2011) Organization of Estrogen-Associated Circuits in the Mouse Primary Auditory Cortex. J Exp Neurosci 2011:45-60

Tremere LA, Pinaud R (2011) Brain-generated estradiol drives long-term optimization of auditory coding to enhance the discrimination of communication signals. J Neurosci 31:3271-3289

Vates GE, Broome BM, Mello CV, Nottebohm F (1996) Auditory pathways of caudal telencephalon and their relation to the song system of adult male zebra finches. J Comp Neurol 366:613-642

Vyas A, Harding C, Borg L, Bogdan D (2009) Acoustic characteristics, early experience, and endocrine status interact to modulate female zebra finches' behavioral responses to songs. Horm Behav 55:50-59

Vyas A, Harding C, McGowan J, Snare R, Bogdan D (2008) Noradrenergic neurotoxin, N-(2 chloroethyl)-N-ethyl-2-bromobenzylamine hydrochloride (DSP-4), treatment eliminates estrogenic effects on song responsiveness in female zebra finches (Taeniopygia guttata). Behav Neurosci 122:1148-1157

Wang L, Narayan R, Grana G, Shamir M, Sen K (2007) Cortical discrimination of complex natural stimuli: can single neurons match behavior? J Neurosci 27:582-589

Ward S, Speakman JR, Slater PJ (2003) The energy cost of song in the canary, Serinus canaria. Anim Behav 66:893-902

Watkins PV, Barbour DL (2011) Rate-level responses in awake marmoset auditory cortex. Hear Res 275:30-42

Wharton JA, Church GT (1990) Influence of menopause on the auditory brainstem response. Audiology 29:196-201

Wild JM, Karten HJ, Frost BJ (1993) Connections of the auditory forebrain in the pigeon (Columba livia). J Comp Neurol 337:32-62

Wild JM, Krützfeldt NO, Kubke MF (2010) Connections of the auditory brainstem in a songbird, Taeniopygia guttata. III. Projections of the superior olive and lateral lemniscal nuclei. J Comp Neurol 518:2149-2167

Wingfield JC, Crim JW, Mattocks PW, Jr., Farner DS (1979) Responses of photosensitive and photorefractory male white-crowned sparrows (Zonotrichia leucophrys gambelii) to synthetic mammalian luteinizing hormone releasing hormone (syn-LHRH). Biology of reproduction 21:801-806

Wingfield JC, Farner DS (1978) The annual cycle of plasma irLH and steroid hormones in feral populations of the white-crowned sparrow, Zonotrichia leucophrys gambelii. Biol Reproduct 19:1046-1056

Woolley SM, Gill PR, Fremouw T, Theunissen FE (2009) Functional groups in the avian auditory system. J Neurosci 29:2780-2793

Woolley SM, Wissman AM, Rubel EW (2001) Hair cell regeneration and recovery of auditory thresholds following aminoglycoside ototoxicity in Bengalese finches. Hear Res 153:181-195

Xu XF, Hoebeke J, Björntorp P (1990) Progestin binds to the glucocorticoid receptor and mediates antiglucocorticoid effect in rat adipose precursor cells. J Steroid Biochem 36:465-471

Yoder KM, Vicario DS (2012) To modulate and be modulated: estrogenic influences on auditory processing of communication signals within a socio-neuro-endocrine framework. Behav Neurosci 126:17-28

Zakon HH (1998) The effects of steroid hormones on electrical activity of excitable cells. Trends Neurosci 21:202-207

Zaretsky MD, Konishi M (1976) Tonotopic organization in the avian telencephalon. Brain Res 111:167-171

Appendix 2.1 Supplementary Information for Chapter 2

Supplementary Table 2.1.
Number of missing ABR latency data points filled in with mean values

	PEAK 1*				PEAK 2**			
	Non-breeding		Breeding		Non-breeding		Breeding	
	Male	Female	Male	Female	Male	Female	Male	Female
Click	0	0	0	0	0	0	0	0
500 Hz	3	1	4	4	3	1	4	4
1000 Hz	1	0	4	3	1	0	4	3
2000 Hz	1	0	2	2	1	0	2	2
3000 Hz	1	0	0	1	1	0	2	1
4000 Hz	1	0	0	0	1	0	1	0
6000 Hz	1	0	1	0	1	0	1	0
8000 Hz	1	0	2	2	1	0	2	1

* Filled in values represent 35 out of 312 total peak 1 data points (11.2%)
** Filled in values represent 37 out of 312 total peak 1 data points (11.9%)

Appendix 2.1

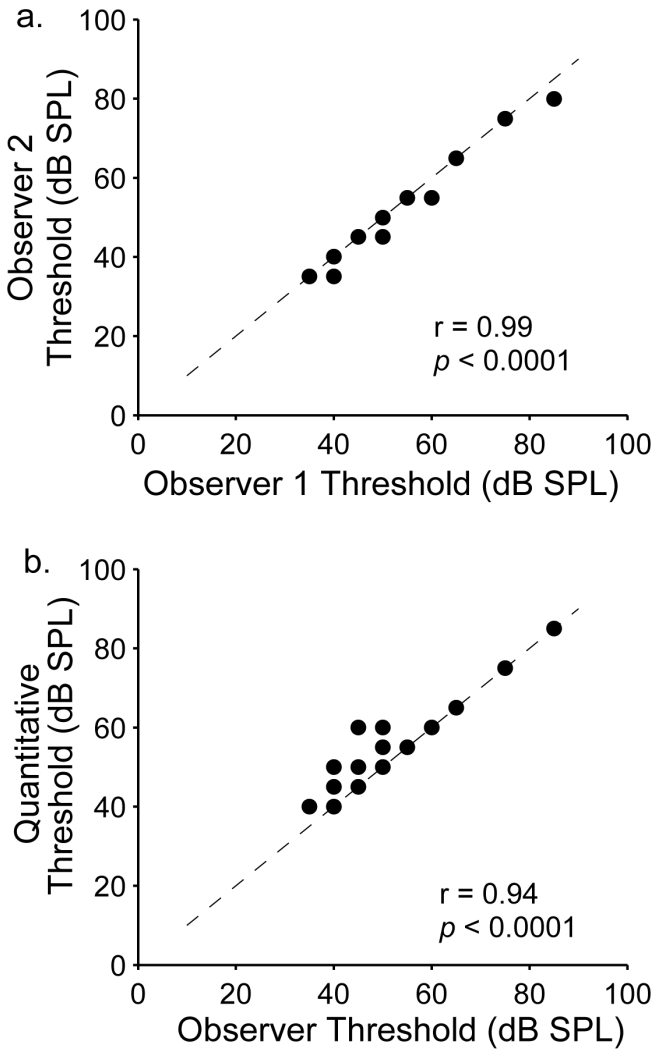

Supplementary Fig 2.1. Blind observer and quantitative analyses verify visual estimates of ABR thresholds. Each circle represents the threshold value for a representative ABR response. The dashed line represents the unity line. Pearson's r and *p* value are indicated for each comparison. *a)* Blind observer threshold estimates (*y*-axis) for a subset (10%) of all ABR responses significantly correlate with estimates made by one author (*x*-axis). *b*) Visual estimates (*x*-axis) significantly correlate with an automated estimate (*y*-axis) comparing the maximum voltage response in a 10 msec post-stimulus window with the maximum pre-stimulus voltage displacement plus 2 standard deviations.

Appendix 2.1

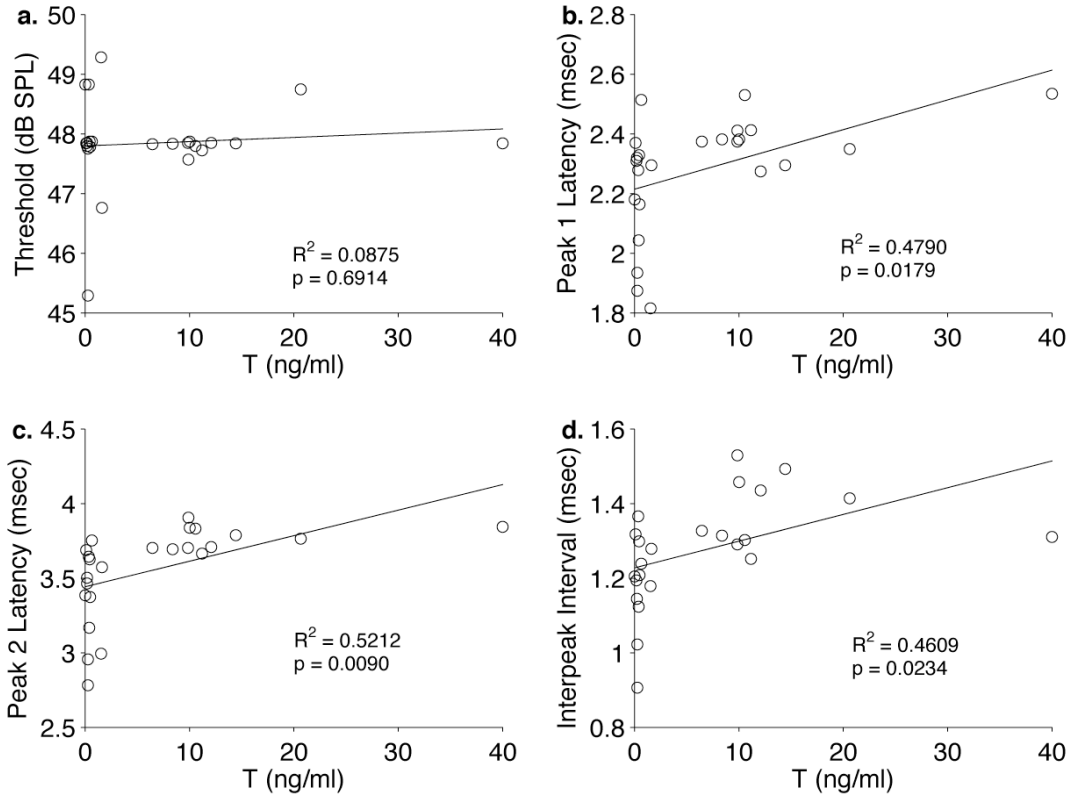

Supplementary Fig 2.2. ABR latencies, but not thresholds, correlate with male plasma T level. *a*) Individual ABR thresholds were averaged across all stimulus frequencies to give a single threshold value for each bird. These values are plotted as a function of individual T levels. Thresholds do not correlate with hormone level in male white-crowned sparrows. *b*) Individual iso-intensity peak 1 latencies were averaged across all stimulus frequencies to give a single peak 1 latency for each bird. Peak 1 latencies significantly correlate with T level ($p<0.05$). Similar results were found for Peak 2 latencies (*c*) and Inter-peak intervals (*d*).

Appendix 2.1

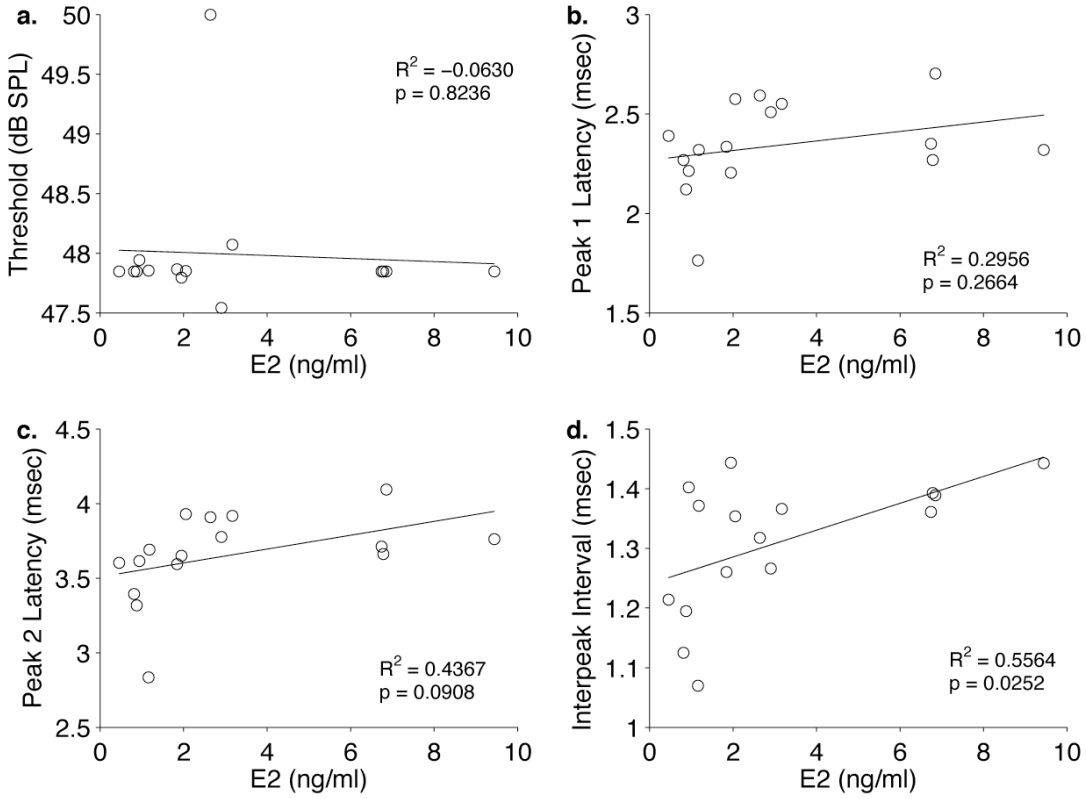

Supplementary Fig 2.3. ABR latencies and thresholds do not correlate with female plasma E_2 level. *a*) Individual ABR thresholds were averaged across all stimulus frequencies to give a single threshold value for each bird. These values are plotted as a function of individual E_2 levels. Thresholds do not correlate with hormone level in female white-crowned sparrows. *b*) Individual iso-intensity peak 1 latencies were averaged across all stimulus frequencies to give a single peak 1 latency for each bird. Peak 1 latencies do not significantly correlate with E_2 level. Similar results were found for Peak 2 latencies (*c*) and Inter-peak intervals (*d*).

Appendix 2.1

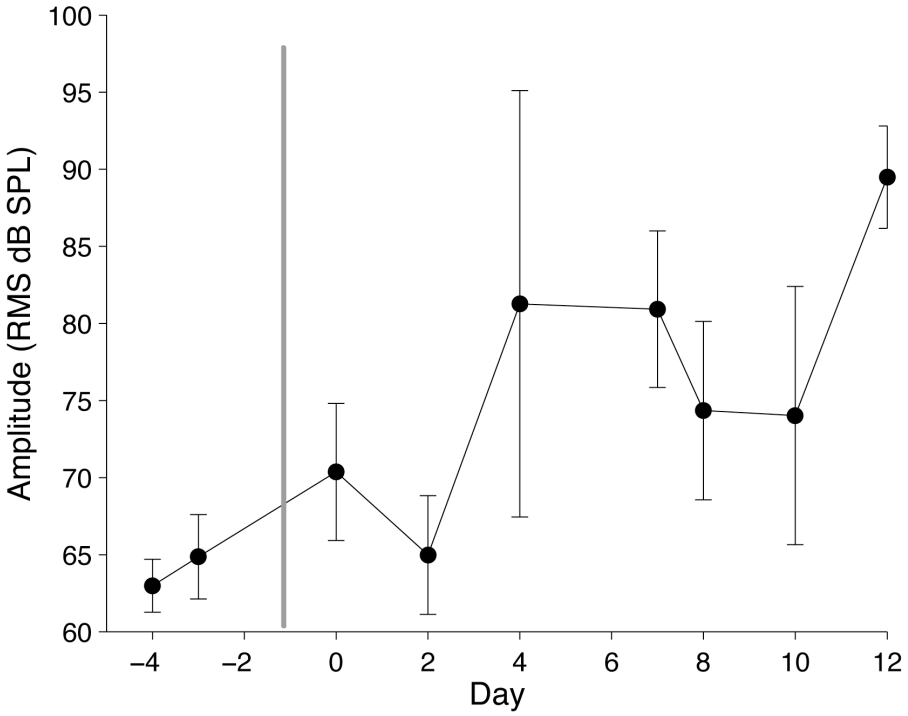

Supplementary Fig 2.4. Non-breeding songs have lower amplitudes than breeding songs. We recorded an individual male white-crowned sparrow under non-breeding conditions until day 0, at which point we implanted him with a subcutaneous T pellet and switched him to a long-day photoperiod. The vertical grey line separates songs produced under non-breeding conditions (left) from those produced during the transition into breeding (right). After exposure to breeding-like conditions, song amplitude gradually rises from 70.4 +/- 4.45 dB SPL on day 0 to 87.5 +/- 4.15 dB SPL on day 12. Data are mean +/- STDEV.

Appendix 3.1 Supplementary Information for Chapter 3

Chapter 3 explored the modulatory role of estradiol on field L auditory processing in female white-crowned sparrows. In a series of related experiments, I also explored the role of testosterone on field L auditory processing in male white-crowned sparrows. The methods and materials used in this study were identical to those described in Chapter 3, with the exception of the type of hormone administered (testosterone vs. estradiol), and the sex under investigation (male vs. female). Here I present results from this study that may be of interest to the reader. Given the preliminary nature of these findings, I have decided not to include an in-depth discussion of the results, though a brief summary is provided below:

Similar to the results reported in Chapter 3, male white-crowned sparrows exhibit two functionally distinct cell populations in field L: monotonic and non-monotonic (Supplementary Fig. 3.1A). These populations overlap considerably in anatomical location, though under breeding condition, non-monotonic neurons were found more dorsally than under non-breeding condition (Supplementary Fig. 3.1B). This finding may reflect a true hormonal difference in cellular distribution, or may be explained by uneven sampling across the two experimental groups. Regardless, the relative proportions of monotonic and non-monotonic neurons do not change as a function of breeding condition (Supplementary Fig. 3.1C).

Systemic administration of testosterone does not affect neuronal firing rates (Supplementary Figs. 3.2 and 3.5), auditory response strengths (Supplementary Figs. 3.3 and 3.4A-B), or

thresholds (Supplementary Figs. 3.3 and 3.4C-D). Similarly, while breeding condition does not affect pure tone dynamic ranges (Supplementary Fig. 3.3E-F), or song dynamic ranges in cells with monotonic tone responses (Supplementary Fig. 3.4E), breeding condition increases song dynamic ranges in cells with non-monotonic tone responses (Supplementary Fig. 3.4F, but note the extremely small sample size for the non-breeding group). More data are needed for meaningful conclusions to be drawn.

Appendix 3.1

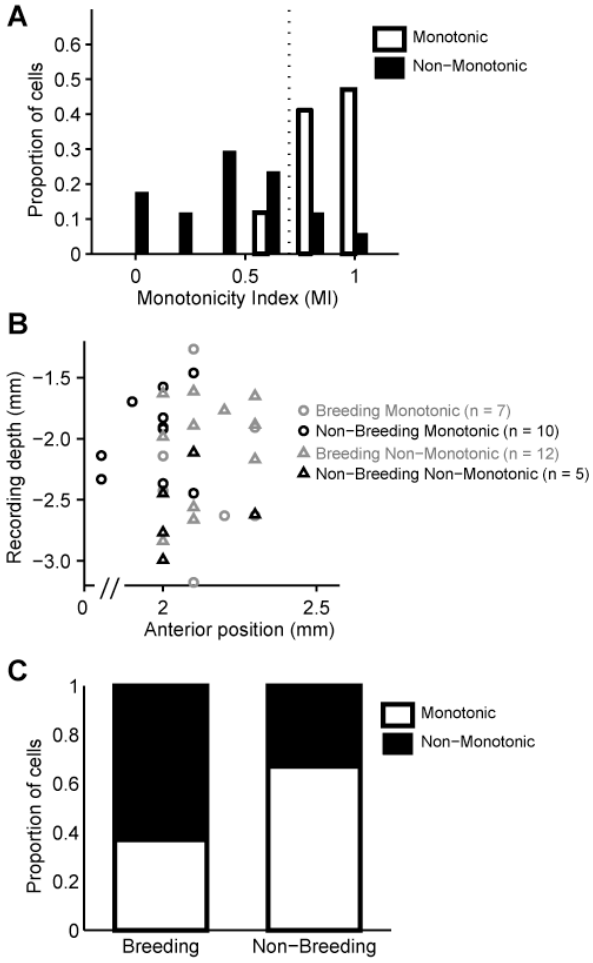

Supplementary Figure 3.1. Monotonic and non-monotonic neurons constitute separate cell populations in male white-crowned sparrows. **A**.Group histograms for monotonic (white) and non-monotonic (black) neurons showing the proportion of cells with various MIs. Increasing MI values represent increasing degrees of monotonicity. The majority of monotonic neurons have MI values >0.70 (dotted vertical line), while the majority of non-monotonic neurons have MI values < 0.70. These differences are significant ($t_{32} = 5.41$, $p < 0.001$) **B.** The anatomical location of individual tone responsive neurons are plotted as a function of recording depth and anterior distance from the birfucation of the midsagittal sinus. Breeding (grey) and non-breeding (black) monotonic neurons (circles) are evenly distributed across the anterior-posterior and dorsal-ventral extents of field L ($p > 0.05$). Non-monotonic neurons (triangles) recorded under breeding condition, however, are located more dorsally than those recorded under non-breeding conditions ($F_{1,15} = 5.634$, $p < 0.05$). **C.** Breeding condition does not significantly affect the proportion of monotonic and non-monotonic neurons ($\chi^2_{(1, N = 34)} = 2.982$, $p > 0.05$).

Appendix 3.1

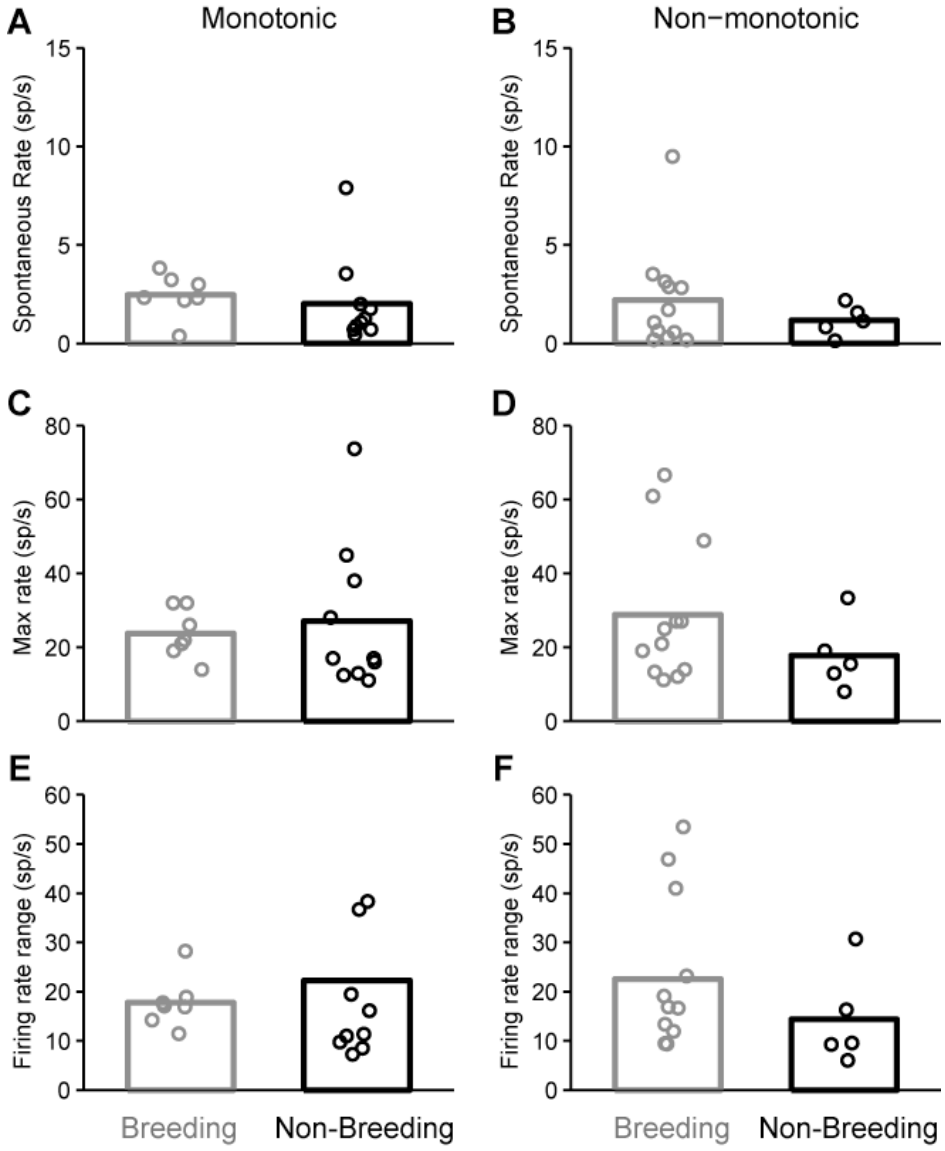

Supplementary Figure 3.2. Breeding condition does not modulate neuronal activity in male white-crowned sparrows

Breeding condition (grey) does not affect monotonic or non-monotonic spontaneous firing rates (A-B), maximum firing rates (C-D), or firing rate ranges (E-F). Bars are mean values, circles represent individual neurons. The number of cells and number of birds (in parentheses) are as follows: Monotonic neurons: breeding = 7(4), non-breeding = 10(6). Non-monotonic neurons: breeding = 12(6), non-breeding = 5(4). A separate one-way MANOVA was run for monotonic and non-monotonic cells. All $p > 0.05$.

Appendix 3.1

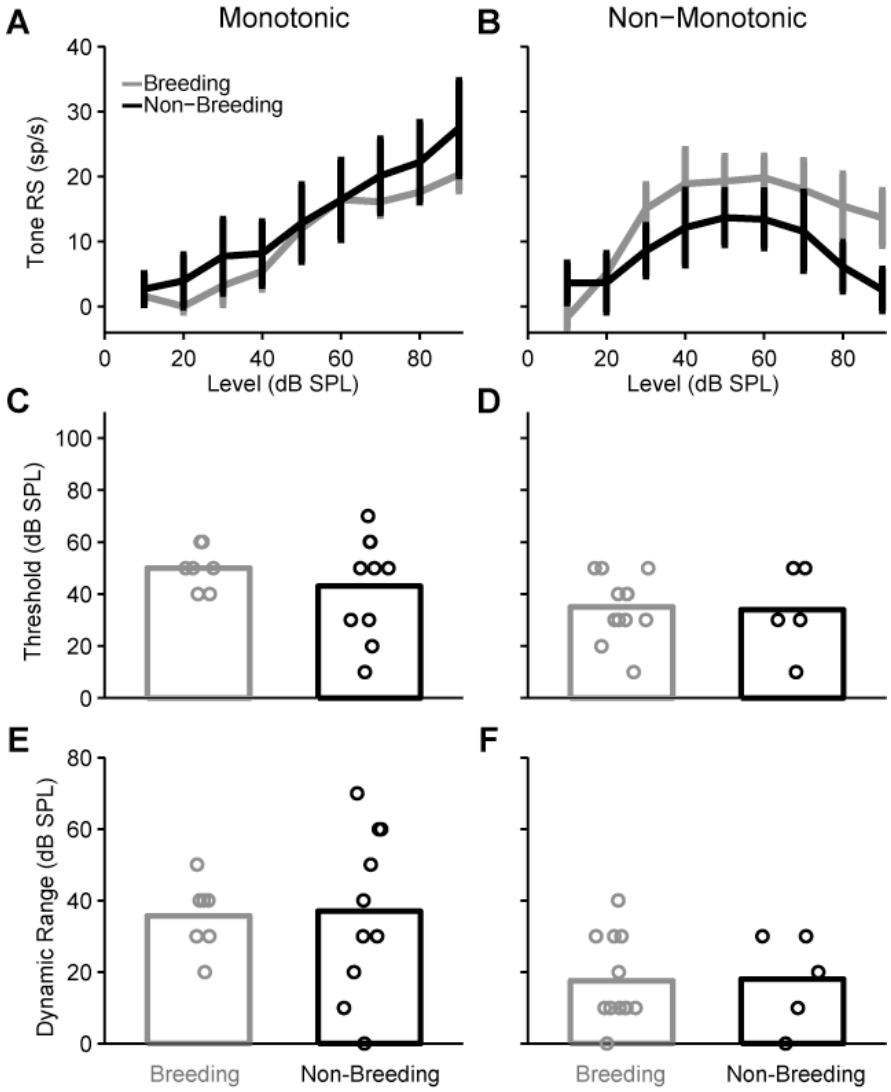

Supplementary Figure 3.3. Breeding condition does not affect tone responses in male white-crowned sparrows

Breeding condition (grey) does not affect CF-evoked response strengths (A-B), CF threshold (C-D) or dynamic range (E-F) in monotonic or non-monotonic neurons. Bars are mean values, circles represent individual neurons. The number of cells and number of birds (in parentheses) are as follows: Monotonic neurons: breeding = 7(4), non-breeding = 10(6), except at 90 dB SPL in panel A, non-breeding = 7(5). Non-monotonic neurons: breeding = 12(6), non-breeding = 5(4), except at 90 dB SPL in panel B, breeding = 10(5). Separate 2-way mixed-model ANOVAs (breeding condition x dB SPL) were run for monotonic and non-monotonic cells. A separate one-way MANOVA that included threshold and dynamic range as dependent variables was run for monotonic and non-monotonic cells. All $p > 0.05$.

Appendix 3.1

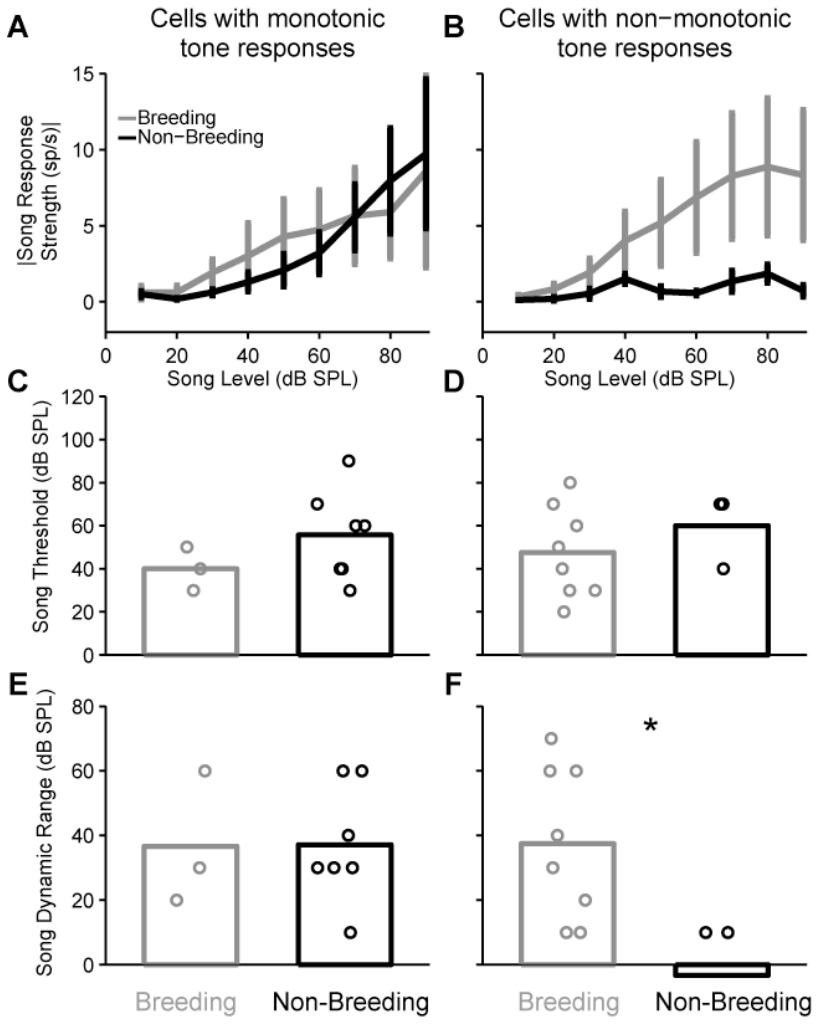

Supplementary Figure 3.4. Breeding condition may affect song dynamic range in cells with non-monotonic tone responses in male white-crowned sparrows
Breeding condition (grey) does not affect song-evoked response strengths (A-B) or song thresholds (C-D) in cells with monotonic or non-monotonic tone responses (all $p > 0.05$). Breeding condition does not affect song dynamic range in monotonic neurons (E), but does increase song dynamic range in cells with non-monotonic tone responses ($F_{1,9} = 6.526$, $p < 0.05$). Bars are mean values, circles represent individual neurons. The number of cells and number of birds (in parentheses) are as follows: Monotonic neurons: breeding = 3(2), non-breeding = 7(6), except at 10 dB SPL in panel A, non-breeding = 3(3). Non-monotonic neurons: breeding = 8(5), non-breeding = 3(3), except at 10 dB SPL in panel B, breeding = 5(4), non-breeding = 1(1); and 20 dB SPL in panel B, breeding = 6(4). Separate 2-way mixed-model ANOVAs (breeding condition x dB SPL) were run for monotonic and non-monotonic cells. A separate one-way MANOVA that included threshold and dynamic range as dependent variables was run for monotonic and non-monotonic cells.

Appendix 3.1

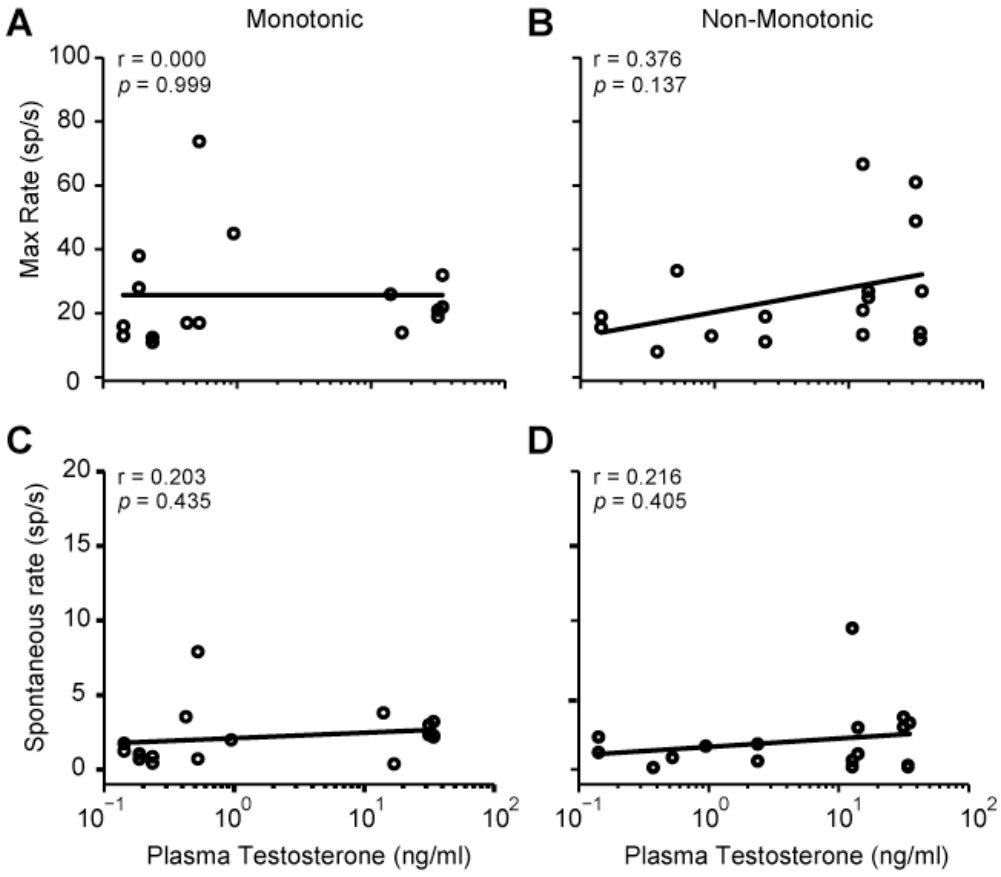

Supplementary Figure 3.5. Plasma testosterone concentrations do not predict neuronal firing rates in male white-crowned sparrows. Maximum (A-B) and spontaneous (C-D) firing rates of both monotonic and non-monotonic neurons do not correlate with plasma testosterone levels.

Melissa Lynne Caras

Education

Mar 2013 — PhD Neurobiology and Behavior
Seasonal and hormonal effects on auditory processing in a wild songbird
University of Washington, Seattle, WA

Jun 2007 — B.S. Neuroscience with Highest Honors, Summa cum laude
B.S. Biology
Investigating the motivational mechanism of altered saline consumption following 5-HT$_{1A}$ manipulation.
Brandeis University, Waltham, MA

Research Experience

Jul 2008 – Mar 2013 — Doctoral Candidate in Neurobiology and Behavior
University of Washington, Seattle, WA
Hormonal modulation of auditory processing in a seasonally breeding songbird
Advisors: Drs. Eliot Brenowitz and Edwin Rubel

Apr 2008 -Jun 2008 — Rotation Student
University of Washington, Seattle, WA
Effects of efferent innervation on seasonality in auditory tuning in the midshipman fish
Advisor: Dr. Joseph Sisneros

Jan 2008 – Mar 2008 — Rotation Student
University of Washington, Seattle, WA
Feeding behavior in divergent populations of three-spined stickleback fish
Advisor: Dr. Catherine Peichel

Sep 2007 – Dec 2007 — Rotation Student
University of Washington, Seattle, WA
Effects of downstream target ablation on neuronal recruitment in the song nucleus HVC
Advisor: Dr. Eliot Brenowitz

May 2004- Aug 2007 — Undergraduate Researcher
Brandeis University, Waltham, MA
Investigating the motivational mechanism of altered saline consumption following 5-HT$_{1A}$ manipulation.
Advisor: Dr. Donald B. Katz

Research Support

Jun 2010- Jun 2013 — NIH Predoctoral National Research Service Award (F31) Role: PI
Seasonal and hormonal effects on auditory processing

Jun 2008- Jun 2010 — NIH Speech and Hearing Sciences Predoctoral Training Grant (T32)
Role: Trainee

Academic Honors and Awards

2010	International Society for Neuroethology Student Travel Award
2010	Graduate and Professional Student Senate Travel Award
2010	Association for Research in Otolaryngology Travel Award
2009	NSF Graduate Research Honorable Mention
2007-2009	Achievement Reward for College Scientists (ARCS) Fellowship
2007	Doris Brewer Cohen Endowment Award
2006	Nathan and Bertha Richter Scholarship
2003-2007	Brandeis University Dean's List
2003-2007	Stephen Phillips Memorial Scholarship

Publications

Caras, M.L., O'Brien, Matthew, Brenowitz, E. and Rubel, E.W. (2012). Estradiol selectively enhances auditory function in avian forebrain neurons. *Journal of Neuroscience.* In press.

Caras, M.L., Brenowitz, E. and Rubel, E.W. (2010) Peripheral auditory processing changes seasonally in Gambel's white-crowned sparrows. *Journal of Comparative Physiology A.* 196(8): 581-599.

Caras, M.L., MacKenzie, K., Rodwin B., and Katz, D.B. (2008) Investigating the motivational mechanism of altered saline consumption following 5-HT_{1A} manipulation. *Behavioral Neuroscience.* 122(2): 407-415.

Poster Presentations

Caras, M.L., O'Brien, M., Brenowitz, E., Rubel, E.W. (2012) Estradiol selectively enhances auditory function in monotonically driven forebrain neurons. *Society for Neuroscience Annual Meeting.* New Orleans, LA. Abstract 503.08.

Caras, M.L., O'Brien, M., Brenowitz, E., Rubel, E.W. (2012) Estradiol selectively enhances auditory function inmonotonically driven forebrain neurons. *Gordon Research Conference: Auditory System.* Lewiston, ME.

Caras, M.L., Brenowitz, E., Rubel, E.W. (2011) Hormonal effects on forebrain auditory processing in male and female songbirds. *Society for Neuroscience Annual Meeting.* Washington, D.C. Abstract 945.07

Caras, M.L., Pollak, J., Fung, S., Mehravari, A., Watari, H. (2011) Sustainability of outreach programs over time: A look back through the first five years. *Society for Neuroscience Annual Meeting.* Washington,D.C. Abstract 27.17.

Caras, M.L. (2011) The effects of breeding condition on auditory processing in a wild songbird. *Gordon Research Seminar: Neuroethology: Behavior, Evolution & Neurobiology.* Easton, MA.

Smarr, B., Corke, A., Lee, M., Georgi, S., Watari, H., **Caras, M.L.,** Chudler, E. (2010) Expanding out reach: Using technology and the internet in neuroscience outreach. *Society for Neuroscience Annual Meeting.* San Diego, CA.

Caras, M.L., Brenowitz, E. and Rubel, E.W. (2010) Peripheral auditory processing changes seasonally in Gambel's white-crowned sparrows. *International Congress for Neuroethology.* Salamanca, Spain. Abstract 277

Caras, M.L., Brenowitz, E. and Rubel, E.W. (2010) Peripheral auditory processing changes seasonally in Gambel's white-crowned sparrows. *Association for Research in Otolaryngology Midwinter Meeting.* Anaheim, CA.Abstract 247

Georgi, S., Harris, R., Watari, H., White, B., **Caras, M.L**., Smarr, B., Chudler, E. (2008) Expanding our reach: Ideas and resources for neuroscience outreach. *Society for Neuroscience Annual Meeting*

Caras, M.L., MacKenzie, K., Rodwin B., and Katz, D.B. (2007) Investigating the motivational mechanism of altered saline consumption following 5-HT_{1A} manipulation. *Society for Neuroscience Annual Meeting.* San Diego, CA.

Oral Presentations

Caras, M.L. (2012) Neural coding of intensity discrimination. *Northwest Auditory and Vestibular Research Meeting.* Oregon Health and Sciences University, Portland, OR.

Caras, M.L. (2012) Estradiol selectively enhances auditory function. *Gordon Research Seminar: Auditory System.* Lewiston, ME.

Caras, M.L. (2012) Estradiol enhances songbird auditory forebrain function in a cell-specific and dose dependent manner. *Neurobiology and Behavior Spring Symposium.* Seattle, WA.

Caras, M.L. (2011) The effects of breeding condition on auditory processing in a wild songbird. *Gordon Research Seminar: Neuroethology: Behavior, Evolution & Neurobiology.* Invited presentation. Easton, MA.

Caras, M.L. (2011) How hormones affect hearing: studies in a wild songbird. *ARCS Annual Spring Luncheon.* Invited presentation. Seattle, WA.

Caras, M.L. (2010) Hormonal effects on auditory processing in a wild songbird. *Northwest Auditory and Vestibular Research Meeting.* University of Washington, Seattle, WA.

Caras, M.L. (2010) Hormonal effects on auditory processing in a wild songbird. *Graduate Program in Neurobiology and Behavior Annual Retreat*. Invited presentation. University of Washington, Seattle, WA.

Skills

Physiology	Single unit extracellular recording *in vivo* Auditory brainstem response recording Distortion product otoacoustic emission recording
Hormone Analysis	Enzyme-Linked Immunosorbent Assay Blood and plasma collection

Histology	Immunohistochemistry Stereological cell counts Morphological analysis
Behavior	Song recording, quantification and analysis (birds) Video capture of feeding and drinking behavior (fish and rats) Video coding of palatability (rats)
Programming	MATLAB

Teaching Experience

Courses

Mar 2012– Jun 2012 Teaching assistant for undergraduate neurobiology journal club
University of Washington, Seattle, WA

Jan 2008- Mar 2008 Teaching assistant for undergraduate introductory neurobiology course
University of Washington, Seattle, WA

Supervised Students/Mentorships

Feb 2010- Mar 2012 Matthew O'Brien, Undergraduate student
University of Washington, Seattle, WA

Nov 2010-May 2011 Scott Mitchell, High school student
Northwest association for biomedical research expo project
Seattle/Bellevue, WA

2007 Benjamin Rodwin, Undergraduate student
Brandeis University, Waltham, MA

University Membership and Service

2010-2012 Graduate Student Representative, Admissions Committee.
Graduate Program in Neurobiology and Behavior.
University of Washington, Seattle, WA.

Scientific Outreach and Advocacy

2007- 2013 Neurobiology and Behavior Community Outreach.
K-12 Liaison, Webmaster.
University of Washington, Seattle, WA

2012 Host for Neuroscience Olympiad Champion at Society for Neuroscience
Annual Meeting New Orleans, LA

2012 Presenter at Expanding Your Horizons Workshop for High School Girls

2011 Brain Awareness Week Open House Coordinator.
University of Washington, Seattle, WA.

2009 Capitol Hill Lobbying Day
American Society for Biochemistry and Molecular Biology Representative
Washington, D.C